
UNIVERSIDAD
DE ANTIOQUIA
1 8 0 3

# Methodology to recognize atypical functioning in emotional processing of Colombian ex-combatants using EEG brain connectivity

**Mónica Viviana Rodríguez Calvache**

Universidad de Antioquia UDEA
Facultad de Ingeniería
Medellín, Colombia
2017

# Methodology to recognize atypical functioning in emotional processing of Colombian ex-combatants using EEG brain connectivity

**Mónica Viviana Rodríguez Calvache**

In Partial Fulfillment of the
Requirements for the Degree of
**Master in Engineering**

Advisors:
Prof. José David López Hincapié, PhD.
Prof. Natalia Trujillo Orrego, PhD.

Field:
Bioengineering
Research Group:
Sistemas Embebidos e Inteligencia Computacional –SISTEMIC–

Universidad de Antioquia
Facultad de Ingeniería
Medellín, Colombia
2017

# Acknowledgments

I feel grateful because in the course of my master degree studies I was guided by many excellent researchers. I would like to express my deepest gratitude to my advisors PhD. José David López Hincapié and PhD. Natalia Trujillo Orrego, for their important support through the development of this thesis. Their scientific interest and knowledge made me go towards interesting research directions. A great thanks goes to Andrés Quintero Zea who invested his time to teach me a lot of fundamental knowledge during the realization and fulfillment of the objectives.

I am thankful to the project team, for their help in research and data collection; with special attention to: Sandra Trujillo, Stella Valencia, Diana Gómez, Leonardo Duque Muñoz and to the undergraduate students. Also, I thank my friends for being there for me.

Last but not least important, I would like to thank to my parents, my sister, my brother and to my boyfriend Luis Fernando Pulido, for being my greatest support and motivation to finish all of the projects that I have assumed in my life.

*Mónica Rodríguez Calvache*

This work was financially supported by the project *"Evaluación de la eficacia de modelos experimentales para la reintegración política y social de adultos con experiencia de combate en el marco del conflicto armado colombiano"*, Colciencias.

# Abstract

Reintegration is the process through which ex-combatants adapt to society after being part of an illegal armed group. Social reintegration process of ex-combatants is overshadowed because chronic exposure to violence changes their personality expression, social behavior, and cognition; and affects their emotional processing (EP). EP is necessary for the analysis of everyday situations and is affected by trauma exposition. Because of that, researchers suggest that the assessment of cognitive and behavioral profile on EP is crucial to characterize ex-combatants after chronic exposition to war. Furthermore, the characterization of EP will contribute to the design of cognitive trainings aimed to help ex-combatants on their reintegration process.

EP activates cortical and subcortical structures of the brain associated with the identification of valence of real live stimuli, faces and schematic objects. The study of EP has been performed with brain connectivity analysis, using computerized cognitive tasks synchronized with electroencephalography (EEG) recordings. Brain connectivity technique focuses on how the brain is processing the information in order to establish the pattern of activation required to generate a cognitive process. Atypical connectivity patterns represent a disruption on the connection among areas used for different kinds of processing.

This thesis focuses on the development of a methodology to recognize atypical functioning in EP of Colombian ex-combatants using brain connectivity analysis from scalp EEG recordings. For that purpose, at first, a model for preprocessing the EEG data and removing the artefactual components is developed. Secondly, the performance of five brain connectivity measures is compared: Correlation, Cross-Correlation, Coherence, Imaginary part of Coherency and the Phase-Lag Index; in order to analyze their advantages and drawbacks when tested on Colombian ex-combatants' EP related tasks data. Thereafter, using the proposed methodology the EP of ex-combatants is characterized. Finally, differences in EP of ex-combatants who received a social cognitive training intervention and those who did not receive it are analyzed.

**Keywords: Brain Connectivity, Colombian Ex-combatants, EEG, Emotional Processing.**

# Resumen

La reincorporación es el proceso mediante el cual los excombatientes se adaptan a la sociedad después de formar parte de un grupo armado ilegal. El proceso de reincorporación social de los excombatientes se dificulta debido a que la exposición crónica a la violencia modifica la expresión de la personalidad, el comportamiento social y la cognición; y afecta su procesamiento emocional (PE). El PE es necesario para el análisis de las situaciones cotidianas y se ve afectado por la exposición al trauma. Debido a esto, los investigadores sugieren que la evaluación del perfil cognitivo y conductual en PE es crucial para caracterizar a los ex combatientes después de la exposición crónica a la guerra. Además, la caracterización del PE contribuirá al diseño de entrenamientos cognitivos destinados a ayudar a los excombatientes en su proceso de reintegración.

El PE activa estructuras corticales y subcorticales del cerebro asociadas con la identificación de valencias de estímulos vivos reales, caras y objetos esquemáticos. El estudio de PE se ha realizado mediante el análisis de conectividad cerebral, utilizando tareas cognitivas computarizadas sincronizadas con registros de electroencefalografía (EEG). La técnica de conectividad cerebral se centra en cómo el cerebro procesa la información con el fin de establecer el patrón de activación requerido para generar un proceso cognitivo. Patrones de conectividad atípicos representan una interrupción en la conexión entre las áreas utilizadas para diferentes tipos de procesamiento.

Esta tesis se centra en el desarrollo de una metodología para reconocer el funcionamiento atípico en el PE de excombatientes colombianos utilizando análisis de conectividad cerebral a partir de grabaciones de EEG. Para ello, en primer lugar, se desarrolla un modelo para el preprocesamiento de los datos EEG y la eliminación de los componentes artefactuales. En segundo lugar, se compara el desempeño de cinco métricas comúnmente utilizadas: Correlación, Correlación Cruzada, Coherencia, Parte Imaginaria de la Coherencia y el Índice de Desfase; con el fin de analizar sus ventajas y desventajas cuando se utilizan en datos de las tareas de PE de los excombatientes colombianos. Entonces, utilizando la metodología propuesta el PE de los excombatientes es caracterizado. Por último, se analizan las diferencias en el PE de los excombatientes que recibieron una intervención de formación social cognitiva y aquellos que no la recibieron.

**Palabras clave: Conectividad cerebral, Excombatientes colombianos, EEG, Procesamiento Emocional.**

# Contents

# List of Figures

# List of Tables

# 1. Background

## 1.1. Introduction

Over the last 50 years, Colombia has been suffering from an internal armed conflict between the State and several illegal armed groups. Many deceases, disappeared people, drug traffic, poverty, closed to 6.000.000 forced internally displacement, kidnappings, the use of antipersonnel mines and around of 400.000 refugees are some of the consequences of the armed conflict in Colombia [1]. In order to end this conflict, the State established a demobilization policy. With this policy, thousands of Colombian ex-combatants have returned to civilian life, and that number is increasing after the signature of the peace agreements [2].

A pitfall in the social reintegration process is that chronic exposure to violence changes the expression of personality traits, social behavior, and cognition [3], and increases the incidence of Post-Traumatic Stress Disorder (PTSD) symptoms [4]. In this sense, it has been suggested that integration of behavioral assessments sync with electrophysiological techniques such as electroencephalography (EEG) is crucial for the comprehension of this complex phenomena. For instance, Emotional Processing (EP) is fundamental for the selection and implementation of adaptive/surviving strategies. This processing activates multiple sources of cortical and subcortical brain structures during the observation of visual stimuli with valence content [5].

In this work, the use of brain connectivity analysis is proposed to study the EP of Colombian ex-combatants. Brain connectivity refers to a pattern of structural-anatomical relations ("Structural Connectivity"), statistical dependencies on linear and nonlinear covariations ("Functional Connectivity"), or causal interactions ("Effective Connectivity") between neurons, neuronal populations or brain regions [6]. The functional connectivity is modified for life experiences. Then, it can be used to understand how these modifications might be disturbing the EP [7].

To analyze the EP of Colombian ex-combatants, thirty Colombian ex-combatants (Two female) from the government's Colombian Agency for Reintegration (ACR) program, and 20 Colombian individuals with no antecedents of being combatant (paired by gender, age and educational level) participated in the study. The participants performed an emotional recognition computerized task that used visual stimuli from the International Affective Picture

System (IAPS) [8], synchronized with EEG recordings. In general, these stimuli are able to generate emotional activation in a similar way of real conditions [9–11].

This work addresses the development of a methodology based on EEG signal preprocessing and brain connectivity analysis, aimed on analyzing the EP differential modulation of Colombian ex-combatants. Additionally, in order to determine the effectiveness of a training intervention, this methodology is used to analyze differences in EP of ex-combatants who received a Social Cognitive Training Intervention (SCTI) and those who did not receive it.

### 1.1.1. Motivation

EP is necessary to analyze everyday situations and to select and implement adaptive strategies [12]. EP of ex-combatants is affected by chronic exposure to violent events. In that sense, researchers suggest that the assessment of neurocognitive and behavioral profile on EP is crucial to characterize ex-combatants after chronic exposure to war. Furthermore, the characterization of EP can contribute to the design of social cognitive intervention trainings aimed to improve ex-combatants reintegration process.

Some neurophysiological methodologies provide biological markers of the impact of chronic exposure to combat. Brain connectivity analysis is proposed as a useful methodology to evaluate interconnected activation during EP [13, 14]. This technique focuses on how the brain processes the information in order to establish the pattern of activation required to generate a cognitive process [15]. In that sense, brain connectivity analysis can be meaningful to recognize how different interconnected structures are contributing to the expression of atypical modulation in emotional processing of Colombian ex-combatants.

### 1.1.2. Problem Statement

EP has been widely studied in veterans with the aim of analyzing the exposure to combat consequences on the mental health [16–20]. The Colombian armed conflict differs from other conflicts, particularly because of its chronicity, since it is a long-standing one. Thus, the study of the EP of ex-combatants provide information that would be useful to help them to improve their behavior, and to reintegrate into society.

Different techniques have been used to study the EP of Colombian ex-combatants [21–24]. Event-Related Potential technique was used to estimate the ex-combatants emotional valence attribution in [22]. In their analysis, the researchers only took into account the modulation in EEG patterns in response to stimuli [22–24].

In this work, brain connectivity analysis is proposed to evaluate EP of Colombian ex-combatants. Different neuroimaging techniques are useful to analyze the brain connectivity. Functional Magnetic Resonance Imaging (fMRI) offers a good spatial resolution about neural activation among specific brain regions. On the other hand, Magnetoencephalography (MEG) provides an excellent temporal resolution. However, those neuroimaging modalities are not practical for this study because they are expensive, they cannot be moved to rural locations, and they are not feasible for ex-combatants as they may have metal pieces in their bodies due to combat bullet wound or suffer claustrophobia.

Due to its noninvasiveness, portability, relatively low cost and its good temporal resolution, EEG is an optimal neuroimaging technique for studying brain dynamics in humans. However, the interpretation of the connectivity analysis performed at scalp level is difficult and error-prone, because any neurophysiological interpretation of EEG data is hindered due to volume conduction uncertainties. That is, each EEG channel is assumed to measures a linear mixture of neural and non-neural electrical sources whose activities are volume conducted to the scalp electrodes with broadly overlapping patterns [25,26]. Additionally, they are known to be contaminated by noise artifacts as eye blinking, eye movements (EOG), muscular contractions (EMG), cardiac signals (ECG) and environmental noise [27]. The artifacts must be removed in order to reduce misinterpretations [28].

Despite the problems mentioned above, it is important to know how interconnected cortical areas contributed to the expression of atypical functioning in the EP of ex-combatants. Then a question arises, is it possible to establish a methodology to characterize the EP of Colombian ex-combatants using a brain functional connectivity analysis?

## 1.2. Objectives

### 1.2.1. General

To develop a brain functional connectivity methodology focused on analyzing emotional processing from EEG data of Colombian Ex-combatants of illegal armed groups.

### 1.2.2. Specific

- To analyze the advantages and drawbacks in the theory and implementation of state-of-the-art techniques in brain connectivity analysis applied to EEG emotional processing tasks.

- To propose a brain connectivity methodology based on the characteristics of those techniques that provided better performance when tested on Colombian ex-combatant's

data.

- To validate the proposed methodology with emotional processing tasks applied to Colombian ex-combatants, by previously defining performance metrics to this context.

## 1.3. Outline

This work is divided into seven chapters. Chapter 2 contains the description of the psychological profile of Colombian ex-combatants and the definition of emotional processing. Additionally, it contains the theory related to EEG recordings and provides a review of brain connectivity analysis. Thereafter, the Chapter describes the research setting and provides a definition of the computerized task used in this study.

Chapter 3 describes each of the steps involved in the acquisition and the preprocessing of EEG data. This Chapter contains the description of the proposed methodology that we used to remove the artefactual components in the EEG signals. Additionally, the results of each the preprocessing step are illustrated over an EEG segment.

Chapter 4 presents a review of five functional brain connectivity metrics. Additionally, the Chapter contains a comparative performance analysis of these connectivity metrics for classifying the two groups (ex-combatants vs. control group).

Chapter 5 contains the description of our proposed methodology to find modulations in EP of Colombian ex-combatants. In this Chapter we present the results of the statistical analyses performed to find significant differences between both groups.

In Chapter 6, the proposed methodology was employed to find differences between the EP EEG data of ex-combatants after receiving a social cognitive training intervention, and those who did not receive it.

Finally, Chapter 7 provides the conclusions, the main contribution derived from this study, and the future work.

## 1.4. Publications

The following articles were published during the development of this work:

- M. Rodríguez-Calvache, A. Quintero-Zea, S. Trujillo, N. Trujillo, and J. López, "Classifying artifacts and neural EEG components using SVM," in Computational Intelligence

(LA-CCI), 2016 IEEE Latin American Conference on. IEEE, 2016, pp. 1-5.

- A. Quintero, M. Rodríguez-Calvache, S. Trujillo, F. Vargas, N. Trujillo, and J. López, "EEG Graph Analysis for identification of Ex-Combatants: A Machine Learning Approach," in Computational Intelligence (LA-CCI), 2016 IEEE Latin American Conference on. IEEE, 2016, pp. 1-6.

- A. Quintero-Zea, L. M. Sepúlveda-Cano, M. Rodríguez-Calvache, S. Trujillo, N. Trujillo, and J. López, "Characterization framework for ex-combatants based on eeg and behavioral features," in VII Latin American Congress on Biomedical Engineering CLAIB 2016, Bucaramanga, Santander, Colombia, October 26th-28th, 2016. Springer, 2017, pp. 205-208.

- S. Trujillo, S. Valencia, N. Trujillo, J. Ugarriza, J. López, M. Rodríguez-Calvache, J. Rendón, D. Pineda, A. Ibanez and M. Parra, " Atypical modulations of N170 component during emotional processing and their links to social behaviors in ex-combatants," Frontiers in Human Neuroscience, ol. 11, 2017. [Online]. Available: http://journal.frontiersin.org/article/10.3389/fnhum.2017.00244

# 2. Theory

## 2.1. Introduction

In this Chapter, a review of the concepts and techniques that are fundamental to the understanding of this thesis is provided. The chapter begins with the description of ex-combatant and their psychological profile, where the concept of emotional processing is explained. Thereafter, main concepts of EEG and the ways to obtain EEG recordings are described, as well as different techniques to analyze emotional processing using EEG signals, that is, event-related potentials and brain connectivity analysis. Finally, the research setting is reported.

## 2.2. Ex-combatant

In this work, an ex-combatant is a person who, after being part of an Illegal Armed Group (IAG), makes a personal or political decision to return to civilian life. According to official numbers provided by the ACR, by February 2017, 49.550 ex-combatants had started the process of reintegration with the ACR program. In total, 2.901 ex-combatants were people between 18 and 25 years old, 32.461 between 26 and 40 years old, 12.625 between 41 and 60 years old and 872 older than 60 years old. Additionally, 86,64% of the ex-combatants were men. In 2016 the number of active ex-combatants under ACR reintegration program were 15.043 [29].

### 2.2.1. Psychological Profile of Ex-combatants

The psychological profile of ex-combatants is characterized by poor social-affective cognition and behavior [30]. Recent studies of Colombian ex-combatants show that they have differences on the expression of social skills (this is better in ex-combatants [24]), on the empathic dispositions and also on the emotional recognition compared to civilian people [21–23, 30].

In the cognitive domain, ex-combatants level of education is about seven years, although some of them describe functional illiteracy. Also, a group of them exhibit deficits in the executive function [21]. In addition, it has been considered that military training also constraints autonomous thinking and increases the use of aggressive response to solve everyday live problems [30, 31]. Taken together, these findings suggest that the chronic exposition to

combat experiences increases the expression of the atypical socio-cognitive process specially on EP.

### 2.2.2. Emotional Processing (EP)

EP is a cognitive process based on the analysis of the positive or negative valence of stimuli or situations [32]. It is crucial for human adaptation and survival. The process starts when the subject identifies changes in external or internal circumstances that involve differences in valence, operating as a trigger situation [33]. EP facilitates a rapid response appropriate to the social context [34, 35].

Determining how ex-combatants are processing emotional information is crucial to provide an adequate intervention training. Thus, it is necessary to obtain quantifiable information, which in our case is achieved by analyzing EEG recordings.

## 2.3. Electroencephalography (EEG)

EEG consists of the recording of the electrical activity generated by the synchronized activity of thousands of mainly cortical neurons using electrodes attached to the scalp. EEG measures the difference between the potential at the location of interest (Sensors) to a reference point [36]. Due to its temporal resolution in the millisecond range and other properties such as noninvasiveness, portability and relatively low cost, EEG is a good technique for studying brain dynamics in humans [37]. The EEG is useful to identify problems such as sleep disorders, to evaluate the neural basis of changes in the behavioral patterns and in other cases to assess the activity of the brain after a head injury. EEG is a safety procedure, subjects do not feel any kind of electrical discharge on the scalp or in another part of the body.

EEG signals are known to be contaminated by noise artifacts. Generally, the artifacts can be divided into two groups: Environmental and physiological. Environmental noise can be caused by the power line noise (50/60 Hz), or by the movement of electrodes or cables during the EEG registration [27]. The most common physiological artifacts are perhaps those generated by the frontal and temporal muscles. This includes eyes blinking, eye movements (EOG), muscular contractions (EMG), cardiac signals (ECG) and pulsations. In addition, breathing in a rhythmic activity and muscle movement can cause alterations in the EEG signals. There are also artifacts caused by the skin, if there are deformities, such as scars, they can change the impedance [27].

As described, there are many types of artifacts, which are inevitable but must be removed in order to reduce misinterpretations in the analysis of these signals.

### 2.3.1. EEG recordings

The two most common ways to obtain EEG recordings are: resting state or task related procedures. The first strategy is used to study intrinsic activity of the brain [5]. Resting state data can help to diagnose diseases, cognitive impairments and disturbances in consciousness. However, resting state lacks of works reporting utility for studying specific variation of the emotional processing [38]. In the second strategy, the EEG recordings are obtained by evoking stimuli in the brain using specific tasks. This technique is known as Event-Related Potentials ERP [39]. Some ERP tasks are useful to stimulate the emotional process in the brain [40].

### 2.3.2. Event-Related Potentials ERP

Event Related Potential (ERP) is an electrophysiological activity measure sensitive to evaluate different processes such as emotional recognition. Its implementation takes place by syncing EEG recordings with an experimental cognitive task. ERPs are potentials of early (i.e., 100-300 ms) and late (i.e., 300-700 ms) latency of the mental processes. The latency is understood as the time between the association of the stimulus presentation and related brain responses. These potentials have been widely used in the study of normal functioning of the human brain, by providing a metric for comparing neurological and psychiatric conditions among subjects or groups. Thus, this comparison is obtained by observing the result of the synchronization of neuronal subpopulations in response to the processing of auditory, visual, or somatosensory stimuli [39].

## 2.4. Brain Connectivity Analysis

Interaction among brain regions within the nervous system have to be understood to explore the neural basis and mechanisms of any specific cognitive process. A tool to analyze these interactions is brain connectivity [41]. Brain connectivity refers to different interrelated aspects of the brain organization. It can be described at several levels: anatomical or structural, functional and effective connectivity. Fig. **2-1** illustrates the differences among the structural, functional and effective connectivity, which are explained in the following subsections.

### 2.4.1. Structural Connectivity

Structural, also called anatomical connectivity refers to the delineation and assessment of synaptic, axonal projections, or fiber pathways within certain group of neurons. Therefore, it describes the physical networks of anatomical links [42]. Structural connectivity can only be analyzed using structural Magnetic Resonance Imaging (sMRI).

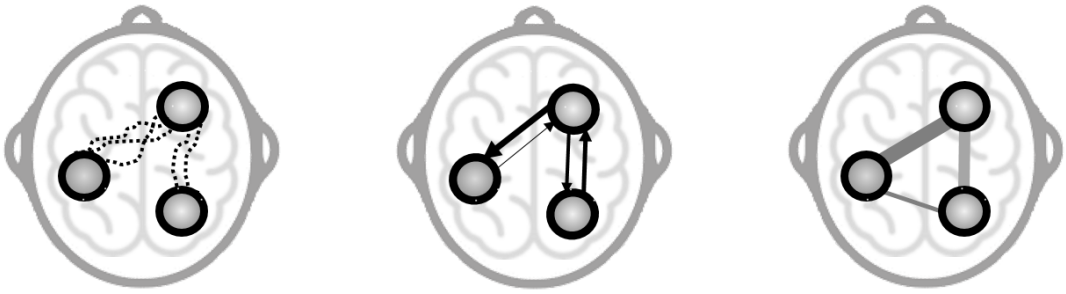

Structural Connectivity | Effective Connectivity | Functional Connectivity

Figure **2-1**.: Brain connectivity analysis is normally divided into three different categories. Structural connectivity (anatomical links among brain regions), effective connectivity (causal interactions among neurons or neuronal populations), and functional connectivity (statistical dependencies among neurons or neuronal populations).

### 2.4.2. Effective Connectivity

Effective connectivity describes the causal interactions among activated brain areas reflecting directional effects within a neuronal network. The directionality is usually determined by the temporal order of activation across the different brain regions [6].

### 2.4.3. Functional Connectivity

Functional connectivity is defined as the temporal dependency of neural activation patterns of brain areas. It does not include directionality information. It relies on statistical measures such as correlation, covariance, spectral coherence, or phase locking. Commonly, the computation of functional connectivity requires high temporal resolution, then it requires to use electromagnetic recording techniques such as MEG or EEG [6].

Functional connectivity is modified by life experiences [6, 43], this type of connectivity can be useful to understand how these contingencies might be disturbing the EP. Therefore, in this work we will focus on this type of brain connectivity analysis.

## 2.5. Volume conduction uncertainties

Neural activity is propagated through the head volume to electrodes at scalp level by the volume conduction [44, 45]. Volume conduction can lead to uncertainties for many but not

all connectivity analyzes. Uncertainties are due to the fact that the connectivity may reflect true interactions among electrodes or could be due to those electrodes measuring activity from a single brain source [45].

Volume conduction uncertainties are illustrated in Fig. **2-2**. Ideally, each electrode measures only the brain activity below them (See Fig. **2-2** Column A) and thus, connectivity among two electrodes reflects connectivity among two physically distinct brain regions. However, volume conduction uncertainties occurs for two principal reasons (See Fig. **2-2** (Columns B/C)):

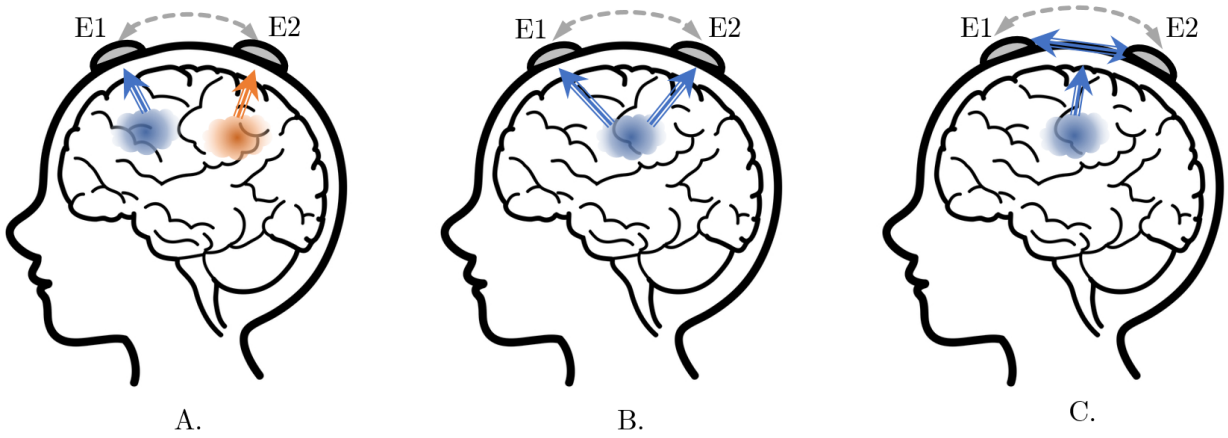


Figure **2-2**.: Volume conduction uncertainties. E1 and E2 represent two electrodes, colored clouds represent the sources of neural activity. Ideally, each electrode measures only neural activity below the electrode (A). Each electrode measures activity from two brain regions (B). Electrical fields can spread through the skull/scalp (C).

- Brain sources generate electromagnetic fields that are measured by more than one electrode (See Fig. **2-2** Column B) [45]. In Fig. **2-2**, the gray arrow between the electrodes illustrates measured connectivity, and the blue and orange arrows represent the electrical activity from the brain sources.

- Electrical fields spread through head tissues (skull, skin, etc.). Thus, they spread to neighboring electrodes causing further uncertainties for EEG connectivity analysis (See Fig. **2-2** Column C) [45].

There are several connectivity metrics and each metric is more or less affected by this phenomenon. In Chapter 4, these effects are discussed in more detail.

## 2.6. Research Setting

### 2.6.1. Participants

The ex-combatants that participated in this work were recruited through the ACR program. Fifty participants took part in the experiment, 30 Colombian ex-combatants (Two female) from the government's ACR program and 20 civilian people with no antecedents of being combatant (paired by gender, age and educational level). All the participants read and signed an informed consent before the beginning of the study. The study's procedures and informed consent were approved by the Bioethical Committee of the Faculty of Medicine from University of Antioquia, Medellin, Colombia.

None of the participants manifested to have psychiatric, neurological or drug abuse disorders. Demographic information is provided in Table **2-1** (M= Mean, SD= Standard Deviation). A Wilcoxon signed-rank test was performed in order to ensure consistency across groups for age, gender and educational level differences, $p$-values are reported in the last column of Table **2-1**.

Table **2-1**.: Descriptive statistics of demographic variables.

| | Ex-combatants n=30 | Civilians n=20 | $p$-values |
|---|---|---|---|
| Gender (female:male) | 2:28 | 2:18 | 0.678 |
| Age (years) | M=37.5 SD= 8.22 | M=36.15 SD=9.17 | 0.589 |
| Educational level (years) | M=10.33 SD= 3.10 | M=11.05 SD=2.14 | 0.373 |

### 2.6.2. Emotional Processing Experimental Task

Participants performed an emotional categorization task based on the International Affective Picture System (IAPS) [8]. The task aims providing a standardized group of real-life pictographic stimuli for use in experimental research. This system consists of a set of visual stimuli with a wide range of semantic categories (positive, negative and neutral), positive and negative images contain high emotional intensity. These visual stimuli generate emotional activation in a similar way to real conditions: induction of mental representations, psycho-physiological changes, and facial action [9].

The task was designed in the E-prime Software [46]. Participants were asked to categorize the stimulus displayed on a computer screen according to their valence, responding whether

the stimuli were positive, neutral or negative as quickly as possible. In total, 60 images were selected from the IAPS according to their Colombian validation [47]. The task was divided into four blocks. Each block consisted of 60 trials with images (20 positive, 20 neutral and 20 negative). Each stimulus was presented randomly per block, in total 240 stimulus were presented.

IAPS images were controlled in brightness, color and intensity. They were presented in a 17-inch screen, 60 cm apart from the participant. Fig. **3-1** shows the task sequence.

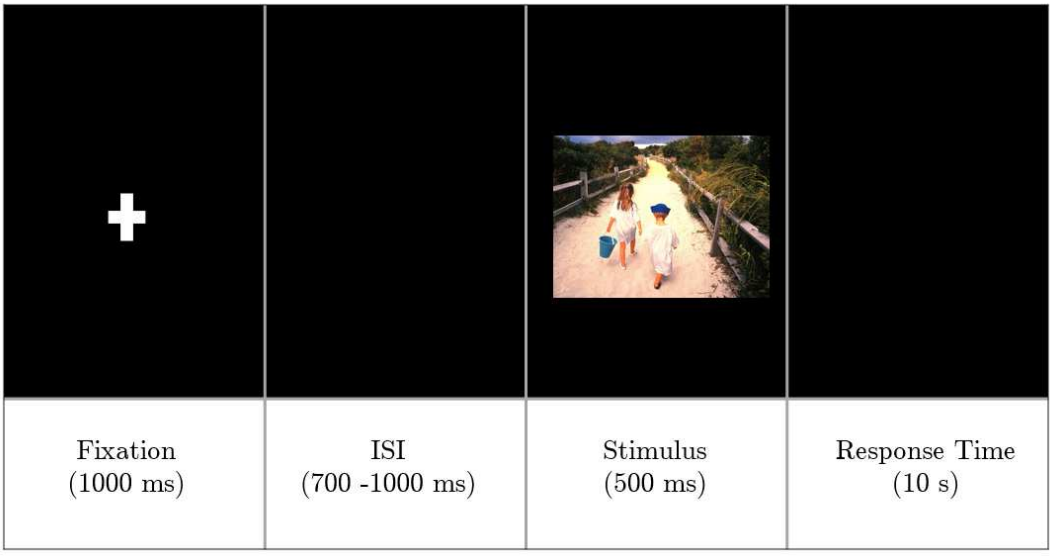


Figure **2-3**.: Stimulus design. The trial starts with a fixation cross, followed by a random Inter-stimulus Interval (ISI) between 700 and 1000 ms. The target stimulus is presented for 500 ms. Participants must response within 10 s.

The task sequence consists of four steps per trial as shown in Fig. **3-1**:

1. A fixation cross is presented for 1000 ms, in order to promote attentional focus on the center.

2. A random inter-stimulus interval ranging from 700 to 1000 ms. This avoids habituation and the prediction of the next stimulus presentation.

3. The stimulus. IAPS images with difference valence: positive, negative or neutral. This step has a duration of 500 ms.

4. A response time of maximum 10 s.

## 2.7. Summary

This Chapter described the main concepts used in this study for the characterization of EP of Colombian ex-combatants using brain connectivity analysis. Aspects of the psychological profile of ex-combatants were presented and an emotional task based on the IAPS (that is used in this work to generate emotion) is explained. Additionally, the definitions of EEG and different measures used to estimate cognitive processes from EEG recordings were presented. For instance, ERP was described as a classic measure used to evaluate different processes such as emotional recognition, and an overview about brain connectivity analysis and its categories: structural, effective and functional is provided.

As mentioned in this Chapter, before using EEG signals for any analysis, the removal of the artifactual noise is essential. The next Chapter describes the preprocessing stages developed in this work.

# 3. Preprocessing of EEG Emotional Processing Data

## 3.1. Introduction

EEG has been widely used in many fields such as clinical research, biomedical engineering, and cognitive science [48]. It is also known that cognitive tasks have been synchronized with EEG recordings in order to expand the evidence on how the brain performs the processing of emotional information. However, EEG signals are often contaminated by environmental noise and physiological factors commonly known as artifacts, which affect the quality of the signal. Then, the preprocessing of EEG signals is a crucial stage when analyzing any dataset.

This chapter describes the methodology used to preprocess the EEG data acquired. An automatic method was developed to classify between artifactual and neural components of EEG signals using Independent Component Analysis (ICA) and a Support Vector Machine (SVM). Additionally, this chapter contains the results of our proposed preprocessing methodology.

## 3.2. Data Acquisition

EEG data were acquired by the mental health (GISAME) research group of University of Antioquia. EEG registers were acquired with a 64-electrode NeuroScan EEG SynAmps2 amplifier [49] at a sampling rate of 1000 Hz and 24-bit resolution. The electrodes were placed according to the international 10-20 system [50, 51].

During the registration the participants performed the emotional categorization task based on IAPS described in the Section 2.6.2. Participants were seated in a comfortable chair in front of a computer monitor at a distance of 60 cm, located in a Faraday cage with the lights-off for guaranteeing isolated electric conditions (See Fig. **3-1**). Participants were asked to try not to blink, move, nor speak while performing the task. We use the software Scan 4.5 for recording the data [49]. Fig. **3-1** shows the position of the most important elements during the data acquisition.

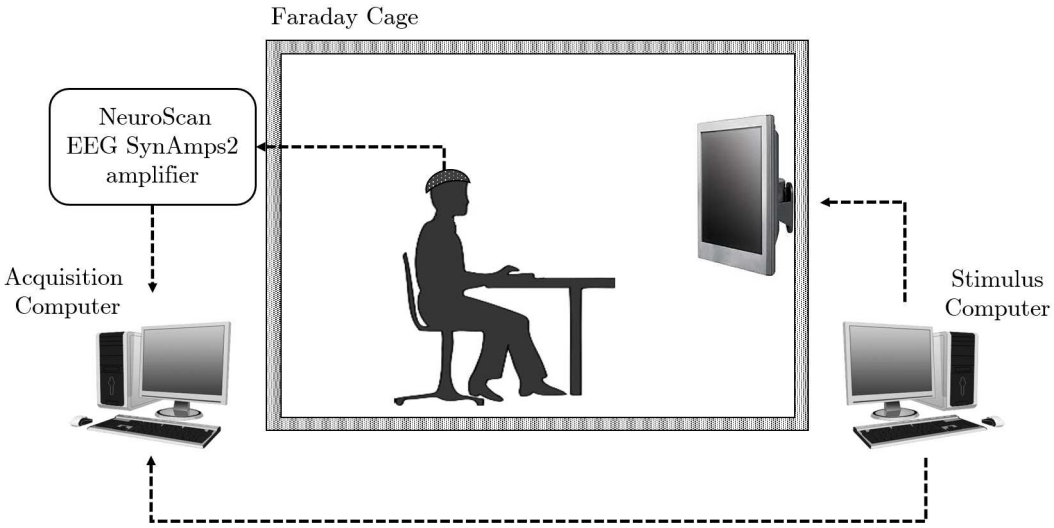


Figure **3-1**.: EEG acquisition scheme. Devices that may generate environmental artifacts were placed outside the Faraday cage

The impedances were maintained below 10 kΩ in order to obtain a good conductivity between the scalp and the electrodes. Fig. **3-2** shows the electrode impedances once they have been corrected. After correcting the impedances, EEG signals were recorded. EEG recordings were preprocessed with the EEGLab toolbox for MATLAB [52]. Fig. **3-3** shows a segment of one signal, the initial state over each of the sources (electrodes). It can be seen a lot of noise over the entire segment. The power line noise is identified as a low frequency periodic behavior throughout the signal.

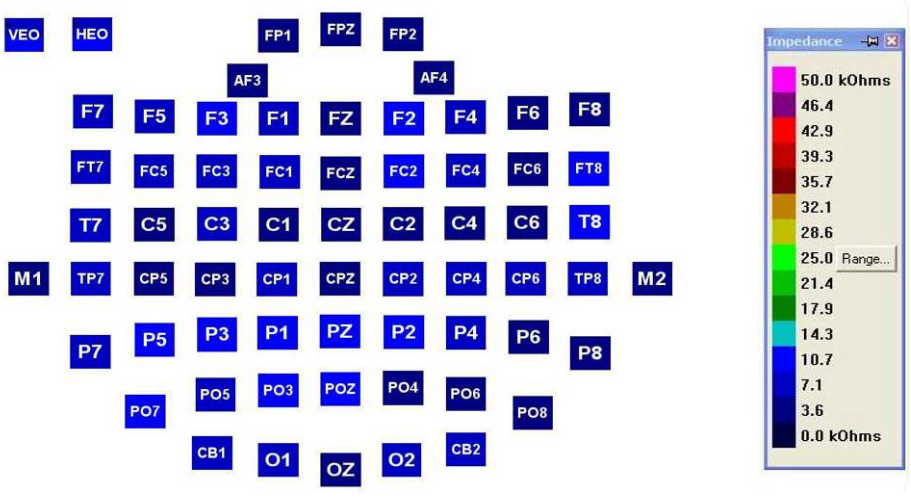


Figure **3-2**.: Impedances between the electrodes and the scalp. The colors that appear on the screen are in a range from an intense pink that indicates 50 kΩ to a gamma of blues that indicates that the impedance is below of 10 kΩ.

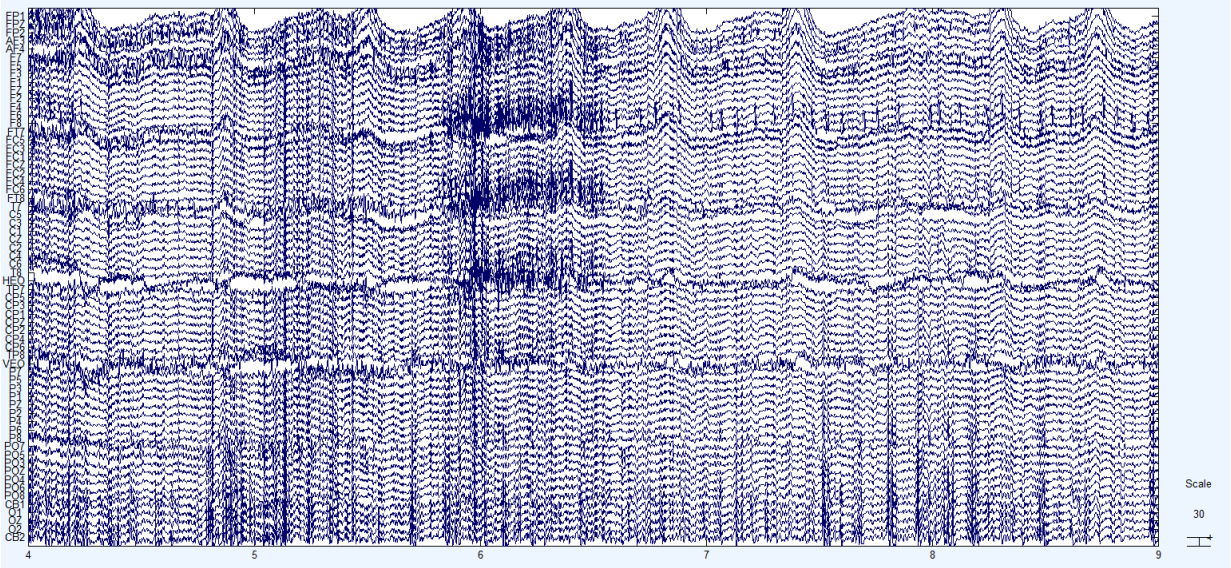


Figure **3-3**.: Section of an EEG recording. Showing time in $x$-axis and 64-channels in $y$-axis. The noise can be observed at all electrodes.

## 3.3. Downsampling

The first step in the preprocessing was to downsample the signal. The term downsampling refers to the process of reducing the sampling rate of a signal. In this case from 1000 Hz to 500 Hz. Downsampling was implemented using the `pop\_resample()` function from EEGLab Toolbox [52], which employs a zero-phase antialiasing filter prior to downsampling.

## 3.4. Off-line Re-reference

Second step is to re-reference the signals using a common reference for all the channels. In this case the EEG data was re-referenced to mastoids using `pop\_reref()` function from EEGlab Toolbox [52]. Fig. **3-4** shows the downsampling and the off-line re-reference results. In Fig. **3-4** we can observe the changes in the same portion of the signal in Fig. **3-3**. A reduction of noise can be observed as a result of re-referencing to mastoids process.

## 3.5. Filtering

To reduce environmental artifacts (power line noise) in the EEG data and to extract specific frequency bands associated with the human cognition, it is necessary to filter the signals before epoching or artifact removal. In this case a band-pass IIR digital filter was applied using `pop\_eegfilt()` function from EEGLab Toolbox [52]. The cutoff frequencies were 0.1

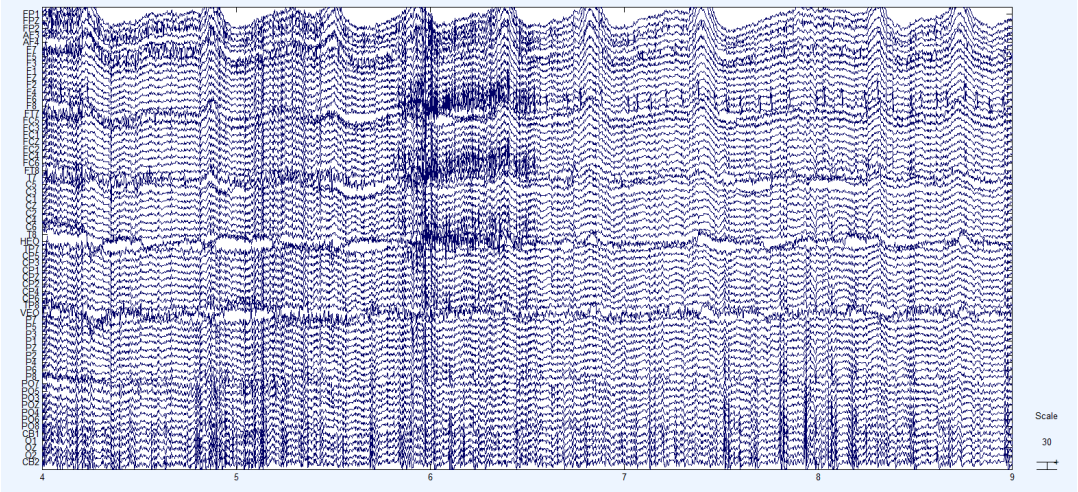


Figure **3-4**.: Section of an EEG recording. A decrease in the the signal noise can be observed for each of the sources (electrodes) after performing the downsampling and the off-line re-reference.

and 60 Hz and the order was 12. Fig. **3-5** shows the same portion of the signal of Fig. **3-4** at the same scale. A noise reduction, specially the elimination of power line noise can be seen once the filtering was performed.

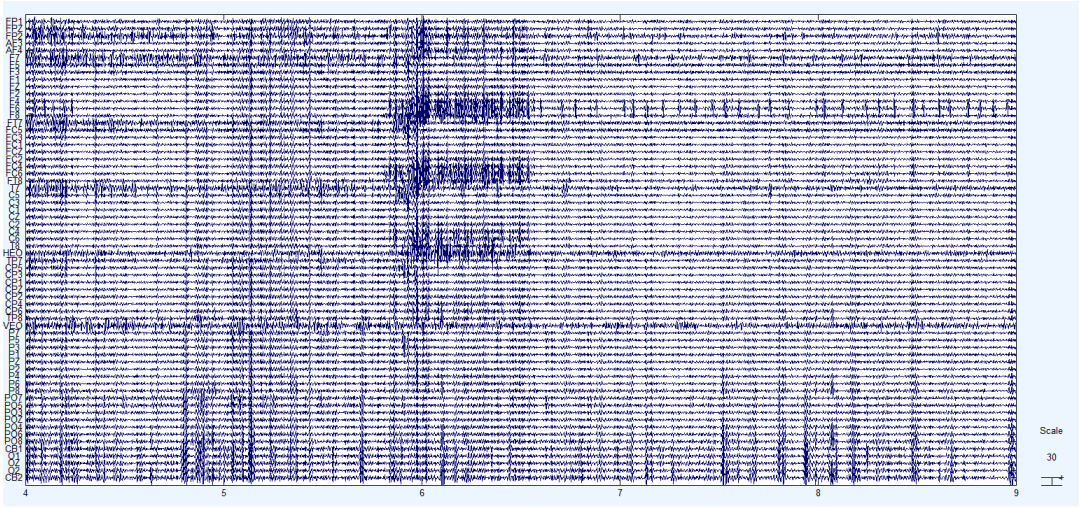


Figure **3-5**.: Section of an EEG recording. The behavior of the signal can be observed after performing the band-pass IIR filtering. Figure shows a decrease in the noise and the absence of power line noise.

Adittionally, in order to illustrate the effect of the digital filter on the frequency, an electrode was taken from the frontal region (FP1) and two spectrogram were created before (Fig. **3-6**) and after applying the filter (Fig. **3-7**), using the MATLAB `spectrogram` function.

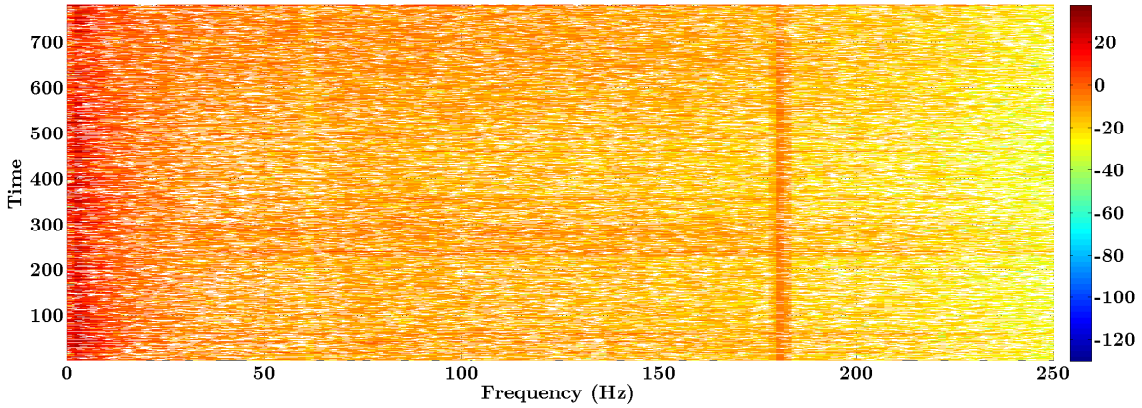


Figure **3-6**.: Spectrogram of one EEG recording before performing the band-pass IIR filtering. Figure shows that the power of the signal was distributed in all the frequencies.

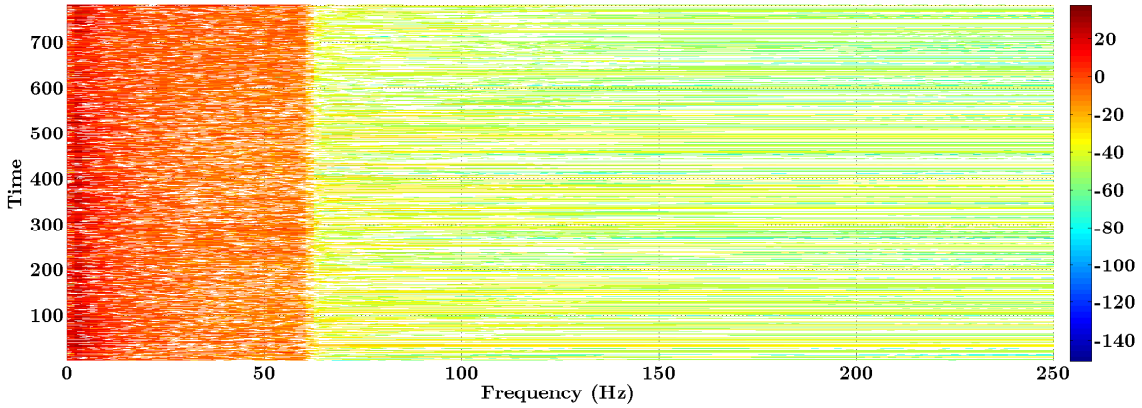


Figure **3-7**.: Spectrogram of one EEG recording after performing the band-pass IIR filtering. Figure shows that the power of the signal was distributed in the cutoff frequencies.

## 3.6. Artifacts and Neural Component Classification

As mentioned, EEG signals are contaminated by environmental and biological artifacts that must be removed in order to reduce misinterpretations. The hypothesis that an artifactual

component is statistically independent from the rest of the signals is widely accepted [53–56]. Therefore, the Independent Component Analysis (ICA) has been used to remove artifacts from EEG signals [57]. ICA results must be analyzed by an expert, who classifies each component individually. This inspection is slow and human error prone [28].

Then, here, we propose to use the Infomax ICA algorithm combined with C-SVM for classifying between neural and artifacts EEG components. This classifier would severely reduce the processing time. It is based on ICA and a robust technique to classify large datasets called Support Vector Machine (SVM). Another database of GISAME research group was used to train and validate the proposed approach. The database consists of the EEG recordings obtained from 32 subjects that performed an EP experimental task with the same protocol previously mentioned in the Section 2.6.2. The participants were 32 young university students (15 female, Mean=22 years old, STD=4 years). The exclusion criteria for the sample were history of neurological diseases and presence of visual impairments [28].

### 3.6.1. Independent Component Analysis (ICA)

ICA is a solution to the Blind Source Separation (BSS) problem. It consists in obtaining unmixed components of a mixed register. For the EEG signals, the model is an $n \times m$ system with same number of unmixed components (brain sources, $n = 1, 2, \ldots, N$) as observations (electrodes, $m = 1, 2, \ldots, M$), i.e., $N = M$. These unmixed components:

$$\mathbf{S}(t) = [\mathbf{s}_1(t), \mathbf{s}_2(t), \ldots, \mathbf{s}_N(t)]^\top, \quad t = 1, 2, \ldots, T, \quad \mathbf{S}(t) \in \mathbb{R}^{N \times T} \tag{3-1}$$

are independent in terms of variance and conform the original signal $\mathbf{X}(t) \in \mathbb{R}^{M \times T}$, where $T$ is the total number of the time samples in the register. Then, $\mathbf{X}(t)$ is a weighted sum or linear combination whose columns are computed as:

$$\mathbf{x}_i(t) = \sum_{j=1}^{N} a_{ij}\, \mathbf{s}_j(t), \quad i = 1, 2, \ldots, M, \quad \mathbf{x}_i(t) \in \mathbb{R}^T \tag{3-2}$$

where $a_{ij} \in \mathbb{R}^{M \times N}$, are real coefficients. The objective behind ICA is to estimate independent (in variance) components of the obtained data [58]. To achieve this, the first step is to estimate the matrix $\mathbf{A}$ (commonly known as mixed matrix) that contains the $a_{ij}$ elements. Thereafter, we compute the inverse of the matrix $\mathbf{A}$, called weighted matrix $\mathbf{W} \in \mathbb{R}^{M \times N}$ using the Infomax algorithm for ICA. Infomax is an algorithm proposed in [59] for BSS and consist in maximizing the output entropy for computing $\mathbf{W}$. Finally, the independent components are obtained with:

$$\hat{\mathbf{S}}(t) = \mathbf{W}\, \mathbf{X}(t). \tag{3-3}$$

This methodology is widely used in EEG because ICA allows decomposing the signals into different independent components. Some of them are expected to be sources of artifacts, while the others pure brain activity. Noise artifacts could be physiological or technical; all of them are assumed to be normal independent sources, *i.e.*, orthogonal variance components.

In this study, the infomax ICA algorithms are used from `pop\_runica()` function of EEGLab Toolbox to decompose the EEG signals [52]. The weights **W** from ICA provide the weights at each electrode. In case of EEG data, the ICA components are expected to be independent from each other, *e.g.*, eye blink, EOG, ECG or EMG. These weights give the scalp topography of each component, and provide evidence of their physiological origins [60, 61].

For each register, 64 components were generated and analyzed. Each component of the inverse weighted matrix is labeled by an expert as artifact or neural, depending on how its topography map looks like (such as in Fig. **3-8**). Fig. **3-8** illustrates the differences in topography of the features used for classification. Neural components are shown in the A and B columns of the figure, and artifactual components in the C and D columns.

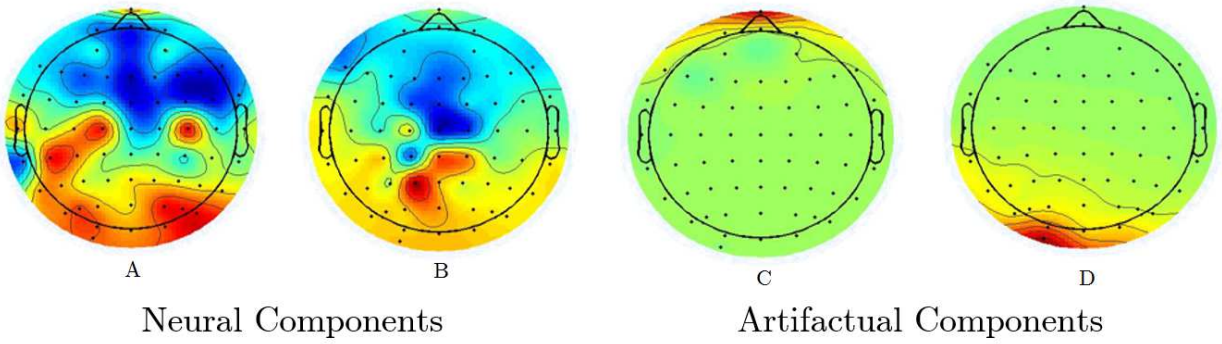


Figure **3-8**.: Topographic plots illustrating the differences between the ICA topographies containing artifactual and neural components. The third and forth columns contains eyes blinking and ECG artifactual components respectively.

A strong activation focused in the front of the head usually corresponds to eye blinking, such as the image shown in the C column of Fig. **3-8** [28]. In the ECG artifacts the activation is at the bottom of the D column of Fig. **3-8**. After the labeling process, the final database consisted of 1.574 neural and 474 artifact components.

### 3.6.2. Support Vector Machines (SVM)

Once the independent components are estimated, a SVM was used. SVM is a classifier developed on statistical learning theory by Vapnik [62] and modified by Cortes and Vapnik [63].

SVM is a type of supervised learning algorithms based on the idea of finding an optimal hyperplane to separate data points of two classes.

There are several studies reporting artefactual removal using BSS algorithms and SVM classifiers. In [64], the authors proposed a method to remove ocular artifacts (eye blinks and EOG) using the BSS Second-Order Blind Identification (SOBI [65]) algorithm and a SVM. They tested their classifiers using 200 independent components, 100 components which contains eye blinks and 100 free of artifacts components [64]. Additionally, in [66] a combination of two BSS algorithms with SVM was proposed to isolate EMG and EOG artifacts. In their study the authors evaluated one BSS algorithm (AMUSE [67]) and three ICA algorithms (JADE [68], Infomax [59] and FastICA [69]) to determine their artifact isolation capabilities. Then, four SVMs were trained with data recorded specifically for this purpose. The SVMs were all trained with a balanced database (equal number of artifacts and nonartifacts). After the selection of the best performing algorithms, they decided to work with a combination between AMUSE and Infomax.

Additionally, [70] presented a two stage artifact removal tool for EOG and EMG. In the first stage the classification of the EOG artifacts was done with the combination of AMUSE algorithm and SVM and in the second stage the classification of EMG was done with the Infomax algorithm and SVM. The database for training the SVMs contained 2000 samples, with one half being artifact-contaminated and the other half artifact-free.

Despite the aforementioned works exhibit classifiers with an accuracy up to 99%, they exclusively remove some physiological artifacts (See Table **3-4**). In some cases [64, 66, 70] authors train their SVM approaches with balanced databases, disregarding that artifacts and neural components are highly unbalanced. SVM (and in general any learning algorithm) is highly sensitive to unbalanced data, as they tend to classify all samples as belonging to the dominant class, which affects the accuracy. Then, in [71] the FastICA algorithm was used to decompose the EEG signals in independent components. The independent components were used as inputs to classify EOG and ECG artifacts using a weighted support vector machine C-SVM. C-SVM manage the unbalanced nature of independent components. SVM operation is shown as follows [72]:

Given the training dataset:

$$Z = \{(\mathbf{p}_i, q_i) \,|\, \mathbf{p}_i \in \mathbb{R}^n,\, q_i \in \{-1, 1\}, i = 1, 2, \ldots, m\} \tag{3-4}$$

where $\mathbf{p}_i$ is a data vector and $q_i$ is the corresponding output. The problem is to find the optimal hyperplane which divides the group of points $\mathbf{p}_i$ depending on the desired output. Here, it is intended to maximize the distance between the hyperplane and the nearest point

$\mathbf{p}_i$ of any of the groups. Any hyperplane can be written as the set of points $\mathbf{p}_i$ satisfying $\mathbf{w}^\top \mathbf{p} + b = 0$, where $\mathbf{w}$ is a vector normal to the hyperplane and $b$ is the bias of the hyperplane.

If the training dataset are linearly separable, it is possible to find two parallel hyperplanes that divided the two classes, in which the distance between the classes is maximum. The region between these two hyperplanes is called the 'hard margin'. The hyperplane that divides the region into two equal parts is called 'maximum-margin hyperplane'. For finding the maximum-margin hyperplane it is necessary to solve the following optimization problem:

$$\underset{\|\mathbf{w}\|}{\text{minimize,}} \text{ subject to: } q_i(\mathbf{w}^\top \mathbf{p_i} + b = 0) \geq 1, \text{ for } i = 1, \ldots, m. \tag{3-5}$$

The maximum-margin hyperplane is defined by the $\mathbf{p}_i$ which lie nearest to it. These $\mathbf{p}_i$ are called support vectors. This problem of constrained optimization corresponds to a problem of quadratic programming and is approachable by the theory of optimization. This theory establishes that a problem of optimization called 'primal' has a 'dual' form if the function to be optimized and the constraints are strictly convex functions. In these circumstances, solving the dual problem allows to obtain the solution of the primal problem. However, the problem is impractical because the real problems that are usually characterized have imperfect data and linearly not separable.

In those cases, in which some dataset are not completely linearly separable, it is required to introduce a set of positive real variables $\xi_i$ called slack variables. Each $\xi_i$ is a slack variable that stands for the distance from $\mathbf{p}_i$ to the hyperplane and allows to quantify implicitly the number of non-separable cases that it is admitting, that is:

$$q_i(\mathbf{w}^\top \mathbf{p_i} + b) \geq 1 - \xi_i, \quad \xi_i \geq 0, \ i = 0, \ldots, m. \tag{3-6}$$

The sum of all the slack variables $\sum_{i=1}^{m} \xi_i$ allows us to measure the cost associated with the number of non-separable cases. The higher this sum, the greater the number of non-separable cases. According to the Eq. (3-6), it is no longer possible to propose a single aim to maximize the margin, because we could do it at the cost of misclassifying too much data. Therefore, the optimal hyperplane can be formulated as the following optimization problem:

$$\begin{aligned} \underset{\mathbf{w},b,\xi}{\text{minimize}} \quad & \frac{1}{2}\|\mathbf{w}\|^2 + C\sum_{i=1}^{m} \xi_i, \\ \text{subject to} \quad & q_i(\mathbf{w}^\top \mathbf{p}_i + b) \geq 1 - \xi_i, \\ & \xi_i \geq 0, \ i = 1, \ldots, m, \end{aligned} \tag{3-7}$$

where $C$ is the penalty factor. The defined hyperplane is called 'soft margin' hyperplane. To transform the original optimization problem ('primal' problem) to its 'dual' form at a firs step, we have to obtain the Lagrangian function:

$$L(\mathbf{w}, b, \xi, \alpha, \beta) = \frac{1}{2} \|\mathbf{w}\|^2 + C \sum_{i=1}^{m} \xi_i - \sum_{i=1}^{m} \alpha_i [q_i(\mathbf{w}^\top \mathbf{p_i} + b) + \xi_i - 1] - \sum_{i=1}^{m} \beta_i \xi_i \tag{3-8}$$

Second step consist into apply Karush-Kuhn-Tucker (KKT) conditions:

$$\frac{\partial L}{\partial \mathbf{w}} \equiv \mathbf{w} - \sum_{i=1}^{m} \alpha_i q_i \mathbf{p_i} = 0 \tag{3-9}$$

$$\frac{\partial L}{\partial b} \equiv \sum_{i=1}^{m} \alpha_i q_i = 0 \tag{3-10}$$

$$\frac{\partial L}{\partial \xi_i} \equiv C - \alpha_i + \beta_i = 0, \quad i = 1, \ldots, m \tag{3-11}$$

$$\alpha_i [1 - q_i(\mathbf{w}^\top \mathbf{p_i} + b) + \xi_i] = 0, \quad i = 1, \ldots, m \tag{3-12}$$

$$\beta_i \cdot \xi_i = 0, \quad i = 1, \ldots, m \tag{3-13}$$

Finally, the dual problem is formalized:

$$\begin{aligned} &\text{maximize} \sum_{i=1}^{m} \alpha_i - \frac{1}{2} \sum_{i,j=1}^{m} \alpha_i \alpha_j q_i q_j (\kappa(\mathbf{p}_i, \mathbf{p}_j)) \\ &\text{subject to} \sum_{i}^{m} \alpha_i \, q_i = 0, \\ &\qquad 0 \leq \alpha_i \leq C, \, i = 1, \ldots, m \end{aligned} \tag{3-14}$$

Solving the optimization problem for quasi-linearly separable problems (Eq. (3-14)) will allows to express the optimal separation hyperplane in terms of $\alpha$. However, the optimization

problem obtained is not directly applicable when the database is non-linearly separable. To solve these problems, it is necessary to convert it into the following Lagrangian dual problem:

$$\begin{aligned} \underset{\alpha}{\text{minimize}} \quad & \frac{1}{2}\sum_{i=1}^{m}\sum_{j=1}^{m} q_i\, q_j\, \alpha_i\, \alpha_j\, \kappa(\mathbf{p}_i, \mathbf{p}_j) - \sum_{j}^{m} \alpha_j \\ \text{subject to} \quad & \sum_{i}^{m} \alpha_i\, q_i = 0, \\ & 0 \leq \alpha_i \leq C,\, i = 1, \ldots, m \end{aligned} \tag{3-15}$$

where $\kappa(\mathbf{p}_i, \mathbf{p}_j)$ represents a kernel function $\kappa : \mathbb{X} \times \mathbb{X} \to \mathbb{R}$. The kernel is a function that assigns to each pair of elments of the input space, $\mathbb{X}$, a real value corresponding to the scalar product of the images of those elements in a new space. This function allows to work in a high-dimensional space without the requirement of computing the coordinates of the data in that space. The decision function finally becomes:

$$f(\mathbf{p}) = \text{sgn}\left(\textstyle\sum_{i}^{m} \alpha_i\; q_i\, \kappa(\mathbf{p}_i, \mathbf{p}) + b\right) \tag{3-16}$$

In this case, the vectors $\mathbf{p}_i$ with $\alpha_i > 0$ are the support vectors. Any function that satisfies Mercer's theorem can be used as a kernel function [73]. In this work we used three types of kernels:

$$\begin{aligned} &\text{The sigmoid: } \kappa(\mathbf{u}, \mathbf{v}) = \tanh\left(\gamma \mathbf{u}^{\top} \mathbf{v}\right) \\ &\text{The polynomial: } \kappa(\mathbf{u}, \mathbf{v}) = \left(\gamma \mathbf{u}^{\top} \mathbf{v}\right)^{d}, \text{with values of } d = 2, 3 \\ &\text{The Gaussian (or radial basis): } \kappa(\mathbf{u}, \mathbf{v}) = \exp\left(\gamma \left\|\mathbf{u} - \mathbf{v}\right\|^2\right) \end{aligned} \tag{3-17}$$

For model selection of the C-SVM classifier, the penalty factor $C$ and the parameter $\gamma$ of the kernels must be tuned by minimizing the estimated generalization error.

The C-SVM was implemented in MATLAB version 8.5 (R2015a) using the libsvm library [74]. The classification performance of four C-SVM designs with different Kernels (Sigmoid, Polynomial degree 2, Polynomial degree 3 and Radial Basis Function -RBF-) were compared to find the best fitted model. The C-SVM performances were obtained using k-fold cross-validation with 10 folds for each case. The performances of the classifiers were evaluated using the following metrics: sensitivity – True Positive Rate (TPR), specificity – True Negative

Rate (TNR), and accuracy (ACC).

$$\begin{aligned} \text{TPR} &= \frac{\text{TP}}{\text{TP} + \text{FN}} \times 100\% \\ \text{TNR} &= \frac{\text{TN}}{\text{FP} + \text{TN}} \times 100\% \\ \text{ACC} &= \frac{\text{TP} + \text{TN}}{\text{TP} + \text{FN} + \text{FP} + \text{TN}} \times 100\% \end{aligned} \tag{3-18}$$

For this, the artifacts components were the positive condition and the neural components were the negative one.

## 3.7. Epoching and Baseline Correction

After identifying the artifactual independent components, they were removed and the original configuration (64-channel EEG) of the signals were reconstructed. Then, the registers were segmented from 200ms and 800ms prior and after the stimulus, respectively. For each epoch, also called trial, the stimulus are recognized in the EEG registers as numbers which correspond to each valence of images, for the emotional processing task the conditions are negative, neutral and positive respectively.

The baseline correction was performed by subtracting the mean of the signal during the time window from 200 to 0ms prior to the stimulus. Epoching and baseline correction were performed using the EEGLAB's `pop\_epoch()` function.

## 3.8. Visual Noise Rejection

Each trial was inspected for leftover noise in the signals to make sure only clean segments go forward for later analysis. Finally, four electrodes (HEO, VEO, CB1 and CB2) were excluded as they did not record neural activity. Fig. **3-9** shows the rejecting of an epoch by visual inspection. In the Fig. **3-9** it is possible to identify the segment contaminated in green, because there is an irregular peak which is marked in the green box. The rest of the signal does not have more visible anomalies.

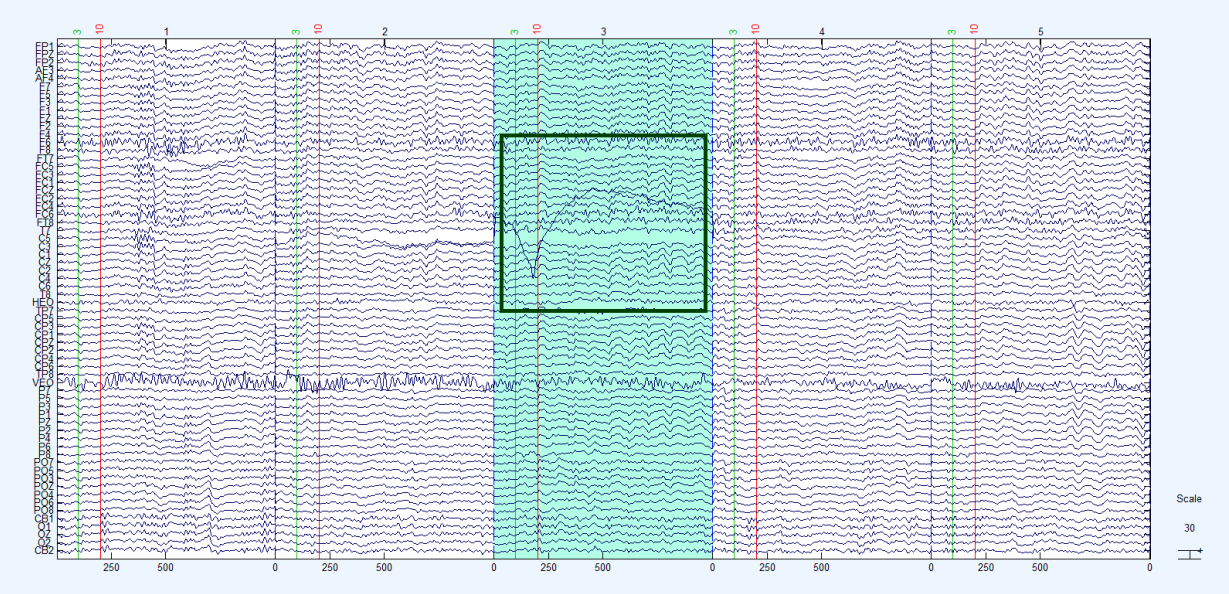


Figure **3-9**.: Selection of noisy segments. Highlighted in green, it can be seen a segment with an abnormal peak.

## 3.9. Results

In this Section, the results of the artifacts and neural components classification are showed. Also, the result of the all preprocessing steps is illustrated.

### 3.9.1. Artifacts and Neural Component Classification

Different weights to the penalty factor $C$ were assigned for each class depending on the number of data per class, to compensate the unbalance in the data. Thereafter, the obtained database is divided for SVM training (90%) and final testing (10%) maintaining unaltered the unbalance among classes.

The weight of C for the positive condition (or class 1) was:

$$W_1 = \frac{\text{neural components}}{\text{total components}} = 0.768 \tag{3-19}$$

and the weight of the negative condition (or class 0) was:

$$W_0 = \frac{\text{artifactual components}}{\text{total components}} = 0.231 \tag{3-20}$$

A grid search was performed with the training database to find the best parameters ($C$ and $\gamma$) for the C-SVM classification with the different Kernels Eq. (3-17). We used cross-validation with 10 folds for each case.

Table **3-1** provides the results for the model selection for every kernel used in the C-SVM.

Table **3-1**.: Grid search results for $C$ and $\gamma$.

| **Kernel Type** | Best $C$ | Best $\gamma$ |
|---|---|---|
| Sigmoid | 2408 | 1.220E-04 |
| Polynomial degree 2 | 0.03 | 0.5 |
| Polynomial degree 3 | 0.125 | 0.0313 |
| Radial Basis Function | 0.693 | 2.32 |

Table **3-2** summarizes the classification results. These results demonstrate that the C-SVM with RBF Kernel outperformed the other three models in specificity and accuracy, while the C-SVM with Polynomial degree 2 Kernel outperformed the others in sensitivity.

Table **3-2**.: Training results with best fitted parameter values after a grid search with C-SVM.

| **Kernel Type** | TNR (Conf. Interval) | TPR (Conf. Interval) | ACC (Conf. Interval) |
|---|---|---|---|
| Sigmoid | 88.50% (87.00% - 89.90%) | 73.60% (71.50% - 75.60%) | 77.10% (75.10% - 79.00%) |
| Polynomial degree 2 | **96.00%** (95.00% - 96.80%) | 87.50% (85.90% - 89.00%) | 89.50% (88.00% - 90.80%) |
| Polynomial degree 3 | 92.50% (91.20% - 93.70%) | 94.80% (93.60% - 95.70%) | 94.30% (93.10% - 95.30%) |
| Radial Basis Function | 89.20% (87.70% - 90.60%) | **99.20%** (98.70% - 99.60%) | **96.90%** (96.00% - 97.60%) |

The designed models were validated with data not used in training. The validation dataset consisted of 47 artifact components and 157 neural components. Table **3-3** summarizes the results for each C-SVM design.

Table **3-3**.: ICA - C-SVM validation results

| **Kernel Type** | TNR (Conf. Interval) | TPR (Conf. Interval) | ACC (Conf. Interval) |
|---|---|---|---|
| Sigmoid | 87.20% (85.50% - 88.60%) | 74.50% (72.50% - 76.50%) | 77.50% (75.40% - 79.30%) |
| Polynomial degree 2 | 80.90% (78.90% - 82.60%) | 75.20% (73.20% - 77.20%) | 76.50% (74.50% - 78.40%) |
| Polynomial degree 3 | 87.20% (85.50% - 88.60%) | 94.30% (93.10% - 95.30%) | 92.60% (91.30% - 93.80%) |
| Radial Basis Function | **87.20%** (85.50% - 88.60%) | **98.10%** (97.30% - 98.70%) | **95.60%** (94.50% - 96.40%) |

The results in Tables **3-2** and **3-3** show that the model with the better performance is the C-SVM with RBF Kernel, with 95.6% of accuracy in validation. This result was consistent with the training results (96.9%).

The performance results obtained with the RBF C-SVM are comparable to other works in the literature [64, 66, 70, 71] described in Section 3.6.2. Table **3-4** compares the accuracy obtained with the proposed approach with the state-of-the-art methods.

Table **3-4**.: Comparison between the proposed method and four benchmark methods.

| **Classifier** | **Reported accuracy** | **Physiological rejected artifacts** |
|---|---|---|
| Proposed ICA-CSVM [28] | 95.60% | Eye Blink, EOG, ECG, EMG |
| SOBI SVM [64] | 92.00% | Eye Blink, EOG |
| AMUSE-ICA SVM [66] | (91.51% - 99.62%) | Eye Blink, EOG, EMG |
| ICA- CSVM [71] | 95.67% | EOG, ECG |
| AMUSE-ICA SVM [70] | 90.00% | EOG, EMG |

As described in Section 3.6.2, the authors of the related works used their classifiers with two or more SVM to reject the physiological artifacts, between ocular artifacts or muscular artifacts. We try to use the features presented in the images of the components in order to discriminate four kinds of physiological artifacts using only one SVM. Additionally, our

proposed method was the combination of the best ICA algorithm selected in [66] and C-SVM to deal with the unbalanced databases. Our approach has the advantage of only using the ICA weights as features to train the model, *i.e.*, it was not necessary to use more than one C-SVM to discriminate artifacts from neural components on EEG recordings. This characteristic provides robustness and repeatability to the method.

The final preprocessing results are shown in Fig. **3-10**. Fig. **3-10** shows that there are no abrupt changes or large peaks along the section of the signal that was selected as example to this Chapter.

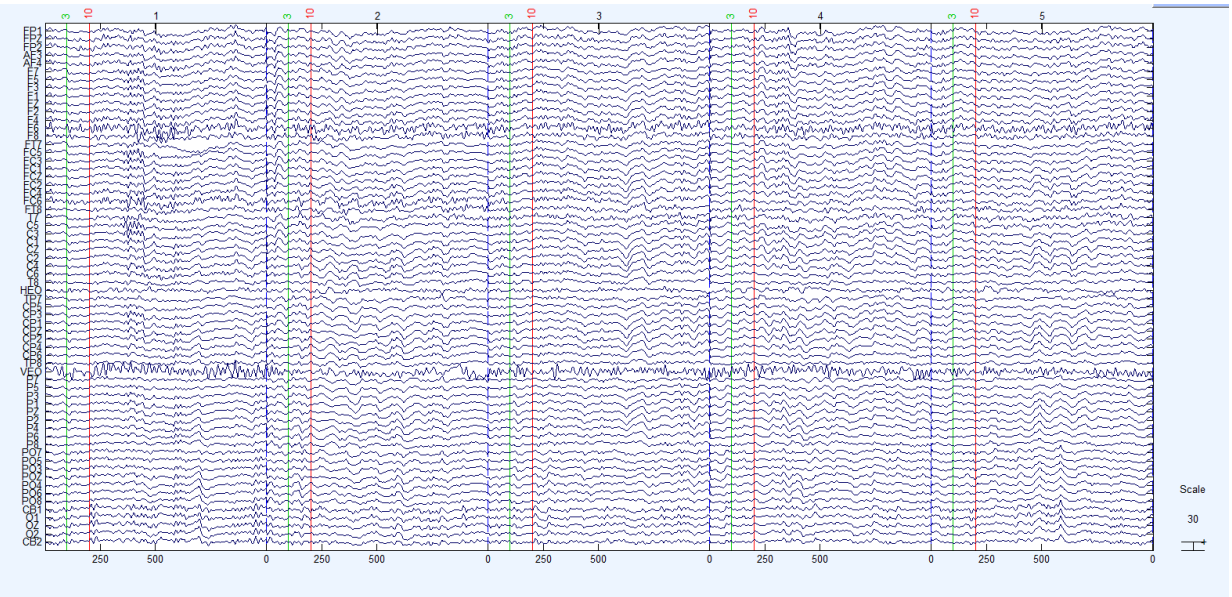


Figure **3-10**.: Results of the pre-processing. A clear reduction in the initial noise can be observed in all electrodes along the whole segment.

## 3.10. Summary

In this Chapter, a methodology for preprocessing EEG data was developed. The first step was to downsample the signal to 500 Hz, followed by a re-reference to the mastoids and a band-pass filtering from 0.1 to 60 Hz.

Additionally, an ICA – C-SVM classifier was developed to discriminate artifactual from neural components on EEG recordings. The proposed methodology uses the columns of the inverse matrix obtained from the ICA decomposition of each EEG signals. The proposed approach was tested with real EEG recordings from a visual attention study. Results show that the proposed approach has the ability to isolate the artifactual components with high

accuracy, and it can eliminate physiological and external noise from the EEG signals. The model that best classified artifacts and neural components was a weighted C-SVM with RBF Kernel. the proposed methodology outperforms similar methodologies proposed in the literature, mainly because it only takes into account a reduced set of features extracted from the ICA decomposition of the signals.

The artifactual free signals were segmented into three tasks conditions, and a baseline correction was performed. Finally, a visual artifact inspection was performed in order to eliminate the leftover noise present in the segmented data.

# 4. Selection of The Connectivity Metric

## 4.1. Introduction

Functional connectivity has been employed to evaluate EP of clinical populations with psychiatric disorders such as autism [75, 76] or schizophrenia [77, 78]. Additionally, functional connectivity has been used in the analysis of EP in adolescent depression [13, 14]. Thus, it is suggested that functional connectivity analysis can be useful for the evaluation of the EP of subjects without clinical conditions but with special characteristics, such as the exposure to an armed conflict.

The main objective of this Section is to select a functional connectivity metric. To achieve this, an explanation about how five of these connectivity metrics work is provided. Additionally, the brain regions of interest for this work were selected. Finally, the performances of the functional connectivity metrics when classifying the EP of both groups (ex-combatants vs. civilian people) were compared.

## 4.2. Metrics for functional connectivity analysis

There are several connectivity metrics used to estimate how different brain areas are working during an experimental task. Functional connectivity is assessed by metrics that find the existence of any type of covariance between two neurophysiological signals without providing any causal information. In the next subsections five metrics divided into three different categories are described (see Fig. **4-1**).

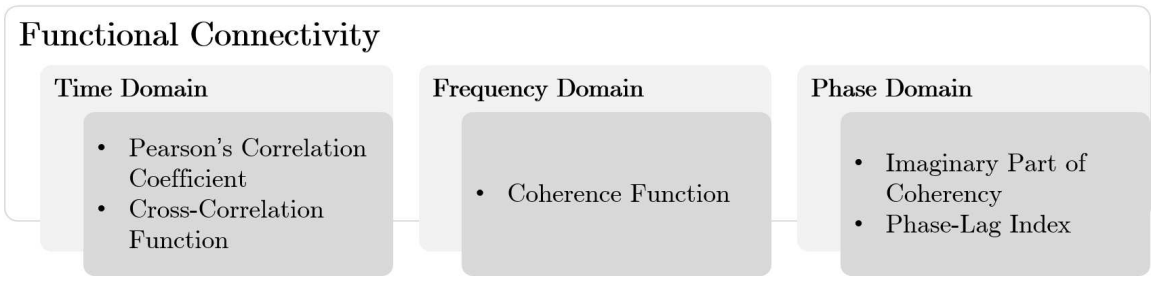


Figure **4-1**.: Functional connectivity metrics are divided into three categories. Metrics that are computed from the time, frequency or phase domain of the EEG signals.

As shown in Fig. **4-1**, functional connectivity metrics are not represented only in the frequency domain. Then, before performing some functional connectivity analysis, it is necessary to extract specific frequency bands associated with human cognition. Five frequency bands of the preprocessed EEG signals were filtered:

- Delta (0.10Hz-3.99Hz).
- Theta(4.00Hz-7.99Hz).
- Alpha (8.00Hz-13.99Hz).
- Beta (14.00Hz-29.99Hz).
- Gamma (30.00Hz-59.9Hz).

The Delta rhythms are slow waves which characterized the EEG during the stages of deep sleep. Its amplitude increases in sleep-deprived subjects and markedly in children. However, in an awake adult, the presence of these waves is associated with pathological disorders [79]. The Theta waves are predominant during somnolence and in the early stages of sleep. Although they have also been recorded during tasks involving functional memory [80]. In an awake and relaxed subject, the Alpha waves are mainly recorded in the occipital areas and are associated as a characteristic rhythm of the inactive state and their activity can be blocked by opening and moving the eyes, evoking an image or performing a mental activity [80]. Beta waves are faster waves, dominant in the EEG of an adult awake and with eyes open. The amplitude of these waves decreases when imagining movements and is prominent during anticipation of an event [81]. Activity higher than 30 Hz is called Gamma rhythm and is related to attention, response to certain sensory stimuli and processes involving short-term memory [82].

### 4.2.1. Pearson's Correlation Coefficient (COR)

Pearson's correlation coefficient is a commonly used correlation metric. COR is defined as the covariance of two signals scaled by their corresponding variance and measures the temporal linear correlation between them. If $\mathbf{x}(t) \in \mathbb{R}^{T_e}$ and $\mathbf{y}(t) \in \mathbb{R}^{T_e}$ are EEG signals at two different electrodes, and $T_e$ the number of time samples per each epoch (trial), the COR between them $r_{xy}$ is defined as:

$$r_{xy} = \frac{\sum_{t=1}^{T_e}(\mathbf{x}(t) - \bar{x})(\mathbf{y}(t) - \bar{y})}{\sqrt{\sum_{t=1}^{T_e}(\mathbf{x}(t) - \bar{x})^2 \sum_{t=1}^{T_e}(\mathbf{y}(t) - \bar{y})^2}}, \quad t = 1, 2, \ldots, T_e \tag{4-1}$$

Where $\bar{x}$ is the sample mean of $\mathbf{x}(t)$:

$$\bar{x} = \frac{1}{T_e} \sum_{t=1}^{T_e} \mathbf{x}(t) \tag{4-2}$$

and analogously for $\bar{y}$. The result of computing $r_{xy}$ is a scalar value at a given time window. For zero mean and unit variance signals, $r_{xy}$ is defined as:

$$r_{xy} = \frac{1}{T_e} \sum_{t=1}^{T_e} \mathbf{x}(t)\, \mathbf{y}(t) \tag{4-3}$$

The range of COR is -1 $\leq r_{xy} \leq$ 1. When $r_{xy}$=-1, signals $\mathbf{x}(t)$ and $\mathbf{y}(t)$ have complete linear inverse correlation. If $r_{xy}$=0, the signals have no linear interdependence, while $r_{xy}$=1 means complete linear direct correlation between the two signals. Therefore, higher correlations indicate stronger functional connection between the related signals.

### 4.2.2. Cross-Correlation function (XCOR)

Cross-Correlation is the cross-covariance of two EEG signals $\mathbf{x}(t) \in \mathbb{R}^{T_e}$ and $\mathbf{y}(t) \in \mathbb{R}^{T_e}$ at two different electrodes, scaled by the variance of each one of them [83]. With $T_e$ the number of time samples per trial, the XCOR measures the linear correlation between the signals as a function of time:

$$C_{xy} = \frac{\sum_{t=1}^{T_e-\tau} (\mathbf{x}(t-\tau) - \bar{x})(\mathbf{y}(t) - \bar{y})}{\sqrt{\sum_{t=1}^{T_e-\tau} (\mathbf{x}(t) - \bar{x})^2 \sum_{t=1}^{T_e-\tau} (\mathbf{y}(t) - \bar{y})^2}}, \quad t = 1, 2, \ldots, T_e - \tau \tag{4-4}$$

where $\bar{x}$ and $\bar{y}$ are the sample mean of $\mathbf{x}(t)$ and $\mathbf{y}(t)$ respectively, and $\tau$ is the time lag that is determined by the argument of the maximum XCOR:

$$\tau = \arg\max_{t}(C_{xy}) \tag{4-5}$$

When $\tau$ =0, XCOR is equal to the Pearson's correlation coefficient. For zero mean and unit variance signals, it is defined as:

$$C_{xy} = \frac{1}{T_e - \tau} \sum_{t=1}^{T_e-\tau} \mathbf{x}(t-\tau) y(t) \tag{4-6}$$

The result of $C_{xy}$ is a scalar value at a given time window. XCOR values range between -1 and 1. When $C_{xy}(\tau)$=-1, signals $\mathbf{x}(t)$ and $\mathbf{y}(t)$ have complete linear inverse correlation. When $C_{xy}(\tau)$=0, signals $\mathbf{x}(t)$ and $\mathbf{y}(t)$ have no linear interdependence at the time lag $\tau$, and $C_{xy}(\tau)$=1 represents complete linear direct correlation between the two signals at the time lag $\tau$.

### 4.2.3. Coherence function (COH)

Coherence refers to the linear relations between signals at a specific frequency. COH is defined as the absolute value of the complex coherency also know as Coherency [84]. Coherency measures how the phases in two different channels are coupled to each other. Coherency is calculated by the cross-spectral density function $S_{xy}$ of two EEG signals $\mathbf{x}(t) \in \mathbb{R}^{T_e}$ and $\mathbf{y}(t) \in \mathbb{R}^{T_e}$ of distinct brain regions (electrodes), normalized by their individual auto-spectral density functions.

If $\mathbf{x}_{an}(t)$ and $\mathbf{y}_{an}(t)$ are the analytic signals of $\mathbf{x}(t)$ and $\mathbf{y}(t)$ respectively, defined as:

$$\begin{aligned} \mathbf{x}_{an}(t) &= \mathbf{x}(t) + i\widetilde{\mathbf{x}}(t) = A_x e^{i\phi_t} \\ \mathbf{y}_{an}(t) &= \mathbf{y}(t) + i\widetilde{\mathbf{y}}(t) = A_y e^{i\phi_t} \end{aligned} \tag{4-7}$$

where $A_x = \sqrt{\widetilde{\mathbf{x}}(t)^2 + \mathbf{x}(t)^2}$ and $\phi_t = \arctan\frac{\widetilde{\mathbf{x}}(t)}{\mathbf{x}(t)}$ are the amplitude and phase of $\mathbf{x}_{an}(t)$ respectively, and similarly for $\mathbf{y}_{an}(t)$. $\widetilde{\mathbf{x}}(t)$ and $\widetilde{\mathbf{y}}(t)$ are the Hilbert transforms of $\mathbf{x}(t)$ and $\mathbf{y}(t)$, computed by:

$$\begin{aligned} \widetilde{\mathbf{x}}(t) &= \frac{1}{\pi}\int_{\infty}^{-\infty} \frac{x(\tau)}{t-\tau} d\tau \\ \widetilde{\mathbf{y}}(t) &= \frac{1}{\pi}\int_{\infty}^{-\infty} \frac{y(\tau)}{t-\tau} d\tau \end{aligned} \tag{4-8}$$

The cross-spectral density function is defined as:

$$S_{xy} = \mathrm{E}[A_x\, A_y e^{i\Delta\phi_t}] \tag{4-9}$$

where E[·] is the expected value operator and $\Delta\phi$ is the phase angle difference between the signals. Then, the cross-spectral density function is the average of $e^{i\Delta\phi_t}$ weighted with the product of the amplitudes $A_x$ and $A_y$ at a frequency $f$. Then, complex coherency is calculated as:

$$C_{xy} = \frac{S_{xy}(f)}{\sqrt{S_{xx}(f) S_{yy}(f)}} \tag{4-10}$$

Then, COH coefficients are computed for each frequency $f$ as follows:

$$\Gamma_{xy} = \frac{|S_{xy}(f)|^2}{S_{xx}(f)S_{yy}(f)} \tag{4-11}$$

The operation of Eq.(4-11) puts coherence on a scale from 0 to 1, with 1: complete coherence, and 0: complete independence between $\mathbf{x}(t)$ and $\mathbf{y}(t)$ at frequency $f$.

### 4.2.4. Imaginary Part of Coherency (ICOH)

Coherency between signals can be defined as their cross-spectral density function divided by the product of their auto-spectral densities. When complex values of the coherency are projected onto the imaginary axis, the ICOH is obtained [85]. ICOH is a metric of phase-synchronization between two signals $\mathbf{x}(t) \in \mathbb{R}^{T_e}$ and $\mathbf{y}(t) \in \mathbb{R}^{T_e}$ which uses the same equation as that for COH Eq.(4-11), except that the imaginary part of coherency is taken before computing the magnitude, as following:

$$IC_{xy} = \frac{E[A_x A_y \sin(\Delta\phi_t)]}{\sqrt{E[A_x^2]E[A_y^2]}} \tag{4-12}$$

ICOH is zero when the cross-spectrum between the two EEG signals $\mathbf{x}(t)$ and $\mathbf{y}(t)$ has a $0°$ or $180°$ phase, and maximum when the cross-spectrum has a phase of $\pm 90°$. Then, ICOH is not affected by the $0°$ or $180°$ cross-spectral relationship between the volume-conducted activities of a single source at two separate sensors.

Discarding contributions to the connectivity estimate along the real axis explicitly removes instantaneous interactions that are potentially spurious due to field spread of volume conduction. Thus, ICOH captures true source interactions at a given time lag [85].

### 4.2.5. Phase-Lag Index (PLI)

Phase-Lag Index is another metric of phase-synchronization that measures the asymmetry of the distribution of phase differences between two signals [86]. PLI is based on the imaginary component of the cross-spectrum, then, it is not spuriously affected by the volume conduction from a single source's activity to two separate sensors, or by a common reference. PLI is computed by averaging the sign of the phase difference between the two signals, $\mathbf{x}(t) \in \mathbb{R}^{N_e}$ and $\mathbf{y}(t) \in \mathbb{R}^{N_e}$ per observation:

$$PLI_{xy} = |\mathrm{E}[\mathrm{sgn}[(\Delta\phi_t)]]| \tag{4-13}$$

PLI ranges between 0 and 1. When $PLI_{xy} = 0$ there is no coupling between the signals $\mathbf{x}(t)$ and $\mathbf{y}(t)$, when $PLI_{xy} = 1$, there is perfect phase locking at a value of $\Delta\phi_t$ between the both signals.

## 4.3. Classification

To select one of the five functional connectivity metrics, their performances when classifying ex-combatants vs. civilian people using linear discriminant analysis were compared for each condition of the emotional processing experimental task (negative, neutral and positive), in the RoIs described in Section 4.4 and for each frequency band described in Section 4.2.

### 4.3.1. Linear Discriminant Analysis (LDA)

LDA is a data analysis technique proposed by R. Fisher in 1936 with the objective of solving a pattern recognition problem [87]. LDA consists on finding a linear combination of features that characterizes or separates two or more classes. That is, finding the optimal hyperplane that minimizes the within-class variance and maximizes the separation between the projected means of classes [88]. Mathematically speaking, if $\mathbf{S_w}$ and $\mathbf{S_b}$ are the within-class and between-class scatter matrices respectively, for $c$ different classes of $N_j$ samples, the optimization problem can be formulated as:

$$\begin{aligned} &\underset{\mathbf{S_w}}{\text{minimize}} \quad \mathbf{S_w} = \sum_{j=1}^{c}\sum_{i=1}^{N_j}(u_{ij} - \mu_j)(u_{ij} - \mu_j)^\top, \text{while,} \\ &\underset{\mathbf{S_b}}{\text{maximize}} \quad \mathbf{S_b} = \sum_{j=1}^{c}(\mu_j - \mu)(\mu_j - \mu)^\top, \end{aligned} \tag{4-14}$$

where $u_{ij}$ is the $i_{th}$ sample of class $j$, $\mu_j$ is the mean of class $j$ and $\mu$ is the mean of all classes. If $\mathbf{S_w}$ is a non-singular matrix, one option to solve the optimization problem consists on maximizing the ratio $\frac{\det|\mathbf{S_b}|}{\det|\mathbf{S_w}|}$. This ratio is a maximum when the column vectors of the projection matrix are the eigenvectors of ${\mathbf{S_w}}^{-1}\mathbf{S_b}$.

## 4.4. Selection of brain Regions of Interest (RoIs)

Several studies have reported that for many aspects of emotion (i.e. affective style, aggressive and violent behavior, emotional processing and emotion regulation), a circuit of activated or deactivated brain regions is implicated. The circuit involves not only subcortical areas (e.g. amydala or the basal ganglia), but also cortical areas, mainly Prefrontal Cortex (PFC), Anterior Cingulate Cortex (ACC), as well as temporal and medial parietal cortices [89–91]. Taking into account these findings, we defined 10 Regions of Interest (RoIs) for further connectivity analysis of interaction patterns. RoIs are reported in Table **4-1**.

Table **4-1**.: Regions of Interest (RoIs) and related electrodes defined for connectivity analysis.

| Name | Region of Interest | Related Electrodes |
|---|---|---|
| RoI 1 | Frontal | Fp1,Fp2, FpZ, Af3, Af4 |
| RoI 2 | Left frontal-central | F1, Fc1, F3, Fc3 |
| RoI 3 | Medial frontal-central | Fz, Fcz |
| RoI 4 | Right frontal-central | F2,F4,Fc2, Fc4 |
| RoI 5 | Left central-parietal | C1, Cp1, C3, Cp3 |
| RoI 6 | Medial central-parietal | CZ, CpZ |
| RoI 7 | Right central-parietal | C2, Cp2, C4, Cp4 |
| RoI 8 | Left parietal-occipital | P1, P3, Po3, Po5 |
| RoI 9 | Medial parietal-occipital | Pz, PoZ |
| RoI 10 | Right parietal-occipital | P2, P4, Po4, Po6 |

## 4.5. Results

Functional connectivity metrics described in Section 4.2 were calculated for each EEG signal, previously divided into frequency bands and task conditions (Negative, Neutral and Positive). All metrics were computed in MATLAB using the Hermes toolbox [92].

### 4.5.1. Connectivity spatial patterns

Several topographic maps were generated to visually compare the connectivity results of the five connectivity metrics. Brain topographic maps were plotted using the `topoplot` function of the EEGLab toolbox [52]. Connectivity results were divided into two groups: Ex-combatants and controls (Civilian people). The measures of the five metrics were averaged per band frequency: Delta, Theta, Alpha, Beta and Gamma. Strong connections between brain regions are represented with red and weak connections in dark blue.

As shown in Fig. **4-2** and Fig. **4-4**, COR and COH analyses for the ex-combatants and control subjects show high connectivity, instead of being concentrated in the central areas, for every condition and frequency band. Connectivity patterns of XCOR metric were similar to the COR patterns for Delta and Gamma bands for both groups in all conditions. Analogously for negative conditions in Alpha, Beta and Gamma bands. For neutral and negative conditions, in Alpha, Beta and Gamma bands the connectivity distribution patterns were stronger in the peripheral brain areas (See Fig. **4-3**).

As shown in Fig. **4-5**, ICOH connectivity distributions were mostly limited in the parietal-occipital regions. Strong connections from the parietal-occipital to central regions were

observed in Delta, Alpha and Theta and Gamma bands with different distributions patterns for both ex-combatants and controls. For the Delta band, PLI showed very weak connections, in the other bands the connections were concentrated in the parietal-occipital areas, similarly to the ICOH patters.

The connectivity spatial pattern of COR, XCOR and COH suggests that their results were influenced by the volume conduction. While, ICOH and PLI patterns were quite similar to each other in both subjects, concentrating on the occipital-parietal brain areas.

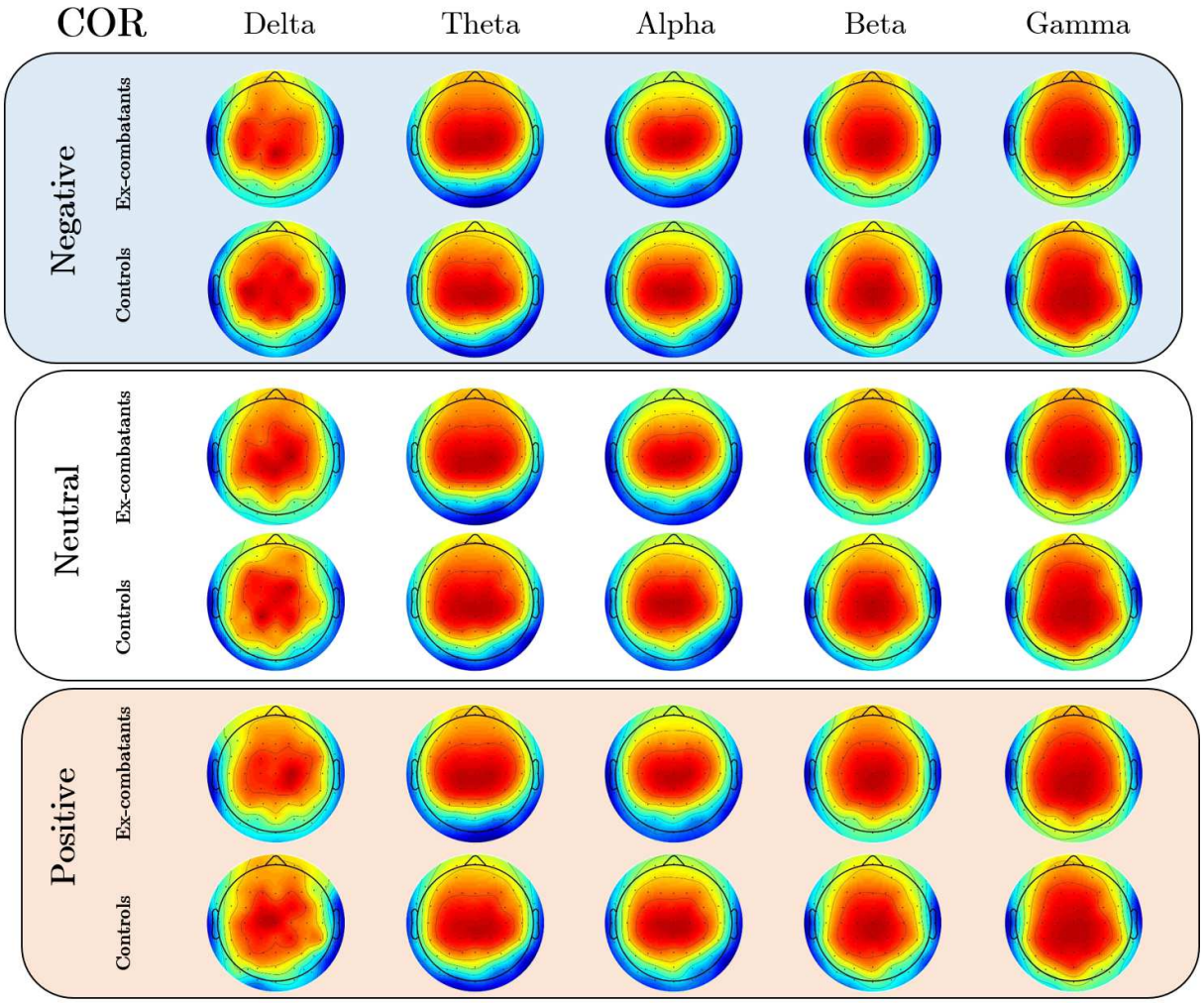


Figure **4-2**.: COR Topographic plots. Figure illustrates the spatial patters of COR analysis of ex-combatants and civilian people per condition (negative, neutral and positive) an frequency band (Delta, Theta, Alpha, Beta and Gamma).

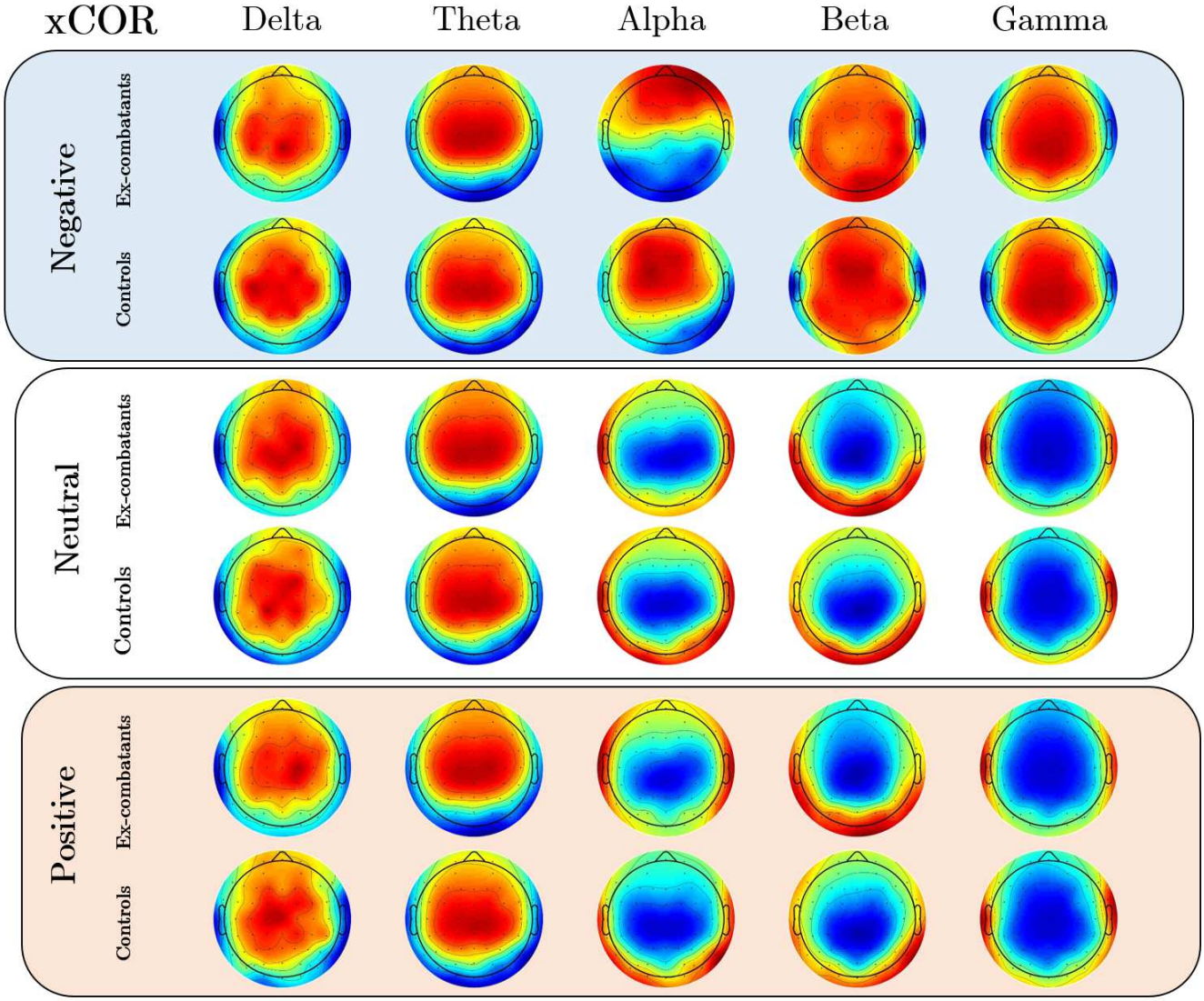


Figure **4-3**.: XCOR Topographic plots. Figure illustrates the spatial patters of XCOR analysis of ex-combatants and civilian people per condition (negative, neutral and positive) an frequency band (Delta, Theta, Alpha, Beta and Gamma).

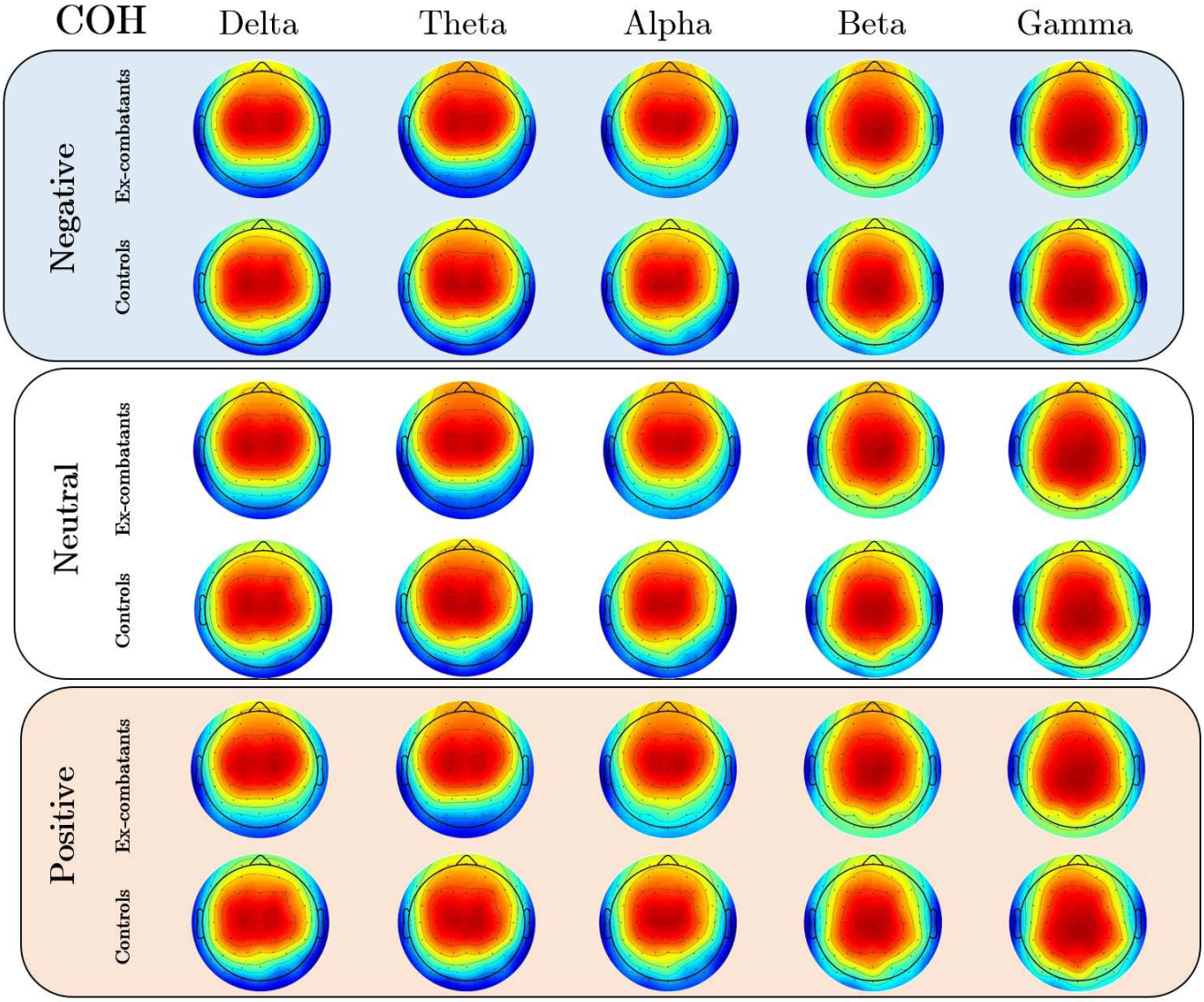


Figure **4-4**.: COH Topographic plots. Figure illustrates the spatial patters of COH analysis of ex-combatants and civilian people per condition (negative, neutral and positive) an frequency band (Delta, Theta, Alpha, Beta and Gamma).

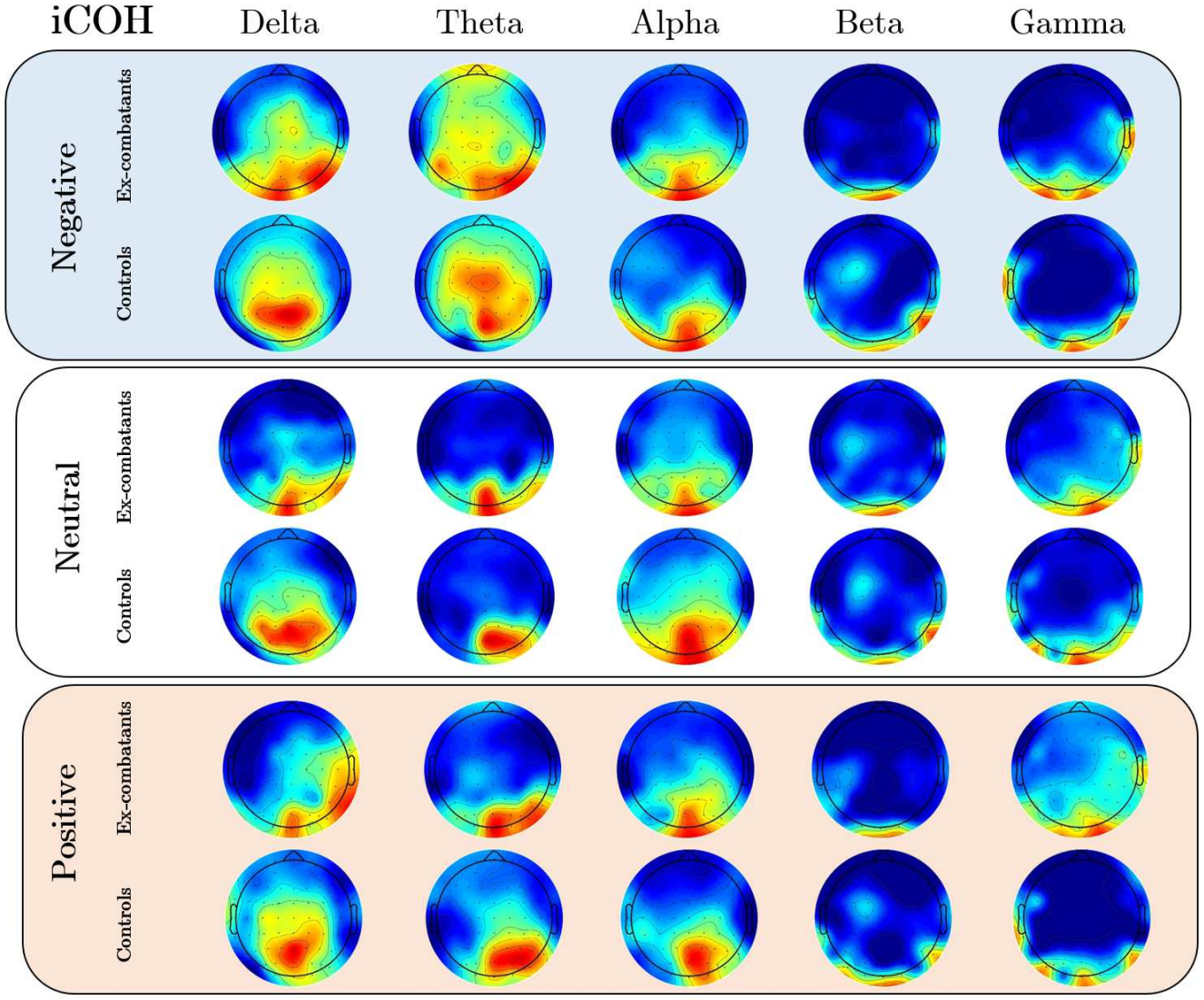


Figure **4-5**.: ICOH Topographic plots. Figure illustrates the spatial patters of ICOH analysis of ex-combatants and civilian people per condition (negative, neutral and positive) an frequency band (Delta, Theta, Alpha, Beta and Gamma).

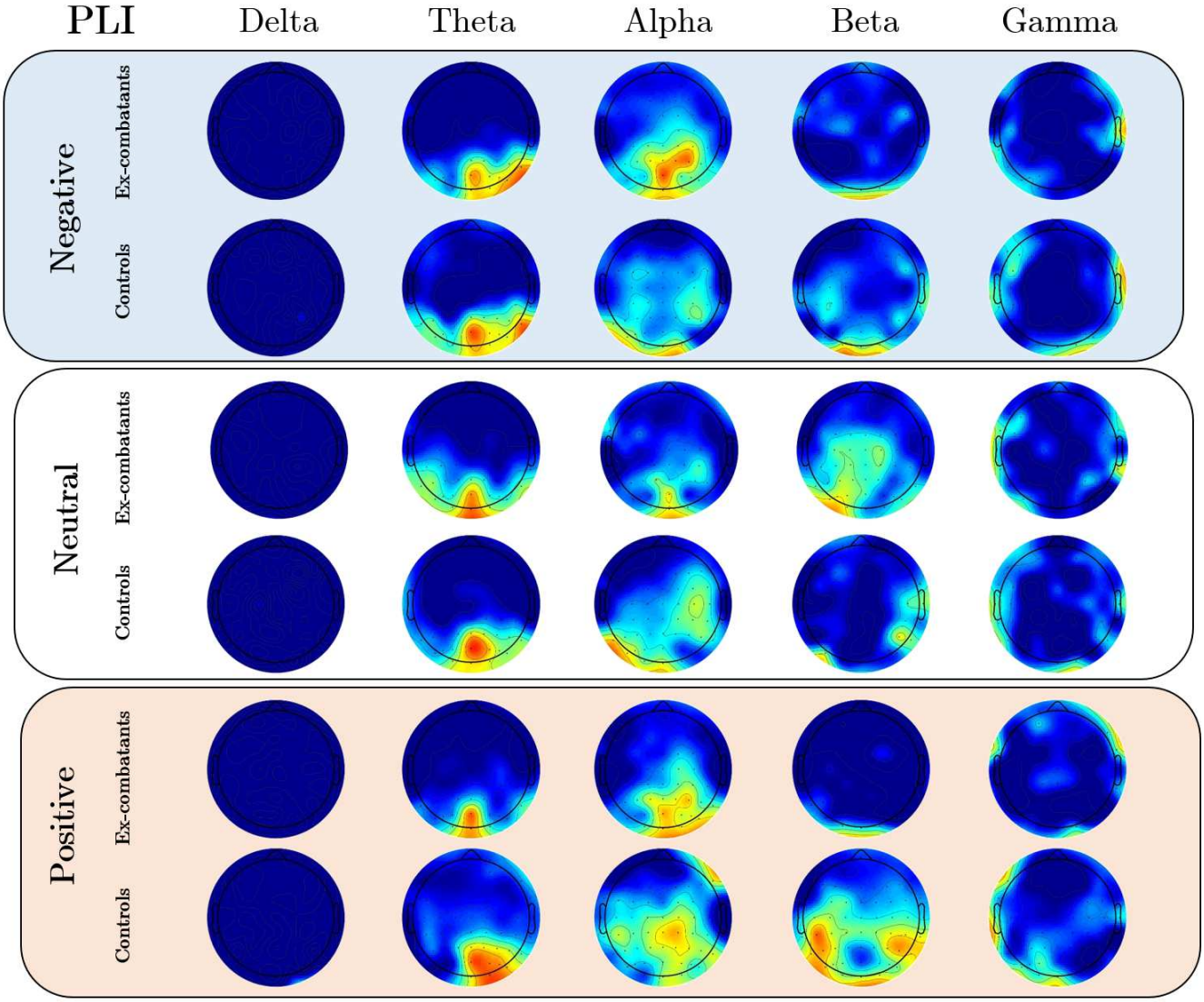


Figure **4-6**.: PLI Topographic plots. Figure illustrates the spatial patters of PLI analysis of ex-combatants and civilian people per condition (negative, neutral and positive) an frequency band (Delta, Theta, Alpha, Beta and Gamma).

### 4.5.2. LDA classification performance

Different LDA were implemented for task conditions and frequency bands. Features for LDA were obtained by averaging the connectivity values from all electrodes between one RoI to another RoI. For instance, the connectivity from left frontal-central to right frontal-central regions is the average connectivity of all pairs from (F1, Fc1, F3 and Fc3) to (F2,F4,Fc2 and Fc4). Then, a vector of 45 features per subject was the input for each LDA classifier.

For this analysis a normal distribution of the data was assumed. The LDA performances were obtained using K-fold cross-validation with 10 folds for each class. LDA classification accuracies for negative, neutral and positive conditions are shown in Table **4-2**, Table **4-3** and Table **4-4**, respectively.

Table **4-2**.: LDA classification results for the negative condition

| | **Task condition: Negative** | | | | |
|---|---|---|---|---|---|
| | **DELTA** | **THETA** | **ALPHA** | **BETA** | **GAMMA** |
| | ACC (Conf. Interval) | ACC (Conf. Interval) | ACC (Conf. Interval) | ACC (Conf. Interval) | ACC (Conf. Interval) |
| **COR** | 54% (39,45% - 67,97%) | 50% (35,71% - 64,28%) | 46% (32,06% - 60,5%) | 56% (41,34% - 69,79%) | 48% (33,88% - 62,4%) |
| **XCOR** | 42% (28,48% - 56,65%) | 50% (35,71% - 64,28%) | 48% (33,88% - 62,4%) | 54% (39,45% - 67,97%) | 48% (33,88% - 62,4%) |
| **COH** | 50% (35,71% - 64,28%) | 52% (37,57% - 66,13%) | 48% (33,88% - 62,4%) | **62%** (47,16% - 75,12%) | 44% (30,26% - 58,59%) |
| **ICOH** | **64%** (49,14% - 76,85%) | **64%** (49,14% - 76,85%) | **68%** (53,16% - 80,26%) | 56% (41,34% - 69,79%) | **54%** (39,45% - 67,97%) |
| **PLI** | 52% (37,57% - 66,13%) | 54% (39,45% - 67,97%) | 42% (28,48% - 56,65%) | 46% (32,06% - 60,5%) | 46% (32,06% - 60,5%) |

The results in the Table **4-2** show that the metric with higher performance for the negative condition was ICOH in four of the five frequency bands. For the Beta band, COH has a better performance than the others.

Table **4-3**.: LDA classification results for the neutral condition

| | **Task condition: Neutral** | | | | |
|---|---|---|---|---|---|
| | **DELTA** | **THETA** | **ALPHA** | **BETA** | **GAMMA** |
| | ACC (Conf. Interval) | ACC (Conf. Interval) | ACC (Conf. Interval) | ACC (Conf. Interval) | ACC (Conf. Interval) |
| **COR** | 36% (23,28% - 50,71%) | 42% (28,48% - 56,65%) | **62%** (47,16% - 75,12%) | 50% (35,71% - 64,28%) | 46% (32,06% - 60,5%) |
| **XCOR** | 48% (33,88% - 62,4%) | 38% (24,99% - 52,71%) | 48% (33,88% - 62,4%) | **66%** (51,14% - 78,57%) | 54% (39,45% - 67,97%) |
| **COH** | 48% (33,88% - 62,4%) | 52% (37,57% - 66,13%) | 50% (35,71% - 64,28%) | 52% (37,57% - 66,13%) | 52% (37,57% - 66,13%) |
| **ICOH** | 48% (33,88% - 62,4%) | **54%** (39,45% - 67,97%) | 58% (43,26% - 71,59%) | 54% (39,45% - 67,97%) | **58%** (43,26% - 71,59%) |
| **PLI** | **58%** (43,26% - 71,59%) | 48% (33,88% - 62,4%) | 54% (39,45% - 67,97%) | 34% (21,59% - 48,68%) | 46% (32,06% - 60,5%) |

For the neutral condition Table **4-3** shows no concrete results about what metric has the better performance, since each metric has the higher accuracy for one of the five frequency bands.

Table **4-4**.: LDA classification results for the positive condition

| | **Task condition: Positive** | | | | |
|---|---|---|---|---|---|
| | **DELTA** | **THETA** | **ALPHA** | **BETA** | **GAMMA** |
| | ACC (Conf. Interval) | ACC (Conf. Interval) | ACC (Conf. Interval) | ACC (Conf. Interval) | ACC (Conf. Interval) |
| **COR** | 60% (45,2% - 73,36%) | 44% (30,26% - 58,59%) | 48% (33,88% - 62,4%) | 50% (35,71% - 64,28%) | 50% (35,71% - 64,28%) |
| **XCOR** | 60% (45,2% - 73,36%) | 42% (28,48% - 56,65%) | 50% (35,71% - 64,28%) | 68% (53,16% - 80,26%) | **52%** (37,57% - 66,13%) |
| **COH** | **62%** (47,16% - 75,12%) | 46% (32,06% - 60,5%) | **56%** (41,34% - 69,79%) | 62% (47,16% - 75,12%) | 50% (35,71% - 64,28%) |
| **ICOH** | 52% (37,57% - 66,13%) | **60%** (45,2% - 73,36%) | 50% (35,71% - 64,28%) | **76%** (61,51% - 86,77%) | 44% (30,26% - 58,59%) |
| **PLI** | 54% (39,45% - 67,97%) | 44% (30,26% - 58,59%) | 64% (49,14% - 76,85%) | 56% (41,34% - 69,79%) | **52%** (37,57% - 66,13%) |

For the positive condition the results show that the performance of ICOH was considerably better in the Beta band than the other metrics. Additionally, in Theta band ICOH had a better performance than the others. COH shows better performance in Delta and Alpha bands. Finally, in Gamma band XCOR and PLI metrics were the best metrics with the same performance.

## 4.6. Summary

Functional connectivity analysis was presented as a promising tool to evaluate the EP. Different connectivity metrics have been used to measure functional connectivity at scalp level. In this Chapter, five of connectivity metrics (COR, XCOR, COH, ICOH and PLI) were analyzed and evaluated. These metrics were compared using their connectivity spatial pattern representations and LDA in the 10 RoIs selected in Section 4.4.

According to the spatial connectivity patterns, ICOH and PLI present similar results which suggests that their calculated indexes were no influenced by volume conduction. Additionally, the LDA results show that ICOH has the better performance when classifying ex-combatants vs. civilian people. Thus, ICOH was selected for the further analysis.

# 5. Characterization of Emotional Processing in Ex-combatants

## 5.1. Introduction

EP is a neural mechanism in charge of the perception, recognition, evaluation and generation of a response to stimuli and relevant emotional information in the environment [93, 94]. Studies in veterans have shown that experiences of combat and trauma during deployment were significantly associated with aggressive and violent behaviors. Veterans mainly manifest differences on the processing of emotional information [17, 18, 20]. On Colombian ex-combatants, an atypical functioning on similar mechanisms is hypothesized.

In [21], in order to evaluate how Colombian ex-combatants are processing the emotional information, the authors proposed to use two psychological tests: the Reading Minds in the Eyes (RME) [95], and a computerized test designed for the recognition of emotional faces [96]. The participants of this study were 63 ex-combatants and 22 controls. For performing the statistical analyzes the authors used the Fisher's exact test. Using these tests there was a slight tendency of ex-combatants to poorly recognizing of positive emotional valence (specifically, in the number of hits recognizing the happy faces) but no statistical significance compared to the control group [21].

Another way for studying EP consists on evaluating the ERP modulation through computerized tasks synchronized with EEG recordings [22–24]. In [24] the authors analyzed the relationship between the EP in ex-combatants and the social cognition and behavior (SCB) patterns using an emotional recognition task which consisted in identifying faces and words with emotional content. The database used in this study consist in the the same of this thesis, 30 ex-combatants and 20 controls. The demographic variables and SCB scales were analyzed using independent-samples t-test or Chi square (for gender) and to analyze the behavioral data, two two-way mixed ANOVA models were used, one for Faces and one for Words. The results of [24] suggest that in ex-combatants the links between EP and SCB functions are reorganized. This may be associated to chronic exposure to war experiences.

In [22], the authors found associations between the ex-combatants' ERPs responses to emotional images from the IAPS system with their empathy levels. The participants from this

work were 40 ex-combatants and 20 civilians. ANOVA test was used to analyze the ERP information. In their study, authors concluded that ex-combatants showed adequate early cortical responses to affective stimuli (EPN) but presented a higher reactivity of LPP; and found poor executive functioning and high cortical reactivity to emotional processing information.

In [23] the authors used the same emotional recognition task and database of [24] to characterize the emotional processing of Colombian ex-combatants using ERPs analyzes. The authors concluded that using ERP modulations and the analysis of aggressive responses and social interactions, both groups ex-combatant and civilian could be automatically separated using supervised machine learning techniques: Partial Least Square Regression (PLS), k-Neareast Neighbors Classifier (KNN) and Support Vector Machines (SVM).

In the last studies, researchers only took into account psychological tests and the ERPs modulations in response to visual stimuli. Using these approaches, it is not possible to recognize how different cortical structures are contributing to the expression of failures in emotional processing of ex-combatants.

Brain connectivity analysis is proposed as a method to estimate EP [13, 14]. Brain connectivity techniques focus on how the information is processed on the brain, to establish the activation pattern required to generate a cognitive process [6]. In a recent study [97] brain connectivity analysis was used to analyze the data obtained from 39 male combat veterans with Post-Traumatic Stress Dissorder (PTSD) symptoms which performed a task designed to assess cognitive inhibition and activation using fMRI. The authors concluded that PTSD and neuropsychological performance relate dysregulation of functional connectivity.

Atypical connectivity patterns represent a disruption on the connection among areas used for different kinds of processing as the EP. Taking into account the above, we proposed to employ brain connectivity analysis (functional connectivity analysis) to characterize atypical functioning in EP of Colombian ex-combatants. The Imaginary Part of Coherency (ICOH) [85] was chosen as the metric to evaluate the connectivity. According to the results reported in Chapter 4 it is the best choice to separate ex-combatants vs. civilians. Additionally, its spatial patterns suggest that their results were not influenced by the volume conduction.

This Chapter contains the description of the proposed methodology. Additionally, the selection of the brain regions of interest and the statistical results are presented.

## 5.2. Proposed Methodology

The stages of the proposed methodology are shown in Fig. **5-1** and consist on:

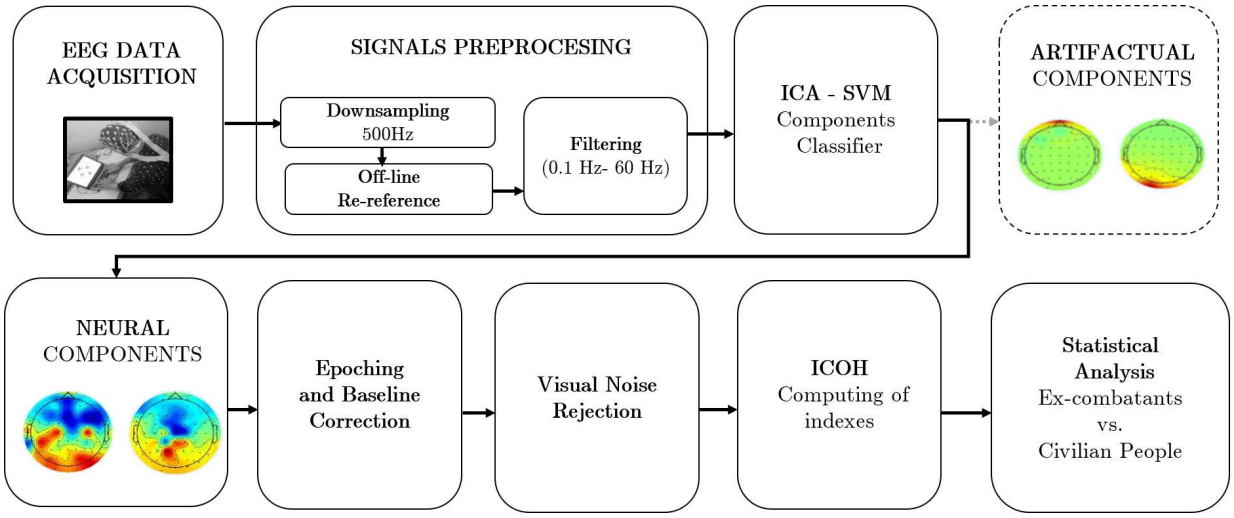


Figure **5-1**.: Block diagram of the proposed methodology to recognize atypical functioning in EP of Colombian ex-combatants.

1. EEG data acquisition. EEG registers while participants performed the emotional processing experimental task (Section 3.2).

2. Signals preprocessing.
   - Downsampling. From 1000 Hz to 500 Hz (Section 3.3).
   - Off-line re-reference to Mastoids (Section 3.4).
   - Filtering. IIR digital band-pass filter from 0.1 to 60 Hz (Section 3.5).

3. Automatic artifacts rejection (Section 3.6)
   - Independent Component Analysis (ICA)
   - Support Vector Machine (SVM)

4. EEG segmentation. Epoching and baseline correction (Section 3.7).

5. Visual noise rejection. Visually classification of EEG segments

6. Functional connectivity analysis. Calculating indexes of Imaginary Part of Coherency (ICOH) (Section 4.2.4).

7. Statistical analysis. Wilcoxon test “Ex-combatants vs. Controls” (section 5.3).

## 5.3. Statistical Analysis

### 5.3.1. Wilcoxon Rank-Sum Test

Frank Wilcoxon proposed a non-parametric statistical test called the Rank-Sum Test [98]. His approach is used for establishing significant differences between two sample groups. This test is described as the non-parametric version of the two-sample t-test and its null hypothesis is that a randomly selected value from one sample is different (less or greater) than a randomly selected value from the other sample. Mathematically speaking the test is based on calculating magnitude-based ranks. If the ranks of the groups are significantly separated, then the both groups are significantly different [98].

The Rank-Sum test is widely used in EEG studies [99–101] because this test does not require or had very limited assumptions to be made about the distribution of the data (*e.g.* it does not assume a normal distribution of the data). Additionally, non-parametric methods are useful for working with data with outlier observations [102].

Once the ICOH indexes are computed for each pair of RoIs reported in Table. **4-1**, three between-group Wilcoxon Rank-Sum test are calculated:

1. Group (Ex-combatants vs. Controls).
2. Condition × Group.
3. Condition × Band × Group.

With these comparisons we expect to find significant differences in the EP between Colombian ex-combatants and people not directly exposed to the armed conflict.

### 5.3.2. False Discovery Rate (FDR)

The statistical analysis for functional connectivity metrics incurs in a serious multiple testing problem for determining significant differences, this is because the data dimensionality exponentially increases due to the number of considered pairs and/or frequency bands. FDR is a procedure used for correct multiple hypothesis comparisons [103]. It is commonly used in statistical analysis adopted in EEG and other neuroimaging techniques [104].

From the resultant $p$-values of Wilcoxon Sum-Rank test, a significance threshold is calculated with a corresponding $q$-value using the procedure for controlling the False Discovery Rate (FDR) proposed in [103]:

- List the $p$-values in ascending order $p_1 \leq p_2 \cdots \leq p_m$ corresponding to the hypoteses $H_1, H_2, \cdots, H_m$.

- Set a $q$ value (in this work $q = 0.05$).
- Find the largest $k$ such that $P_k \leq \frac{k}{m} q$.
- Reject the null hypothesis for all $H_i$ for $i = 1, \cdots, k$.

## 5.4. Results

### 5.4.1. Selection of brain Regions of Interest (RoIs)

As mentioned in Section 4.4, according to the literature different brain regions are implicated in the circuitry involved in many aspects of emotion [89–91]. Thus, we select 10 ROIs for the functional connectivity analysis (Table. **4-1**). However, observing the connectivity spatial patterns of ICOH, it exhibits low connectivity in the frontal regions for most frequency bands (See Fig. **4-5**) on every task conditions. Additionally, no significant differences were found between ex-combatants and controls for any of the connections across the frontal regions (RoI1 to RoI4) and the others. Then, these four regions were rejected for the final model. New RoIs are represented in Fig. **5-2**. Fig. **5-2** illustrates the placement for EEG sensors of each RoI. In summary, RoI1= C1, Cp1, C3 and Cp3, RoI2= Cz and CpZ, RoI3= C2, Cp2, C4 and Cp4 , RoI4= P1, P3, Po3 and Po5, RoI5= PZ and PoZ, and RoI6= P2, P4, Po4 and PO6.

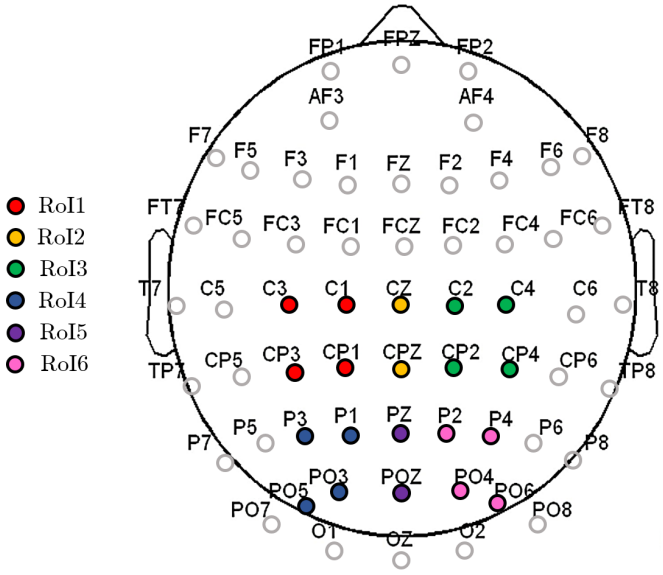


Figure **5-2**.: Final Regions of Interest(RoIs) for brain connectivity analysis. Placement of sensors per each RoI.

### 5.4.2. Statistical analysis results

- Group (Ex-combatants vs. Controls)

  In this test the total information (All frequency bands and all conditions) was included. For each pair, no significant differences were found (See Table **A-1**). However, the p-values suggested a tendency to differentiate the connectivity of both groups across the pairs: RoI1-RoI2 (p=0.021, q=0.173), RoI2-RoI3 (p=0.023, q=0.173) and RoI3-RoI5 (p=0.049, q=0.245). For these three cases, the median connectivity between the RoIs was higher in the controls than the ex-combatants group, the difference percentages in the connectivity were 11%, 8% and 10%, respectively.

- Condition × Group

  No significant differences were found between ex-combatants and controls for negative and neutral conditions. Significant differences between ex-combatants and controls were found in the connectivity across: RoI1-RoI4 (p=0.0027, q=0.0209) and RoI3-RoI4 (p=0.0010, q=0.0152) (See Table **A-2**) for the positive condition. Consistently with the differences found in the first test, the connectivity across these regions were higher for controls. The median of the connectivities from RoI1 to RoI4 was 17.42%, and from RoI3 to RoI4 was 26.79% higher the control group than the ex-combatants group.

- Condition × Band × Group

  No significant differences between ex-combatants and controls were found in the Delta (See Table **A-3**), Theta (See Table **A-4**), Alpha (See Table **A-5**), and Gamma bands (See Table **A-7**) for any condition. Significant differences between ex-combatants and controls were found for positive condition in the Beta band (14-29.99 Hz) for the connectivity across the regions RoI2-RoI4 (p=0.0044, q=0,0336), and across the regions RoI3-RoI4 (p=0.0005, q=0.0088). The connectivity between controls for RoI2-RoI4 was $17,63\%$ and for region RoI3-RoI4 was $27,46\%$ higher than the ex-combatants connectivity (See Table **A-6**).

With the proposed methodology, significant differences in the connectivity between ex-combatants and civilian people were found in the stimulus with positive valence in the Beta frequency band. No significant differences were found for the other stimuli or frequency band. Even though neutral valence is commonly misclassified as negative in normal population; the recognition of emotional stimuli that index potential negative/neutral information is necessary for evolutionary purposes [105]. On this sense, combat experience might main-

tain intact the ability to categorize images with this content.

These results are consistent with the results found in Chapter 4, where the best performance for the metric ICOH in the beta band is shown for the positive stimulus. The Beta band has been associated with emotional processing in the evaluation of all types of valence [106]. Some studies demonstrated a wide posterior and anterior synchronization associated with the evaluation of positive content [106]. The authors found that Beta band was strongly involved during the evaluation of positive content compared to negative valence content [107]. Additionally, it is worth it to mention that these results support the finding in the literature that reports tendency towards the difficulties in the processing of emotional information with positive valence for the ex-combatants [21, 22].

## 5.5. Summary

In this Section, the proposed methodology to find atypical modulations in the EP of Colombian ex-combatants was presented. The proposed methodology begins with the EEG data preprocessing that includes the downsampling, off-line re-reference, filtering and an automatic artifactual noise rejection system. Thereafter, the signals were epoched for the three conditions task (positive, neutral and negative). Then, a visual inspection of the signals was performed. Finally, with the cleaned EEG data, the brain connectivity analysis was performed using the ICOH measure upon the epoched signals.

Using our proposed methodology, significant differences were found in the stimulus with positive valence in the Beta frequency band. No significant differences were found for the other conditions (neutral and negative) or frequency bands. These results support tendency towards the difficulties for the ex-combatants in the processing of emotional information with positive valence previously found in the literature [21, 22].

# 6. Case of Study: Intervention

## 6.1. Introduction

Most of our social interaction is naturally based on emotional information. Colombian ex-combatants have shown atypical processing of emotional information as well as poor social interactions [21–23, 30]. Aimed to ameliorate these deficits and to help ex-combatants in their reintegration to civilian life, the use of a Social Cognitive Training Intervention (SCTI) has been proposed [108].

The SCTI program consists on 12 sessions with a duration of 45 minutes focused on the cognitive-emotional regulation and social-cognition skills of ex-combatants (i.e. the identification of basic emotions, assertive expressions of emotion in everyday situations and aspects of theory of mind).

In this Chapter, the effects of the SCTI program on the EP of ex-combatants were investigated using our proposed methodology (See Chapter. 5). For our analysis the ex-combatants sample (28 subjects, 26 men) was divided into the same two groups of [108]:

1. Social Cognitive Training Intervention Group (SCTI): 15 subjects (13 men) that received the training.

2. Conventional Reintegration Group (CRG): 13 subjects (all men) that did not receive the training but continued the conventional reintegration intervention program.

Initially, 30 ex-combatants were reported in this study, but two of them abandoned the study. Two assessments (EEG registers) that were called PRE and POST were taken from the participants, one (PRE) before the SCTI or waiting time for the CRG group, and another one (POST) 14 weeks after the intervention. In both assessments, participants of the two groups (SCTI and CRG) performed the emotional categorization task following the same protocol described in Section 3.2.

In the next Sections, the spatial patterns of the functional connectivity analysis for the both groups and the statistical results are discussed.

## 6.2. Results

The results of this Chapter were divided into two Sections related to the two groups SCTI and CRG. Both Sections show the connectivity spatial patterns and the statistical analyses for each group. The statistical analysis were performed in a similar way of the Section 5.3 for the two groups (SCTI and CRG), but in this case we compared SCTI in the assessment 1 (PRE) vs. SCTI in the assessment 2 (POST), similar analyzes were performed for CRG.

### 6.2.1. SCTI Connectivity spatial patterns

Connectivity results were divided into two groups: PRE and POST. The topographic plots show the connectivity spatial patterns per each brain frequency band: Delta, Theta, Alpha, Beta and Gamma. Each map represents the within group average value of the connectivity metric per electrode. In the maps, strong connections among brain regions are in red and weak connections in dark blue.

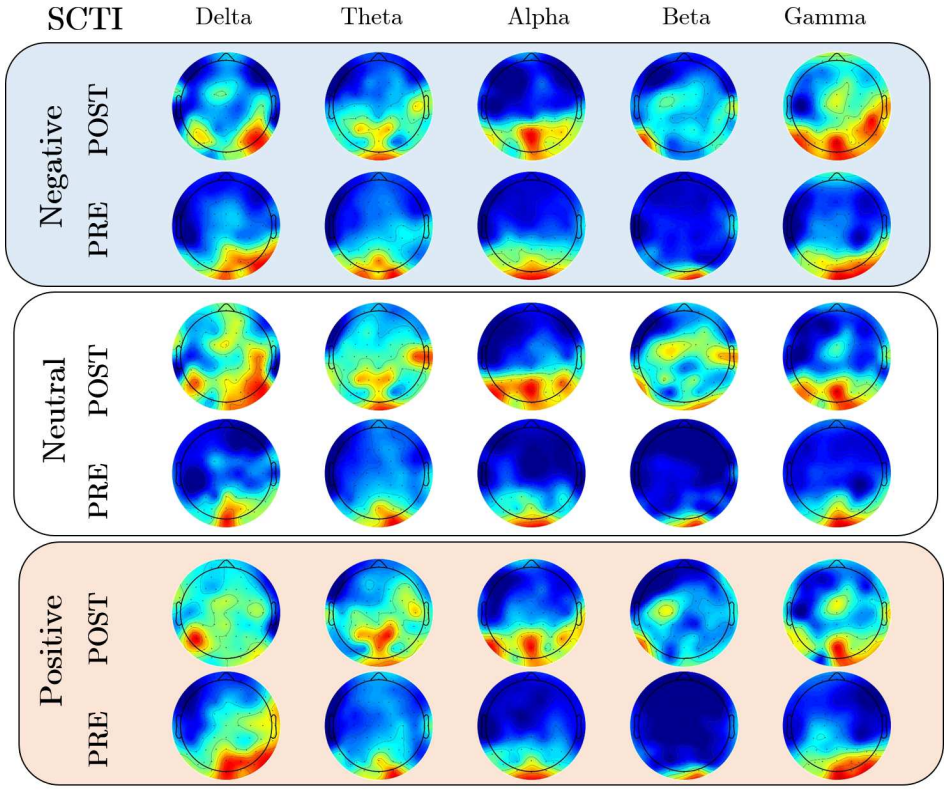


Figure **6-1**.: Topographic plots. Figure illustrates the spatial patters of brain connectivity analysis for SCTI PRE and SCTI POST per each condition (negative, neutral and positive) an frequency band (Delta, Theta, Alpha, Beta and Gamma).

As shown in Fig. **6-1**, the connectivity distribution was mostly limited in the parietal-occipital regions. Long connections from the parietal-occipital areas to central regions were observed in Delta, Theta and Gamma bands. In the figure different distributions patterns for both groups (SCTI PRE, SCTI POST) were observed for the all frequency bands and task conditions.

### 6.2.2. SCTI Statistical analysis

- Group (SCTI PRE vs. SCTI POST)

  The comparison between SCTI PRE vs. SCRI POST with all conditions and all frequency bands revealed significant differences in 13 of the 15 analyzed pairs (See Table **B-1**). Interestingly, the results displayed in Table **B-1** show an increase in the connectivity across the brain regions for the ex-combatants after the social training intervention program.

- Condition × Group

  The results of the Table **B-2** show significant differences between SCTI PRE and SCTI POST in the positive condition for the connectivity across RoI3 and RoI4 (p= 0.003, q= 0.042). Consistent with findings of the previous analysis, the connectivity across these regions was 48% greater after than before the intervention.

- Condition × Band × Group

  The results of Tables **B-3** to **B-7** show that significant differences between PRE and POST intervention are concentrated in the Beta band, specially in regions RoI1-RoI3 (p= 0.003, q= 0,021) and RoI3-RoI4 (p= 0.001, q= 0.018). According to previous analysis an increase in connectivity across the brain regions after psychological intervention was found. The largest increase occurred in regions RoI3-RoI4, it was about 68.79%.

The increment in connectivity the SCTI group may be related to an increment in the neural resources that are involved in the EP. According to [108], ex-combatants who received training tend to recognize more adequately or more precisely the stimuli with emotional content. Then, this increment in connectivity could be related to the increment on the capacities to properly recognize the stimuli.

### 6.2.3. CRG Connectivity spatial patterns

Connectivity results were divided into two groups: CRG PRE and CRG POST. The topographic plots show the connectivity spatial patterns per brain frequency band: Delta, Theta, Alpha, Beta and Gamma for each condition.

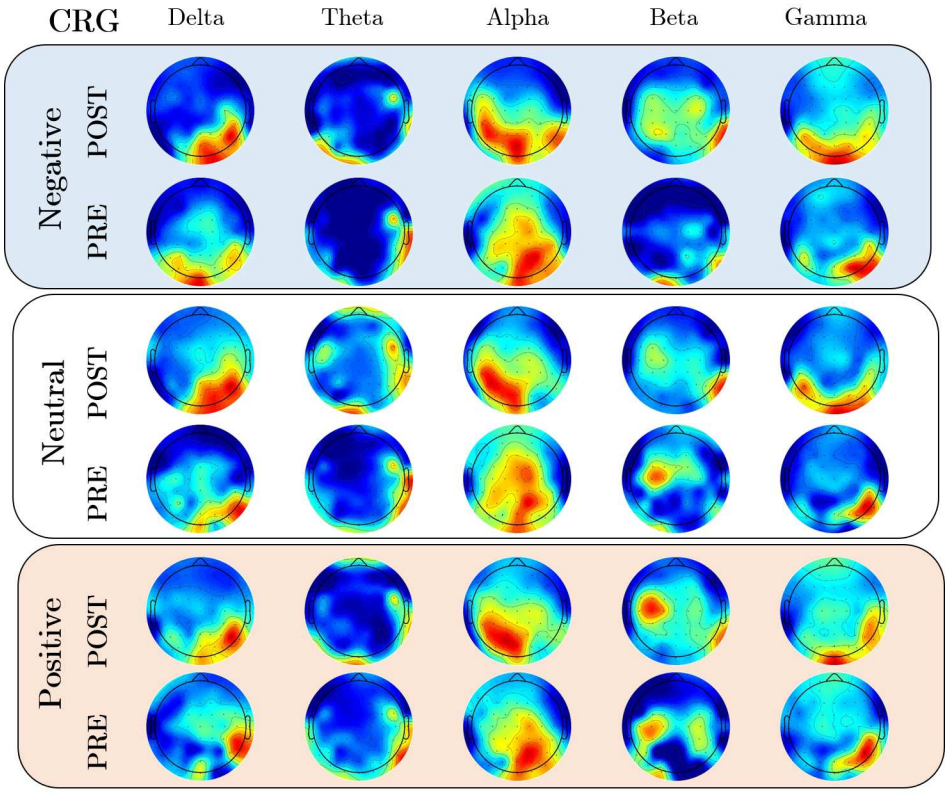


Figure **6-2**.: Topographic plots. Figure illustrates the spatial patters of brain connectivity analysis for CRG PRE and CRG POST per condition (negative, neutral and positive) an frequency band (Delta, Theta, Alpha, Beta and Gamma).

As shown in Fig. **6-2**, the connectivity distribution was limited for central regions in the Beta band. Long connections from the parietal-occipital areas to central region were observed in Alpha and Gamma bands. Additionally, the connectivity was limited for parietal-occipital areas in Delta and Theta bands. In the figure, similar distribution patterns for both groups (CRG PRE, CRG POST) were observed.

### 6.2.4. CRG Statistical analysis

- Group(CRG PRE vs. CRG POST)

  The results of Table **C-1** were obtained when comparing data from all conditions and frequency bands, they show significant differences between CRG PRE and CRG POST in two of the 15 analyzed pairs. The connectivities with significant differences are those across RoI to RoI2 (p= 0.0060, q= 0.0449) and across RoI5 to RoI6 (p= 0.0041, q= 0.0449). The registered data show an increase of 16% and 17% after the waiting time.

- Condition × group

  No significant differences were found for CRG PRE vs. CRG POST (See Table **C-2**).

- Condition × band × group

  No significant differences were found for CRG PRE vs. CRG POST (See Tables **C-3** to **C-7**).

## 6.3. Summary

In this Chapter, the methodology for brain connectivity analysis proposed in Chapter 5. was used to quantitatively evaluate the efficacy of a social cognitive training program. To achieved this, the initial sample of ex-combatants was divided into two groups: Social Cognitive Training Intervention Group (SCTI) that is referred to ex-combatants that received the training, and the Conventional Reintegration Group (CRG) formed with ex-combatants that did not receive the training but continued with the conventional reintegration intervention program.

For SCTI group the statistical analysis showed significant differences between the data obtained before (PRE) and after (POST) the social cognitive training program in all levels (Condition × Band × Group) and, additionally, an increase in the connections across the

brain regions after the intervention. Interestingly, after comparing the data obtained before (PRE) and after (POST) of the ex-combatants who did not receive the intervention, the group level for two RoIs showed differences, in contrast to the findings on the SCTI group.

These results suggest that Colombian ex-combatants that received the social cognition training improved their EP, especially in the processing of emotional information with positive valence.

# 7. Conclusions and further research

## 7.1. General conclusions and main contributions

Colombia has suffered for over 50 years of an internal armed conflict involving illegal armed groups (guerrilla organizations and paramilitary groups) and the national armed forces. In order to reintegrate Colombian ex-combatants to civilian life, the State created the Disarmament, Demobilization and reintegration (DDR) program. In some cases, social reintegration process of ex-combatants is overshadowed because chronic exposure to violence affects their emotional processing (EP). EP is a cognitive process crucial for human adaptation and survival. In that sense, EP of Colombian ex-combatants has to be understood in order to improve the conventional reintegration programs. Taking into account the above mentioned challenges, this thesis was aimed to develop a methodology focused on analyzing EP from EEG data of Colombian Ex-combatants using functional connectivity analysis.

This work was divided into four parts: (i) preprocessing, (ii) selection of the metric for functional connectivity analysis, (iii) characterization of EP of Colombian ex-combatants and (iv) a case of study. Starting with the preprocessing stage (i), we used a Blind Source Separation (BSS) method to remove the artifactual noise of EEG signals. Then, an automatic classifier was developed for neural and artifactual EEG components which severely reduced the processing time. The classifier consisted on the combination of Independent Component Analysis (ICA) and a Support Vector Machine (C-SVM) trained with 32 EEG registers of university students. Our classifier had the ability to isolate the artifacts components with a high accuracy (95.6%), similar to those reported in the state of the art.

In the second part (ii), we presented the advantages and drawbacks of five widely used functional connectivity metrics: Pearson's Correlation Coefficient (COR), Cross-Correlation function (XCOR), Coherence function (COH), the Imaginary part of Coherency (ICOH), and Phase Lag Index (PLI). For that, their connectivity spatial pattern representations were generated and several Linear Discriminant Analysis (LDA) were implemented. In the spatial patterns we identified that a fundamental difficulty for COR, XCOR and COH metrics is the fact that their results were influenced by the volume conduction. It is because the patterns of these metrics reveled that the connectivity was dominated by local connections among adjacent sensors. In contrast, PLI and ICOH patterns were similar to each other in all frequency bands. Local connections were absent in ICOH and PLI. Then, the volume

conduction related influence was diminished in the case of ICOH and PLI. Additionally, with the results of LDA we could conclude that ICOH presented the best performance, because this metric was the best in classifying between ex-combatants and civilian people for two of the three task conditions.

In the third part (iii), ex-combatants showed significant differences in the processing of emotional information with positive valence. These differences were found in the Beta frequency band for the connectivity across two pairs: the first conformed by the medial central-parietal (Cz-Cpz) region and the right central-parietal (C2, Cp2, C4, Cp4) region and the second conformed by the right central-parietal region and the left parietal-occipital (P1, P3, Po3, Po5) region. With these results, we conclude that Colombian ex-combatants and civilian people show a similar processing of emotional information for stimuli with neutral and negative valence, but differences in the stimuli with positive valence were found. These atypical connectivities may be due to the conditions experienced in the armed conflict. For further analysis, there is potential on using these functional markers in diagnosis and as a first step to guide future intervention treatments. Additionally, we were able to confirm the hypothesis that it is possible to establish a methodology to find significant differences in EP between Colombian ex-combatants and people not directly exposed to the armed conflict using a brain functional connectivity analysis.

Finally, in the forth part (iv), the proposed methodology to recognize atypical functioning of EP was used to quantitatively evaluate the efficacy of a social cognitive training program. Significant differences in the group of ex-combatants who received the intervention training in connectivity per condition and frequency band were found, while no significant differences were found for the group that did no receive the intervention. In addition, there is an increase in connectivity across the regions of interest in the group that received the training.

The results of this work allow identifying problems in the processing of emotional information of Colombian ex-combatants. This study provides new elements for characterizing psychological aspects associated with the emotional recognition of individuals exposed to situations of combat. Thus, the methodology developed in this thesis could be used as a decision support system to evaluate the effectiveness of the intervention protocols.

## 7.2. Future work

For future work, we propose to use this methodology in databases with new tasks of emotional recognition recently acquired with an EEG acquisition device with active electrodes. For the new task, it is hypothesized that the phenomenon under study is better captured.

Additionally, we suggest to improve the methodology using other approaches such as the

graph theory. Graph theory allows representing network as matrices or as graphs. A graph contains nodes (electrodes) and edges (connectivity strengths). The adjacency matrices are useful to visualize large networks, and graphs are useful to interpret relatively small networks. Matrices can be generated using any measure of power-based or phase-based connectivity. In EEG data, it is possible to quantify the strength of the connectivity between any pairs of electrodes. Additionally, graph theory can be used to analyze how the distribution of the functional network behaves, and to evaluate the segregation and integration in functional brain networks.

# A. Statistical Analysis: Ex-combatants vs. Controls

Table **A-1**.: Wilcoxon test results (Ex-combatants vs. Controls)

| RoIs | Ex-combatants Vs. Controls. | | | | | |
|---|---|---|---|---|---|---|
| | Controls | | Ex-combatants | | p-value | q-value |
| | MEDIAN | STD | MEDIAN | STD | | |
| **RoI1-RoI2** | 0,0122 | 0,0100 | 0,0108 | 0,0088 | **0,0214** | 0,1738 |
| **RoI1-RoI3** | 0,0122 | 0,0097 | 0,0112 | 0,0107 | 0,1129 | 0,2707 |
| **RoI1-RoI4** | 0,0135 | 0,0216 | 0,0125 | 0,0195 | 0,1624 | 0,2707 |
| **RoI1-RoI5** | 0,0123 | 0,0186 | 0,0116 | 0,0148 | 0,1364 | 0,2707 |
| **RoI1-RoI6** | 0,0131 | 0,0248 | 0,0125 | 0,0169 | 0,8825 | 0,8825 |
| **RoI2-RoI3** | 0,0124 | 0,0122 | 0,0114 | 0,0095 | **0,0232** | 0,1738 |
| **RoI2-RoI4** | 0,0122 | 0,0161 | 0,0113 | 0,0142 | 0,1542 | 0,2707 |
| **RoI2-RoI5** | 0,0137 | 0,0172 | 0,0136 | 0,0154 | 0,3912 | 0,4890 |
| **RoI2-RoI6** | 0,0130 | 0,0179 | 0,0132 | 0,0148 | 0,8369 | 0,8825 |
| **RoI3-RoI4** | 0,0131 | 0,0200 | 0,0118 | 0,0195 | 0,1118 | 0,2707 |
| **RoI3-RoI5** | 0,0130 | 0,0209 | 0,0123 | 0,0160 | **0,0491** | 0,2453 |
| **RoI3-RoI6** | 0,0137 | 0,0244 | 0,0129 | 0,0198 | 0,3386 | 0,4617 |
| **RoI4-RoI5** | 0,0125 | 0,0113 | 0,0121 | 0,0129 | 0,1101 | 0,2707 |
| **RoI4-RoI6** | 0,0146 | 0,0184 | 0,0141 | 0,0165 | 0,3254 | 0,4617 |
| **RoI5-RoI6** | 0,0147 | 0,0231 | 0,0150 | 0,0168 | 0,7437 | 0,8581 |

Table **A-2**.: Wilcoxon test results (Condition × group)

| RoIs | Condition × group (Ex-combatant vs. Control) | | | | | | | | | | | | | | | | | |
|---|---|---|---|---|---|---|---|---|---|---|---|---|---|---|---|---|---|---|
| | Negative | | | | | | Neutral | | | | | | Positive | | | | | |
| | Control | | Ex-combatant | | p | q | Control | | Ex-combatant | | p | q | Control | | Ex-combatant | | p | q |
| | $\widetilde{x}$ | STD | $\widetilde{x}$ | STD | | | $\widetilde{x}$ | STD | $\widetilde{x}$ | STD | | | $\widetilde{x}$ | STD | $\widetilde{x}$ | STD | | |
| **1-2** | 0,012 | 0,009 | 0,011 | 0,010 | 0,118 | 0,673 | 0,013 | 0,011 | 0,010 | 0,010 | 0,251 | 0,912 | 0,012 | 0,010 | 0,012 | 0,009 | 0,226 | 0,246 |
| **1-3** | 0,012 | 0,009 | 0,011 | 0,012 | 0,404 | 0,673 | 0,011 | 0,011 | 0,012 | 0,012 | 0,745 | 0,931 | 0,013 | 0,009 | 0,011 | 0,010 | **0,025** | 0,092 |
| **1-4** | 0,012 | 0,022 | 0,013 | 0,018 | 0,369 | 0,673 | 0,014 | 0,022 | 0,013 | 0,018 | 0,738 | 0,931 | 0,014 | 0,021 | 0,012 | 0,018 | **0,003** | 0,021 |
| **1-5** | 0,012 | 0,021 | 0,012 | 0,015 | 0,681 | 0,874 | 0,013 | 0,017 | 0,013 | 0,015 | 0,562 | 0,912 | 0,012 | 0,018 | 0,011 | 0,014 | 0,110 | 0,150 |
| **1-6** | 0,012 | 0,027 | 0,014 | 0,017 | 0,328 | 0,673 | 0,014 | 0,025 | 0,013 | 0,017 | 0,988 | 0,988 | 0,013 | 0,023 | 0,012 | 0,016 | 0,229 | 0,246 |
| **2-3** | 0,012 | 0,013 | 0,011 | 0,010 | 0,294 | 0,673 | 0,013 | 0,012 | 0,011 | 0,010 | 0,138 | 0,912 | 0,013 | 0,011 | 0,012 | 0,010 | 0,146 | 0,182 |
| **2-4** | 0,012 | 0,015 | 0,011 | 0,014 | 0,629 | 0,874 | 0,013 | 0,017 | 0,012 | 0,014 | 0,608 | 0,912 | 0,012 | 0,016 | 0,011 | 0,013 | **0,012** | 0,060 |
| **2-5** | 0,013 | 0,017 | 0,014 | 0,015 | 0,264 | 0,673 | 0,015 | 0,017 | 0,014 | 0,015 | 0,488 | 0,912 | 0,014 | 0,017 | 0,012 | 0,016 | 0,074 | 0,112 |
| **2-6** | 0,011 | 0,018 | 0,014 | 0,015 | 0,099 | 0,673 | 0,013 | 0,019 | 0,014 | 0,015 | 0,825 | 0,952 | 0,015 | 0,017 | 0,011 | 0,015 | 0,066 | 0,111 |
| **3-4** | 0,011 | 0,020 | 0,012 | 0,018 | 0,257 | 0,673 | 0,014 | 0,021 | 0,013 | 0,018 | 0,533 | 0,912 | 0,015 | 0,020 | 0,011 | 0,017 | **0,001** | 0,015 |
| **3-5** | 0,012 | 0,023 | 0,012 | 0,016 | 0,996 | 0,996 | 0,014 | 0,019 | 0,013 | 0,016 | 0,141 | 0,912 | 0,013 | 0,020 | 0,012 | 0,015 | 0,050 | 0,107 |
| **3-6** | 0,012 | 0,026 | 0,014 | 0,020 | 0,152 | 0,673 | 0,016 | 0,026 | 0,014 | 0,020 | 0,385 | 0,912 | 0,014 | 0,021 | 0,011 | 0,019 | **0,031** | 0,092 |
| **4-5** | 0,013 | 0,012 | 0,013 | 0,012 | 0,872 | 0,996 | 0,012 | 0,011 | 0,013 | 0,012 | 0,603 | 0,912 | 0,012 | 0,011 | 0,011 | 0,012 | **0,041** | 0,102 |
| **4-6** | 0,014 | 0,020 | 0,014 | 0,018 | 0,699 | 0,874 | 0,014 | 0,019 | 0,014 | 0,018 | 0,571 | 0,912 | 0,016 | 0,017 | 0,014 | 0,015 | 0,067 | 0,111 |
| **5-6** | 0,016 | 0,025 | 0,015 | 0,018 | 0,996 | 0,996 | 0,015 | 0,021 | 0,015 | 0,018 | 0,938 | 0,988 | 0,014 | 0,023 | 0,013 | 0,015 | 0,559 | 0,559 |

Table **A-3**.: Wilcoxon test results (Condition × band (DELTA) × group)

| RoIs | Condition × Delta(0.1 Hz-3.99 Hz) × group | | | | | | | | | | | | | | | | | |
|---|---|---|---|---|---|---|---|---|---|---|---|---|---|---|---|---|---|---|
| | Negative | | | | | | Neutral | | | | | | Positive | | | | | |
| | Control | | Ex-combatant | | p | q | Control | | Ex-combatant | | p | q | Control | | Ex-combatant | | p | q |
| | $\widetilde{x}$ | STD | $\widetilde{x}$ | STD | | | $\widetilde{x}$ | STD | $\widetilde{x}$ | STD | | | $\widetilde{x}$ | STD | $\widetilde{x}$ | STD | | |
| **1-2** | 0,023 | 0,013 | 0,012 | 0,010 | **0,042** | 0,506 | 0,020 | 0,017 | 0,014 | 0,012 | 0,090 | 0,674 | 0,024 | 0,013 | 0,016 | 0,010 | 0,216 | 0,289 |
| **1-3** | 0,018 | 0,013 | 0,014 | 0,012 | 0,642 | 0,740 | 0,023 | 0,016 | 0,016 | 0,014 | 0,263 | 0,674 | 0,021 | 0,013 | 0,015 | 0,010 | 0,051 | 0,161 |
| **1-4** | 0,023 | 0,040 | 0,014 | 0,021 | 0,317 | 0,701 | 0,024 | 0,041 | 0,018 | 0,020 | 0,357 | 0,674 | 0,026 | 0,040 | 0,017 | 0,016 | **0,014** | 0,143 |
| **1-5** | 0,023 | 0,033 | 0,014 | 0,015 | 0,135 | 0,506 | 0,024 | 0,025 | 0,022 | 0,017 | 0,470 | 0,674 | 0,027 | 0,033 | 0,014 | 0,011 | **0,027** | 0,143 |
| **1-6** | 0,031 | 0,049 | 0,017 | 0,014 | 0,327 | 0,701 | 0,018 | 0,045 | 0,021 | 0,019 | 0,820 | 0,878 | 0,030 | 0,049 | 0,015 | 0,015 | **0,029** | 0,143 |
| **2-3** | 0,026 | 0,019 | 0,014 | 0,011 | 0,125 | 0,506 | 0,021 | 0,018 | 0,015 | 0,012 | 0,067 | 0,674 | 0,027 | 0,019 | 0,017 | 0,013 | 0,098 | 0,184 |
| **2-4** | 0,021 | 0,025 | 0,014 | 0,018 | 0,628 | 0,740 | 0,019 | 0,029 | 0,021 | 0,014 | 0,411 | 0,674 | 0,018 | 0,025 | 0,016 | 0,018 | 0,337 | 0,389 |
| **2-5** | 0,025 | 0,026 | 0,018 | 0,015 | 0,520 | 0,740 | 0,026 | 0,020 | 0,023 | 0,016 | 0,446 | 0,674 | 0,028 | 0,026 | 0,021 | 0,016 | 0,115 | 0,192 |
| **2-6** | 0,023 | 0,033 | 0,016 | 0,013 | 0,913 | 0,913 | 0,021 | 0,030 | 0,021 | 0,018 | 0,789 | 0,878 | 0,022 | 0,033 | 0,015 | 0,025 | 0,195 | 0,289 |
| **3-4** | 0,025 | 0,036 | 0,015 | 0,024 | 0,714 | 0,765 | 0,026 | 0,037 | 0,022 | 0,022 | 0,378 | 0,674 | 0,024 | 0,036 | 0,017 | 0,021 | 0,094 | 0,184 |
| **3-5** | 0,024 | 0,036 | 0,016 | 0,015 | 0,317 | 0,701 | 0,032 | 0,026 | 0,024 | 0,019 | 0,400 | 0,674 | 0,031 | 0,036 | 0,017 | 0,012 | 0,054 | 0,161 |
| **3-6** | 0,027 | 0,048 | 0,017 | 0,017 | 0,446 | 0,740 | 0,027 | 0,044 | 0,024 | 0,022 | 0,820 | 0,878 | 0,030 | 0,048 | 0,016 | 0,021 | 0,076 | 0,184 |
| **4-5** | 0,025 | 0,017 | 0,018 | 0,014 | 0,120 | 0,506 | 0,019 | 0,013 | 0,017 | 0,010 | 0,327 | 0,674 | 0,019 | 0,017 | 0,014 | 0,011 | 0,231 | 0,289 |
| **4-6** | 0,024 | 0,028 | 0,016 | 0,013 | 0,572 | 0,740 | 0,023 | 0,024 | 0,020 | 0,016 | 0,494 | 0,674 | 0,021 | 0,028 | 0,024 | 0,009 | 0,368 | 0,394 |
| **5-6** | 0,023 | 0,026 | 0,026 | 0,013 | 0,507 | 0,740 | 0,026 | 0,023 | 0,022 | 0,017 | 0,976 | 0,976 | 0,024 | 0,026 | 0,023 | 0,015 | 0,533 | 0,533 |

Table **A-4**.: Wilcoxon test results (Condition × band (THETA) × group)

| RoIs | Condition × Theta(4.0 Hz- 7.99 Hz) × group | | | | | | | | | | | | | | | | | |
|---|---|---|---|---|---|---|---|---|---|---|---|---|---|---|---|---|---|---|
| | Negative | | | | | | Neutral | | | | | | Positive | | | | | |
| | Control | | Ex-combatant | | p | q | Control | | Ex-combatant | | p | q | Control | | Ex-combatant | | p | q |
| | $\widetilde{x}$ | STD | $\widetilde{x}$ | STD | | | $\widetilde{x}$ | STD | $\widetilde{x}$ | STD | | | $\widetilde{x}$ | STD | $\widetilde{x}$ | STD | | |
| **1-2** | 0,013 | 0,009 | 0,011 | 0,009 | 0,327 | 0,836 | 0,013 | 0,011 | 0,012 | 0,009 | 0,685 | 0,790 | 0,016 | 0,009 | 0,014 | 0,010 | 0,614 | 0,708 |
| **1-3** | 0,013 | 0,010 | 0,011 | 0,014 | 0,789 | 0,912 | 0,014 | 0,009 | 0,015 | 0,011 | 0,255 | 0,765 | 0,018 | 0,010 | 0,014 | 0,011 | 0,446 | 0,669 |
| **1-4** | 0,012 | 0,010 | 0,016 | 0,034 | 0,098 | 0,705 | 0,015 | 0,011 | 0,017 | 0,025 | 0,520 | 0,784 | 0,023 | 0,010 | 0,015 | 0,027 | 0,216 | 0,540 |
| **1-5** | 0,014 | 0,018 | 0,016 | 0,022 | 0,789 | 0,912 | 0,021 | 0,017 | 0,014 | 0,019 | 0,107 | 0,680 | 0,022 | 0,018 | 0,017 | 0,021 | 0,600 | 0,708 |
| **1-6** | 0,014 | 0,022 | 0,017 | 0,028 | 0,546 | 0,900 | 0,024 | 0,020 | 0,021 | 0,023 | 0,533 | 0,784 | 0,024 | 0,022 | 0,018 | 0,021 | 0,559 | 0,708 |
| **2-3** | 0,014 | 0,007 | 0,010 | 0,008 | 0,169 | 0,705 | 0,014 | 0,009 | 0,013 | 0,009 | 0,929 | 0,929 | 0,016 | 0,007 | 0,013 | 0,008 | 0,090 | 0,452 |
| **2-4** | 0,011 | 0,013 | 0,016 | 0,022 | 0,188 | 0,705 | 0,011 | 0,007 | 0,014 | 0,019 | 0,181 | 0,680 | 0,017 | 0,013 | 0,011 | 0,015 | 0,087 | 0,452 |
| **2-5** | 0,018 | 0,014 | 0,018 | 0,019 | 0,961 | 0,961 | 0,020 | 0,018 | 0,016 | 0,017 | 0,327 | 0,784 | 0,024 | 0,014 | 0,015 | 0,020 | 0,175 | 0,525 |
| **2-6** | 0,017 | 0,013 | 0,018 | 0,018 | 0,434 | 0,836 | 0,016 | 0,016 | 0,020 | 0,018 | 0,157 | 0,680 | 0,018 | 0,013 | 0,015 | 0,013 | 0,347 | 0,648 |
| **3-4** | 0,008 | 0,013 | 0,015 | 0,033 | **0,032** | 0,475 | 0,014 | 0,009 | 0,015 | 0,026 | 0,389 | 0,784 | 0,020 | 0,013 | 0,014 | 0,021 | 0,080 | 0,452 |
| **3-5** | 0,017 | 0,020 | 0,016 | 0,022 | 0,804 | 0,912 | 0,024 | 0,018 | 0,019 | 0,019 | 0,090 | 0,680 | 0,025 | 0,020 | 0,013 | 0,022 | 0,175 | 0,525 |
| **3-6** | 0,015 | 0,018 | 0,016 | 0,027 | 0,423 | 0,836 | 0,025 | 0,022 | 0,022 | 0,025 | 0,759 | 0,813 | 0,025 | 0,018 | 0,015 | 0,023 | 0,255 | 0,546 |
| **4-5** | 0,016 | 0,014 | 0,019 | 0,020 | 0,851 | 0,912 | 0,017 | 0,014 | 0,019 | 0,018 | 0,614 | 0,784 | 0,022 | 0,014 | 0,019 | 0,018 | 0,685 | 0,734 |
| **4-6** | 0,022 | 0,025 | 0,020 | 0,023 | 0,600 | 0,900 | 0,020 | 0,025 | 0,023 | 0,027 | 0,533 | 0,784 | 0,025 | 0,025 | 0,024 | 0,022 | 0,389 | 0,648 |
| **5-6** | 0,022 | 0,043 | 0,032 | 0,026 | 0,446 | 0,836 | 0,024 | 0,035 | 0,032 | 0,025 | 0,628 | 0,784 | 0,021 | 0,043 | 0,026 | 0,021 | 0,789 | 0,789 |

Table **A-5**.: Wilcoxon test results (Condition × band (ALPHA) × group

| RoIs | **Condition × Alpha (8.0 Hz - 13.99 Hz) × group** | | | | | | | | | | | | | | | | | |
|---|---|---|---|---|---|---|---|---|---|---|---|---|---|---|---|---|---|---|
| | **Negative** | | | | | | **Neutral** | | | | | | **Positive** | | | | | |
| | **Control** | | **Ex-combatant** | | **p** | **q** | **Control** | | **Ex-combatant** | | **p** | **q** | **Control** | | **Ex-combatant** | | **p** | **q** |
| | $\widetilde{x}$ | **STD** | $\widetilde{x}$ | **STD** | | | $\widetilde{x}$ | **STD** | $\widetilde{x}$ | **STD** | | | $\widetilde{x}$ | **STD** | $\widetilde{x}$ | **STD** | | |
| **1-2** | 0,013 | 0,005 | 0,012 | 0,008 | 0,494 | 0,912 | 0,010 | 0,008 | 0,013 | 0,012 | 0,458 | 0,945 | 0,015 | 0,005 | 0,010 | 0,011 | 0,247 | 0,740 |
| **1-3** | 0,014 | 0,007 | 0,014 | 0,013 | 0,929 | 0,929 | 0,009 | 0,010 | 0,013 | 0,016 | 0,572 | 0,945 | 0,013 | 0,007 | 0,011 | 0,012 | 0,247 | 0,740 |
| **1-4** | 0,012 | 0,013 | 0,014 | 0,024 | 0,729 | 0,912 | 0,016 | 0,018 | 0,016 | 0,018 | 0,898 | 0,945 | 0,015 | 0,013 | 0,013 | 0,022 | 0,729 | 0,893 |
| **1-5** | 0,012 | 0,016 | 0,014 | 0,017 | 0,559 | 0,912 | 0,013 | 0,015 | 0,015 | 0,015 | 0,559 | 0,945 | 0,014 | 0,016 | 0,011 | 0,017 | 0,317 | 0,793 |
| **1-6** | 0,012 | 0,015 | 0,017 | 0,019 | 0,188 | 0,912 | 0,014 | 0,016 | 0,015 | 0,016 | 0,945 | 0,945 | 0,016 | 0,015 | 0,013 | 0,020 | 0,656 | 0,893 |
| **2-3** | 0,013 | 0,014 | 0,014 | 0,011 | 0,789 | 0,912 | 0,013 | 0,013 | 0,014 | 0,012 | 0,774 | 0,945 | 0,018 | 0,014 | 0,012 | 0,011 | 0,209 | 0,740 |
| **2-4** | 0,014 | 0,009 | 0,014 | 0,013 | 0,851 | 0,912 | 0,015 | 0,015 | 0,015 | 0,016 | 0,851 | 0,945 | 0,013 | 0,009 | 0,013 | 0,011 | 0,976 | 0,992 |
| **2-5** | 0,014 | 0,016 | 0,018 | 0,019 | 0,586 | 0,912 | 0,017 | 0,021 | 0,018 | 0,019 | 0,929 | 0,945 | 0,014 | 0,016 | 0,016 | 0,019 | 0,494 | 0,845 |
| **2-6** | 0,015 | 0,011 | 0,016 | 0,015 | 0,494 | 0,912 | 0,016 | 0,018 | 0,017 | 0,016 | 0,347 | 0,945 | 0,016 | 0,011 | 0,015 | 0,014 | 0,992 | 0,992 |
| **3-4** | 0,013 | 0,009 | 0,015 | 0,024 | 0,699 | 0,912 | 0,016 | 0,017 | 0,015 | 0,017 | 0,520 | 0,945 | 0,013 | 0,009 | 0,013 | 0,019 | 0,774 | 0,893 |
| **3-5** | 0,014 | 0,018 | 0,016 | 0,021 | 0,520 | 0,912 | 0,016 | 0,020 | 0,015 | 0,018 | 0,533 | 0,945 | 0,015 | 0,018 | 0,016 | 0,018 | 0,614 | 0,893 |
| **3-6** | 0,012 | 0,015 | 0,017 | 0,026 | 0,151 | 0,912 | 0,022 | 0,020 | 0,015 | 0,023 | 0,175 | 0,945 | 0,015 | 0,015 | 0,012 | 0,024 | 0,507 | 0,845 |
| **4-5** | 0,014 | 0,008 | 0,018 | 0,011 | 0,378 | 0,912 | 0,012 | 0,009 | 0,016 | 0,011 | 0,239 | 0,945 | 0,018 | 0,008 | 0,012 | 0,010 | 0,247 | 0,740 |
| **4-6** | 0,016 | 0,012 | 0,016 | 0,012 | 0,820 | 0,912 | 0,016 | 0,017 | 0,018 | 0,013 | 0,389 | 0,945 | 0,022 | 0,012 | 0,017 | 0,011 | 0,163 | 0,740 |
| **5-6** | 0,022 | 0,015 | 0,026 | 0,013 | 0,614 | 0,912 | 0,022 | 0,013 | 0,020 | 0,013 | 0,898 | 0,945 | 0,018 | 0,015 | 0,022 | 0,011 | 0,507 | 0,845 |

Table **A-6**.: Wilcoxon test results (Condition × band (BETA) × group

| RoIs | Condition × Beta (14.0 Hz - 29.99 Hz) × group | | | | | | | | | | | | | | | | | |
|---|---|---|---|---|---|---|---|---|---|---|---|---|---|---|---|---|---|---|
| | Negative | | | | | | Neutral | | | | | | Positive | | | | | |
| | Control | | Ex-combatant | | p | q | Control | | Ex-combatant | | p | q | Control | | Ex-combatant | | p | q |
| | $\widetilde{x}$ | STD | $\widetilde{x}$ | STD | | | $\widetilde{x}$ | STD | $\widetilde{x}$ | STD | | | $\widetilde{x}$ | STD | $\widetilde{x}$ | STD | | |
| **1-2** | 0,010 | 0,003 | 0,009 | 0,003 | 0,546 | 0,858 | 0,011 | 0,003 | 0,009 | 0,004 | **0,047** | 0,349 | 0,009 | 0,003 | 0,009 | 0,004 | 0,685 | 0,781 |
| **1-3** | 0,012 | 0,005 | 0,009 | 0,004 | 0,327 | 0,858 | 0,011 | 0,004 | 0,010 | 0,005 | 0,714 | 0,992 | 0,012 | 0,005 | 0,009 | 0,004 | 0,231 | 0,493 |
| **1-4** | 0,012 | 0,005 | 0,010 | 0,005 | 0,337 | 0,858 | 0,012 | 0,004 | 0,011 | 0,006 | 0,976 | 0,992 | 0,013 | 0,005 | 0,010 | 0,004 | 0,070 | 0,262 |
| **1-5** | 0,011 | 0,003 | 0,009 | 0,003 | 0,169 | 0,858 | 0,010 | 0,002 | 0,011 | 0,003 | 0,961 | 0,992 | 0,010 | 0,003 | 0,010 | 0,004 | 0,729 | 0,781 |
| **1-6** | 0,011 | 0,003 | 0,010 | 0,004 | 0,685 | 0,858 | 0,011 | 0,003 | 0,010 | 0,005 | 0,898 | 0,992 | 0,010 | 0,003 | 0,011 | 0,004 | 0,411 | 0,561 |
| **2-3** | 0,010 | 0,003 | 0,010 | 0,004 | 0,699 | 0,858 | 0,011 | 0,002 | 0,010 | 0,005 | 0,175 | 0,656 | 0,010 | 0,003 | 0,010 | 0,004 | 0,820 | 0,820 |
| **2-4** | 0,009 | 0,003 | 0,009 | 0,004 | 0,446 | 0,858 | 0,011 | 0,003 | 0,009 | 0,003 | **0,042** | 0,349 | 0,011 | 0,003 | 0,009 | 0,003 | **0,004** | 0,034 |
| **2-5** | 0,009 | 0,002 | 0,010 | 0,003 | 0,337 | 0,858 | 0,010 | 0,003 | 0,011 | 0,004 | 0,992 | 0,992 | 0,012 | 0,002 | 0,009 | 0,005 | **0,039** | 0,193 |
| **2-6** | 0,010 | 0,003 | 0,009 | 0,004 | 0,744 | 0,858 | 0,010 | 0,003 | 0,010 | 0,004 | 0,520 | 0,992 | 0,010 | 0,003 | 0,009 | 0,003 | 0,120 | 0,360 |
| **3-4** | 0,010 | 0,006 | 0,009 | 0,004 | 0,140 | 0,858 | 0,011 | 0,004 | 0,010 | 0,004 | 0,337 | 0,842 | 0,013 | 0,006 | 0,009 | 0,003 | **0,001** | 0,009 |
| **3-5** | 0,010 | 0,004 | 0,010 | 0,004 | 0,670 | 0,858 | 0,011 | 0,002 | 0,011 | 0,005 | 0,820 | 0,992 | 0,010 | 0,004 | 0,010 | 0,005 | 0,559 | 0,699 |
| **3-6** | 0,010 | 0,005 | 0,010 | 0,004 | 0,929 | 0,929 | 0,012 | 0,003 | 0,010 | 0,005 | 0,789 | 0,992 | 0,011 | 0,005 | 0,010 | 0,004 | 0,299 | 0,498 |
| **4-5** | 0,010 | 0,003 | 0,011 | 0,004 | 0,835 | 0,895 | 0,011 | 0,003 | 0,009 | 0,003 | 0,125 | 0,624 | 0,010 | 0,003 | 0,009 | 0,005 | 0,263 | 0,493 |
| **4-6** | 0,011 | 0,003 | 0,011 | 0,006 | 0,656 | 0,858 | 0,010 | 0,003 | 0,010 | 0,005 | 0,628 | 0,992 | 0,011 | 0,003 | 0,010 | 0,008 | 0,255 | 0,493 |
| **5-6** | 0,011 | 0,004 | 0,011 | 0,003 | 0,685 | 0,858 | 0,011 | 0,003 | 0,010 | 0,003 | 0,263 | 0,790 | 0,010 | 0,004 | 0,010 | 0,004 | 0,389 | 0,561 |

Table **A-7**.: Wilcoxon test results (Condition × band (GAMMA) × group

| RoIs | **Condition × Gamma (30.0 Hz - 59.99 Hz) × group** | | | | | | | | | | | | | | | | | |
|---|---|---|---|---|---|---|---|---|---|---|---|---|---|---|---|---|---|---|
| | **Negative** | | | | | | **Neutral** | | | | | | **Positive** | | | | | |
| | **Control** | | **Ex-combatant** | | **p** | **q** | **Control** | | **Ex-combatant** | | **p** | **q** | **Control** | | **Ex-combatant** | | **p** | **q** |
| | $\widetilde{x}$ | **STD** | $\widetilde{x}$ | **STD** | | | $\widetilde{x}$ | **STD** | $\widetilde{x}$ | **STD** | | | $\widetilde{x}$ | **STD** | $\widetilde{x}$ | **STD** | | |
| **1-2** | 0,010 | 0,003 | 0,009 | 0,005 | 1,000 | 1,000 | 0,010 | 0,003 | 0,009 | 0,005 | 0,090 | 0,976 | 0,010 | 0,003 | 0,009 | 0,004 | 0,458 | 0,528 |
| **1-3** | 0,009 | 0,002 | 0,009 | 0,004 | 0,744 | 0,928 | 0,010 | 0,003 | 0,009 | 0,004 | 0,263 | 0,976 | 0,010 | 0,002 | 0,009 | 0,004 | 0,327 | 0,446 |
| **1-4** | 0,009 | 0,004 | 0,012 | 0,008 | 0,073 | 0,471 | 0,011 | 0,005 | 0,010 | 0,009 | 0,357 | 0,976 | 0,010 | 0,004 | 0,009 | 0,008 | 0,061 | 0,306 |
| **1-5** | 0,009 | 0,005 | 0,010 | 0,008 | 0,685 | 0,928 | 0,010 | 0,007 | 0,010 | 0,010 | 0,470 | 0,976 | 0,010 | 0,005 | 0,009 | 0,009 | 0,255 | 0,434 |
| **1-6** | 0,010 | 0,005 | 0,010 | 0,010 | 0,586 | 0,879 | 0,010 | 0,006 | 0,010 | 0,012 | 0,820 | 0,976 | 0,011 | 0,005 | 0,008 | 0,011 | 0,169 | 0,434 |
| **2-3** | 0,009 | 0,003 | 0,010 | 0,004 | 0,327 | 0,613 | 0,011 | 0,003 | 0,009 | 0,005 | 0,067 | 0,976 | 0,009 | 0,003 | 0,009 | 0,004 | 0,992 | 0,992 |
| **2-4** | 0,008 | 0,004 | 0,010 | 0,006 | 0,209 | 0,495 | 0,010 | 0,005 | 0,010 | 0,006 | 0,411 | 0,976 | 0,012 | 0,004 | 0,010 | 0,006 | 0,280 | 0,434 |
| **2-5** | 0,009 | 0,004 | 0,010 | 0,007 | 0,094 | 0,471 | 0,011 | 0,006 | 0,012 | 0,008 | 0,446 | 0,976 | 0,011 | 0,004 | 0,009 | 0,007 | 0,546 | 0,585 |
| **2-6** | 0,010 | 0,005 | 0,010 | 0,010 | 0,231 | 0,495 | 0,011 | 0,007 | 0,010 | 0,009 | 0,789 | 0,976 | 0,010 | 0,005 | 0,009 | 0,009 | 0,146 | 0,434 |
| **3-4** | 0,008 | 0,005 | 0,011 | 0,008 | **0,042** | 0,471 | 0,009 | 0,005 | 0,010 | 0,008 | 0,378 | 0,976 | 0,010 | 0,005 | 0,009 | 0,008 | 0,272 | 0,434 |
| **3-5** | 0,009 | 0,005 | 0,009 | 0,009 | 0,400 | 0,667 | 0,010 | 0,007 | 0,009 | 0,011 | 0,400 | 0,976 | 0,011 | 0,005 | 0,009 | 0,009 | 0,289 | 0,434 |
| **3-6** | 0,009 | 0,005 | 0,010 | 0,012 | 0,188 | 0,495 | 0,010 | 0,007 | 0,009 | 0,014 | 0,820 | 0,976 | 0,010 | 0,005 | 0,008 | 0,013 | 0,255 | 0,434 |
| **4-5** | 0,010 | 0,007 | 0,009 | 0,012 | 0,961 | 1,000 | 0,010 | 0,007 | 0,010 | 0,012 | 0,327 | 0,976 | 0,011 | 0,007 | 0,009 | 0,011 | **0,013** | 0,194 |
| **4-6** | 0,009 | 0,005 | 0,010 | 0,018 | 0,231 | 0,495 | 0,010 | 0,005 | 0,011 | 0,016 | 0,494 | 0,976 | 0,011 | 0,005 | 0,009 | 0,014 | 0,400 | 0,500 |
| **5-6** | 0,011 | 0,005 | 0,010 | 0,005 | 0,804 | 0,928 | 0,011 | 0,007 | 0,011 | 0,006 | 0,976 | 0,976 | 0,012 | 0,005 | 0,009 | 0,006 | **0,035** | 0,262 |

# B. Statistical Analysis: Social Cognitive Training Intervention (SCTI)

Table **B-1**.: Wilcoxon test results. SCTI PRE vs. SCTI POST

| RoIs | SCTI PRE vs. SCTI POST | | | | | |
|---|---|---|---|---|---|---|
| | SCTI PRE | | SCTI POST | | p-value | q-value |
| | MEDIAN | STD | MEDIAN | STD | | |
| **RoI1-RoI2** | 0,0108 | 0,0074 | 0,0125 | 0,0125 | **0,0123** | 0,0181 |
| **RoI1-RoI3** | 0,0109 | 0,0098 | 0,0128 | 0,0120 | **0,0200** | 0,0249 |
| **RoI1-RoI4** | 0,0123 | 0,0220 | 0,0161 | 0,0199 | **0,0005** | 0,0027 |
| **RoI1-RoI5** | 0,0116 | 0,0155 | 0,0142 | 0,0166 | **0,0016** | 0,0060 |
| **RoI1-RoI6** | 0,0123 | 0,0187 | 0,0155 | 0,0199 | **0,0098** | 0,0181 |
| **RoI2-RoI3** | 0,0112 | 0,0094 | 0,0134 | 0,0300 | **0,0130** | 0,0181 |
| **RoI2-RoI4** | 0,0112 | 0,0153 | 0,0135 | 0,0131 | **0,0005** | 0,0027 |
| **RoI2-RoI5** | 0,0142 | 0,0146 | 0,0161 | 0,0164 | **0,0268** | 0,0309 |
| **RoI2-RoI6** | 0,0133 | 0,0169 | 0,0153 | 0,0181 | **0,0132** | 0,0181 |
| **RoI3-RoI4** | 0,0118 | 0,0221 | 0,0152 | 0,0235 | **0,0004** | 0,0027 |
| **RoI3-RoI5** | 0,0119 | 0,0169 | 0,0157 | 0,0199 | **0,0059** | 0,0164 |
| **RoI3-RoI6** | 0,0129 | 0,0219 | 0,0159 | 0,0268 | **0,0066** | 0,0164 |
| **RoI4-RoI5** | 0,0122 | 0,0155 | 0,0148 | 0,0185 | **0,0099** | 0,0181 |
| **RoI4-RoI6** | 0,0156 | 0,0163 | 0,0167 | 0,0230 | 0,1132 | 0,1213 |
| **RoI5-RoI6** | 0,0179 | 0,0201 | 0,0193 | 0,0223 | 0,6463 | 0,6463 |

Table **B-2**.: Wilcoxon test results. (Condition × group)

| RoIs | Condition × group (SCTI PRE vs. SCTI POST) | | | | | | | | | | | | | | | | | |
|---|---|---|---|---|---|---|---|---|---|---|---|---|---|---|---|---|---|---|
| | Negative | | | | | | Neutral | | | | | | Positive | | | | | |
| | PRE | | POST | | p | q | PRE | | POST | | p | q | PRE | | POST | | p | q |
| | $\widetilde{x}$ | STD | $\widetilde{x}$ | STD | | | $\widetilde{x}$ | STD | $\widetilde{x}$ | STD | | | $\widetilde{x}$ | STD | $\widetilde{x}$ | STD | | |
| **1-2** | 0,012 | 0,006 | 0,013 | 0,012 | 0,153 | 0,256 | 0,010 | 0,007 | 0,012 | 0,012 | **0,034** | 0,271 | 0,011 | 0,008 | 0,013 | 0,014 | 0,377 | 0,435 |
| **1-3** | 0,011 | 0,011 | 0,013 | 0,011 | 0,103 | 0,220 | 0,011 | 0,009 | 0,013 | 0,014 | 0,291 | 0,364 | 0,010 | 0,009 | 0,012 | 0,010 | 0,205 | 0,308 |
| **1-4** | 0,012 | 0,025 | 0,015 | 0,018 | **0,047** | 0,177 | 0,014 | 0,019 | 0,016 | 0,022 | 0,129 | 0,271 | 0,011 | 0,021 | 0,016 | 0,019 | **0,009** | 0,055 |
| **1-5** | 0,011 | 0,017 | 0,016 | 0,016 | **0,027** | 0,165 | 0,012 | 0,014 | 0,014 | 0,019 | 0,145 | 0,271 | 0,011 | 0,016 | 0,014 | 0,014 | 0,082 | 0,177 |
| **1-6** | 0,014 | 0,020 | 0,015 | 0,018 | 0,199 | 0,256 | 0,013 | 0,018 | 0,017 | 0,023 | 0,238 | 0,337 | 0,012 | 0,018 | 0,015 | 0,018 | **0,031** | 0,087 |
| **2-3** | 0,011 | 0,008 | 0,014 | 0,030 | **0,025** | 0,165 | 0,011 | 0,009 | 0,014 | 0,031 | 0,092 | 0,271 | 0,011 | 0,010 | 0,012 | 0,029 | 0,718 | 0,770 |
| **2-4** | 0,011 | 0,016 | 0,014 | 0,013 | 0,074 | 0,211 | 0,013 | 0,015 | 0,013 | 0,014 | 0,086 | 0,271 | 0,011 | 0,015 | 0,014 | 0,012 | **0,011** | 0,055 |
| **2-5** | 0,013 | 0,014 | 0,016 | 0,018 | 0,084 | 0,211 | 0,015 | 0,013 | 0,017 | 0,017 | 0,316 | 0,364 | 0,013 | 0,016 | 0,015 | 0,015 | 0,250 | 0,316 |
| **2-6** | 0,014 | 0,015 | 0,015 | 0,017 | 0,177 | 0,256 | 0,016 | 0,017 | 0,017 | 0,019 | 0,143 | 0,271 | 0,012 | 0,019 | 0,015 | 0,018 | 0,146 | 0,273 |
| **3-4** | 0,012 | 0,026 | 0,014 | 0,022 | 0,168 | 0,256 | 0,012 | 0,020 | 0,014 | 0,028 | 0,080 | 0,271 | 0,011 | 0,020 | 0,016 | 0,020 | **0,003** | 0,042 |
| **3-5** | 0,012 | 0,018 | 0,016 | 0,019 | **0,033** | 0,165 | 0,013 | 0,016 | 0,016 | 0,023 | 0,121 | 0,271 | 0,011 | 0,017 | 0,014 | 0,018 | 0,200 | 0,308 |
| **3-6** | 0,014 | 0,023 | 0,015 | 0,025 | 0,219 | 0,256 | 0,015 | 0,022 | 0,018 | 0,030 | 0,193 | 0,322 | 0,011 | 0,022 | 0,015 | 0,025 | **0,035** | 0,087 |
| **4-5** | 0,014 | 0,016 | 0,015 | 0,017 | 0,222 | 0,256 | 0,013 | 0,015 | 0,015 | 0,023 | 0,247 | 0,337 | 0,011 | 0,015 | 0,014 | 0,014 | **0,035** | 0,087 |
| **4-6** | 0,015 | 0,018 | 0,015 | 0,022 | 0,334 | 0,358 | 0,016 | 0,016 | 0,018 | 0,028 | 0,516 | 0,552 | 0,016 | 0,015 | 0,016 | 0,018 | 0,253 | 0,316 |
| **5-6** | 0,019 | 0,020 | 0,020 | 0,025 | 0,641 | 0,641 | 0,017 | 0,022 | 0,020 | 0,025 | 0,934 | 0,934 | 0,019 | 0,018 | 0,019 | 0,016 | 0,804 | 0,804 |

Table **B-3**.: Wilcoxon test results. (Condition × band (DELTA) × group)

| RoIs | Condition × Delta (0.1 - 3.99 Hz) × Group (SCTI PRE vs. SCTI POST) | | | | | | | | | | | | | | | | | |
|---|---|---|---|---|---|---|---|---|---|---|---|---|---|---|---|---|---|---|
| | Negative | | | | | | Neutral | | | | | | Positive | | | | | |
| | PRE | | POST | | p | q | PRE | | POST | | p | q | PRE | | POST | | p | q |
| | $\widetilde{x}$ | STD | $\widetilde{x}$ | STD | | | $\widetilde{x}$ | STD | $\widetilde{x}$ | STD | | | $\widetilde{x}$ | STD | $\widetilde{x}$ | STD | | |
| **1-2** | 0,016 | 0,006 | 0,020 | 0,013 | 0,340 | 0,610 | 0,013 | 0,009 | 0,016 | 0,013 | 0,407 | 0,872 | 0,017 | 0,011 | 0,016 | 0,011 | 0,361 | 0,967 |
| **1-3** | 0,016 | 0,011 | 0,018 | 0,012 | 0,213 | 0,610 | 0,013 | 0,008 | 0,016 | 0,014 | 0,184 | 0,872 | 0,015 | 0,012 | 0,018 | 0,015 | 0,709 | 0,967 |
| **1-4** | 0,016 | 0,017 | 0,030 | 0,026 | 0,199 | 0,610 | 0,017 | 0,022 | 0,023 | 0,019 | 0,678 | 0,964 | 0,018 | 0,019 | 0,031 | 0,028 | 0,081 | 0,611 |
| **1-5** | 0,022 | 0,013 | 0,035 | 0,026 | 0,407 | 0,610 | 0,022 | 0,018 | 0,022 | 0,018 | 0,407 | 0,872 | 0,022 | 0,012 | 0,021 | 0,024 | 0,836 | 0,967 |
| **1-6** | 0,028 | 0,014 | 0,019 | 0,024 | 0,934 | 0,934 | 0,021 | 0,020 | 0,024 | 0,018 | 0,967 | 0,967 | 0,019 | 0,019 | 0,022 | 0,027 | 0,407 | 0,967 |
| **2-3** | 0,025 | 0,011 | 0,026 | 0,036 | 0,340 | 0,610 | 0,015 | 0,014 | 0,018 | 0,030 | 0,300 | 0,872 | 0,017 | 0,016 | 0,023 | 0,020 | 0,934 | 0,967 |
| **2-4** | 0,017 | 0,013 | 0,025 | 0,018 | 0,213 | 0,610 | 0,022 | 0,014 | 0,014 | 0,015 | 0,481 | 0,901 | 0,017 | 0,023 | 0,025 | 0,019 | 0,340 | 0,967 |
| **2-5** | 0,026 | 0,013 | 0,028 | 0,025 | 0,803 | 0,861 | 0,029 | 0,016 | 0,028 | 0,017 | 0,967 | 0,967 | 0,029 | 0,019 | 0,027 | 0,019 | 0,934 | 0,967 |
| **2-6** | 0,025 | 0,013 | 0,021 | 0,020 | 0,648 | 0,810 | 0,027 | 0,022 | 0,026 | 0,017 | 0,836 | 0,964 | 0,024 | 0,031 | 0,025 | 0,022 | 0,803 | 0,967 |
| **3-4** | 0,015 | 0,022 | 0,039 | 0,029 | 0,199 | 0,610 | 0,021 | 0,023 | 0,019 | 0,025 | 0,648 | 0,964 | 0,016 | 0,026 | 0,033 | 0,028 | 0,074 | 0,611 |
| **3-5** | 0,023 | 0,016 | 0,037 | 0,027 | 0,384 | 0,610 | 0,025 | 0,021 | 0,030 | 0,022 | 0,407 | 0,872 | 0,027 | 0,014 | 0,021 | 0,027 | 0,967 | 0,967 |
| **3-6** | 0,025 | 0,018 | 0,026 | 0,027 | 0,590 | 0,804 | 0,025 | 0,026 | 0,025 | 0,025 | 0,709 | 0,964 | 0,017 | 0,027 | 0,027 | 0,030 | 0,481 | 0,967 |
| **4-5** | 0,020 | 0,012 | 0,024 | 0,014 | 0,320 | 0,610 | 0,015 | 0,011 | 0,018 | 0,010 | 0,213 | 0,872 | 0,018 | 0,013 | 0,016 | 0,014 | 0,648 | 0,967 |
| **4-6** | 0,021 | 0,009 | 0,030 | 0,020 | 0,158 | 0,610 | 0,016 | 0,017 | 0,025 | 0,016 | 0,229 | 0,872 | 0,026 | 0,011 | 0,025 | 0,014 | 0,534 | 0,967 |
| **5-6** | 0,027 | 0,014 | 0,029 | 0,023 | 0,803 | 0,861 | 0,026 | 0,022 | 0,025 | 0,018 | 0,772 | 0,964 | 0,029 | 0,017 | 0,021 | 0,014 | 0,125 | 0,624 |

Table **B-4**.: Wilcoxon test results. (Condition × band (THETA) × group )

| RoIs | Condition × Theta (4.0 - 7.99 Hz) × group (SCTI PRE vs. SCTI POST) | | | | | | | | | | | | | | | | | |
|---|---|---|---|---|---|---|---|---|---|---|---|---|---|---|---|---|---|---|
| | Negative | | | | | | Neutral | | | | | | Positive | | | | | |
| | PRE | | POST | | p | q | PRE | | POST | | p | q | PRE | | POST | | p | q |
| | $\widetilde{x}$ | STD | $\widetilde{x}$ | STD | | | $\widetilde{x}$ | STD | $\widetilde{x}$ | STD | | | $\widetilde{x}$ | STD | $\widetilde{x}$ | STD | | |
| **1-2** | 0,010 | 0,009 | 0,015 | 0,019 | 0,263 | 0,555 | 0,011 | 0,009 | 0,013 | 0,021 | 0,135 | 0,513 | 0,013 | 0,009 | 0,015 | 0,026 | 0,901 | 0,967 |
| **1-3** | 0,011 | 0,018 | 0,015 | 0,018 | 0,648 | 0,727 | 0,015 | 0,014 | 0,015 | 0,026 | 0,868 | 0,930 | 0,014 | 0,012 | 0,014 | 0,012 | 0,803 | 0,967 |
| **1-4** | 0,014 | 0,045 | 0,024 | 0,019 | 0,263 | 0,555 | 0,017 | 0,033 | 0,026 | 0,039 | 0,320 | 0,599 | 0,016 | 0,035 | 0,017 | 0,020 | 0,901 | 0,967 |
| **1-5** | 0,014 | 0,028 | 0,021 | 0,009 | **0,028** | 0,209 | 0,013 | 0,021 | 0,031 | 0,028 | **0,010** | 0,152 | 0,020 | 0,026 | 0,016 | 0,014 | 0,481 | 0,967 |
| **1-6** | 0,018 | 0,037 | 0,034 | 0,018 | 0,213 | 0,555 | 0,025 | 0,027 | 0,038 | 0,035 | 0,263 | 0,563 | 0,018 | 0,027 | 0,015 | 0,019 | 0,967 | 0,967 |
| **2-3** | 0,010 | 0,008 | 0,020 | 0,054 | **0,025** | 0,209 | 0,011 | 0,010 | 0,016 | 0,058 | 0,361 | 0,602 | 0,015 | 0,009 | 0,012 | 0,058 | 0,561 | 0,967 |
| **2-4** | 0,016 | 0,029 | 0,022 | 0,016 | 0,407 | 0,555 | 0,014 | 0,025 | 0,024 | 0,020 | 0,171 | 0,513 | 0,012 | 0,019 | 0,018 | 0,008 | 0,361 | 0,967 |
| **2-5** | 0,019 | 0,019 | 0,025 | 0,019 | 0,300 | 0,555 | 0,017 | 0,017 | 0,026 | 0,024 | 0,147 | 0,513 | 0,017 | 0,023 | 0,019 | 0,017 | 0,836 | 0,967 |
| **2-6** | 0,025 | 0,022 | 0,021 | 0,022 | 0,678 | 0,727 | 0,022 | 0,022 | 0,027 | 0,027 | 0,619 | 0,748 | 0,018 | 0,016 | 0,016 | 0,027 | 0,590 | 0,967 |
| **3-4** | 0,014 | 0,045 | 0,025 | 0,028 | 0,678 | 0,727 | 0,016 | 0,035 | 0,021 | 0,051 | 0,263 | 0,563 | 0,016 | 0,027 | 0,018 | 0,024 | 0,534 | 0,967 |
| **3-5** | 0,012 | 0,029 | 0,024 | 0,020 | 0,097 | 0,485 | 0,022 | 0,022 | 0,027 | 0,035 | **0,042** | 0,316 | 0,021 | 0,027 | 0,019 | 0,021 | 0,934 | 0,967 |
| **3-6** | 0,018 | 0,037 | 0,035 | 0,035 | 0,320 | 0,555 | 0,026 | 0,031 | 0,039 | 0,049 | 0,481 | 0,691 | 0,015 | 0,030 | 0,022 | 0,036 | 0,901 | 0,967 |
| **4-5** | 0,022 | 0,026 | 0,023 | 0,023 | 0,740 | 0,740 | 0,023 | 0,021 | 0,029 | 0,041 | 0,507 | 0,691 | 0,019 | 0,023 | 0,024 | 0,023 | 0,407 | 0,967 |
| **4-6** | 0,020 | 0,024 | 0,040 | 0,029 | 0,384 | 0,555 | 0,032 | 0,015 | 0,027 | 0,048 | 0,967 | 0,967 | 0,030 | 0,017 | 0,023 | 0,025 | 0,534 | 0,967 |
| **5-6** | 0,040 | 0,030 | 0,026 | 0,039 | 0,407 | 0,555 | 0,052 | 0,030 | 0,031 | 0,044 | 0,648 | 0,748 | 0,039 | 0,025 | 0,024 | 0,024 | 0,300 | 0,967 |

Table **B-5**.: Wilcoxon test results (Condition × band (ALPHA) × group)

| RoIs | **Condition × Alpha (8.0 - 13.99 Hz) × group (SCTI PRE vs. SCTI POST)** | | | | | | | | | | | | | | | | | |
|---|---|---|---|---|---|---|---|---|---|---|---|---|---|---|---|---|---|---|
| | **Negative** | | | | | | **Neutral** | | | | | | **Positive** | | | | | |
| | **PRE** | | **POST** | | **p** | **q** | **PRE** | | **POST** | | **p** | **q** | **PRE** | | **POST** | | **p** | **q** |
| | $\widetilde{x}$ | **STD** | $\widetilde{x}$ | **STD** | | | $\widetilde{x}$ | **STD** | $\widetilde{x}$ | **STD** | | | $\widetilde{x}$ | **STD** | $\widetilde{x}$ | **STD** | | |
| **1-2** | 0,013 | 0,005 | 0,014 | 0,006 | 1,000 | 1,000 | 0,014 | 0,005 | 0,015 | 0,007 | 0,901 | 0,901 | 0,009 | 0,006 | 0,013 | 0,005 | 0,648 | 0,810 |
| **1-3** | 0,015 | 0,011 | 0,013 | 0,006 | 0,901 | 0,965 | 0,013 | 0,009 | 0,015 | 0,008 | 0,534 | 0,667 | 0,009 | 0,007 | 0,011 | 0,006 | 0,590 | 0,804 |
| **1-4** | 0,012 | 0,025 | 0,022 | 0,014 | 0,263 | 0,563 | 0,015 | 0,011 | 0,028 | 0,014 | 0,229 | 0,382 | 0,012 | 0,018 | 0,016 | 0,011 | 0,106 | 0,345 |
| **1-5** | 0,011 | 0,014 | 0,020 | 0,011 | 0,097 | 0,485 | 0,015 | 0,007 | 0,015 | 0,015 | 0,648 | 0,748 | 0,008 | 0,007 | 0,014 | 0,006 | **0,034** | 0,211 |
| **1-6** | 0,015 | 0,016 | 0,019 | 0,014 | 0,263 | 0,563 | 0,014 | 0,010 | 0,022 | 0,013 | **0,038** | 0,279 | 0,010 | 0,012 | 0,022 | 0,010 | **0,042** | 0,211 |
| **2-3** | 0,013 | 0,006 | 0,016 | 0,009 | 0,213 | 0,563 | 0,015 | 0,005 | 0,017 | 0,014 | 0,534 | 0,667 | 0,011 | 0,007 | 0,012 | 0,015 | 0,772 | 0,890 |
| **2-4** | 0,012 | 0,012 | 0,014 | 0,010 | 0,590 | 0,885 | 0,015 | 0,008 | 0,023 | 0,010 | 0,171 | 0,382 | 0,011 | 0,008 | 0,015 | 0,007 | 0,245 | 0,460 |
| **2-5** | 0,011 | 0,017 | 0,019 | 0,014 | 0,081 | 0,485 | 0,017 | 0,006 | 0,021 | 0,013 | 0,229 | 0,382 | 0,015 | 0,008 | 0,013 | 0,012 | 0,934 | 0,967 |
| **2-6** | 0,016 | 0,013 | 0,019 | 0,016 | 0,171 | 0,563 | 0,014 | 0,009 | 0,027 | 0,015 | 0,056 | 0,279 | 0,012 | 0,008 | 0,016 | 0,012 | 0,245 | 0,460 |
| **3-4** | 0,012 | 0,025 | 0,013 | 0,013 | 0,772 | 0,927 | 0,014 | 0,008 | 0,026 | 0,015 | 0,171 | 0,382 | 0,012 | 0,016 | 0,014 | 0,012 | 0,184 | 0,460 |
| **3-5** | 0,012 | 0,016 | 0,016 | 0,015 | 0,074 | 0,485 | 0,016 | 0,007 | 0,018 | 0,015 | 0,184 | 0,382 | 0,010 | 0,008 | 0,016 | 0,009 | 0,507 | 0,760 |
| **3-6** | 0,014 | 0,022 | 0,018 | 0,021 | 0,481 | 0,845 | 0,016 | 0,010 | 0,024 | 0,019 | 0,051 | 0,279 | 0,009 | 0,012 | 0,018 | 0,014 | **0,034** | 0,211 |
| **4-5** | 0,018 | 0,012 | 0,020 | 0,021 | 0,772 | 0,927 | 0,018 | 0,010 | 0,020 | 0,019 | 0,300 | 0,450 | 0,011 | 0,011 | 0,016 | 0,007 | 0,115 | 0,345 |
| **4-6** | 0,017 | 0,012 | 0,019 | 0,025 | 0,507 | 0,845 | 0,018 | 0,010 | 0,026 | 0,022 | 0,074 | 0,279 | 0,017 | 0,011 | 0,016 | 0,019 | 0,361 | 0,602 |
| **5-6** | 0,033 | 0,014 | 0,031 | 0,020 | 0,803 | 0,927 | 0,025 | 0,015 | 0,029 | 0,016 | 0,803 | 0,861 | 0,026 | 0,013 | 0,023 | 0,015 | 0,967 | 0,967 |

Table **B-6**.: Wilcoxon test results (Condition × band (BETA) × group)

| RoIs | **Condition × Beta (14.0 - 29.99 Hz) × group (SCTI PRE vs. SCTI POST)** | | | | | | | | | | | | | | | | | |
|---|---|---|---|---|---|---|---|---|---|---|---|---|---|---|---|---|---|---|
| | **Negative** | | | | | | **Neutral** | | | | | | **Positive** | | | | | |
| | **PRE** | | **POST** | | **p** | **q** | **PRE** | | **POST** | | **p** | **q** | **PRE** | | **POST** | | **p** | **q** |
| | $\widetilde{x}$ | **STD** | $\widetilde{x}$ | **STD** | | | $\widetilde{x}$ | **STD** | $\widetilde{x}$ | **STD** | | | $\widetilde{x}$ | **STD** | $\widetilde{x}$ | **STD** | | |
| **1-2** | 0,009 | 0,003 | 0,010 | 0,005 | 0,135 | 0,203 | 0,009 | 0,002 | 0,011 | 0,005 | **0,042** | 0,423 | 0,008 | 0,003 | 0,010 | 0,005 | **0,034** | 0,086 |
| **1-3** | 0,009 | 0,004 | 0,012 | 0,006 | 0,051 | 0,192 | 0,010 | 0,002 | 0,010 | 0,005 | 0,648 | 1,000 | 0,009 | 0,002 | 0,012 | 0,004 | **0,003** | 0,021 |
| **1-4** | 0,009 | 0,004 | 0,013 | 0,007 | 0,081 | 0,192 | 0,011 | 0,004 | 0,013 | 0,010 | 0,740 | 1,000 | 0,010 | 0,003 | 0,014 | 0,008 | **0,011** | 0,048 |
| **1-5** | 0,009 | 0,003 | 0,009 | 0,008 | 0,229 | 0,301 | 0,010 | 0,003 | 0,010 | 0,010 | 0,934 | 1,000 | 0,008 | 0,005 | 0,012 | 0,008 | 0,097 | 0,157 |
| **1-6** | 0,008 | 0,003 | 0,010 | 0,011 | 0,263 | 0,301 | 0,011 | 0,005 | 0,011 | 0,014 | 0,901 | 1,000 | 0,010 | 0,004 | 0,012 | 0,011 | 0,106 | 0,157 |
| **2-3** | 0,010 | 0,004 | 0,012 | 0,005 | 0,281 | 0,301 | 0,009 | 0,005 | 0,012 | 0,007 | 0,135 | 0,677 | 0,010 | 0,004 | 0,011 | 0,008 | 0,115 | 0,157 |
| **2-4** | 0,008 | 0,004 | 0,013 | 0,005 | 0,115 | 0,192 | 0,008 | 0,004 | 0,010 | 0,005 | 0,056 | 0,423 | 0,008 | 0,002 | 0,011 | 0,004 | **0,014** | 0,048 |
| **2-5** | 0,009 | 0,004 | 0,012 | 0,004 | **0,005** | 0,072 | 0,011 | 0,005 | 0,013 | 0,007 | 0,481 | 0,901 | 0,007 | 0,006 | 0,012 | 0,004 | 0,135 | 0,169 |
| **2-6** | 0,009 | 0,004 | 0,012 | 0,007 | 0,062 | 0,192 | 0,010 | 0,005 | 0,012 | 0,010 | 0,407 | 0,901 | 0,008 | 0,004 | 0,011 | 0,008 | **0,016** | 0,048 |
| **3-4** | 0,010 | 0,004 | 0,011 | 0,008 | 0,081 | 0,192 | 0,010 | 0,005 | 0,011 | 0,009 | 0,245 | 0,736 | 0,008 | 0,003 | 0,013 | 0,006 | **0,001** | 0,018 |
| **3-5** | 0,009 | 0,005 | 0,011 | 0,007 | **0,038** | 0,192 | 0,011 | 0,006 | 0,013 | 0,009 | 0,431 | 0,901 | 0,007 | 0,006 | 0,010 | 0,007 | 0,213 | 0,246 |
| **3-6** | 0,010 | 0,005 | 0,014 | 0,010 | 0,281 | 0,301 | 0,013 | 0,006 | 0,012 | 0,013 | 0,803 | 1,000 | 0,009 | 0,004 | 0,012 | 0,010 | 0,089 | 0,157 |
| **4-5** | 0,010 | 0,004 | 0,011 | 0,004 | 0,115 | 0,192 | 0,009 | 0,003 | 0,010 | 0,003 | 0,678 | 1,000 | 0,009 | 0,007 | 0,011 | 0,007 | 0,340 | 0,364 |
| **4-6** | 0,008 | 0,008 | 0,011 | 0,004 | 0,431 | 0,431 | 0,010 | 0,006 | 0,011 | 0,004 | 1,000 | 1,000 | 0,009 | 0,011 | 0,011 | 0,006 | 0,384 | 0,384 |
| **5-6** | 0,010 | 0,004 | 0,011 | 0,004 | 0,106 | 0,192 | 0,010 | 0,004 | 0,012 | 0,003 | 0,199 | 0,736 | 0,010 | 0,005 | 0,013 | 0,005 | **0,046** | 0,100 |

Table **B-7**.: Wilcoxon test results (Condition × band (GAMMA) × group)

| RoIs | Condition × Gamma (30.0 - 59.99 Hz) × Group (SCTI PRE vs. SCTI POST) | | | | | | | | | | | | | | | | | |
|---|---|---|---|---|---|---|---|---|---|---|---|---|---|---|---|---|---|---|
| | Negative | | | | | | Neutral | | | | | | Positive | | | | | |
| | PRE | | POST | | p | q | PRE | | POST | | p | q | PRE | | POST | | p | q |
| | $\widetilde{x}$ | STD | $\widetilde{x}$ | STD | | | $\widetilde{x}$ | STD | $\widetilde{x}$ | STD | | | $\widetilde{x}$ | STD | $\widetilde{x}$ | STD | | |
| **1-2** | 0,010 | 0,006 | 0,010 | 0,006 | 0,934 | 0,934 | 0,009 | 0,006 | 0,011 | 0,006 | 0,678 | 1,000 | 0,009 | 0,005 | 0,011 | 0,006 | 0,340 | 0,678 |
| **1-3** | 0,009 | 0,005 | 0,009 | 0,005 | 0,619 | 0,934 | 0,010 | 0,005 | 0,010 | 0,004 | 0,868 | 1,000 | 0,009 | 0,005 | 0,009 | 0,004 | 0,619 | 0,810 |
| **1-4** | 0,012 | 0,008 | 0,011 | 0,010 | 0,340 | 0,934 | 0,011 | 0,007 | 0,011 | 0,009 | 0,836 | 1,000 | 0,010 | 0,008 | 0,009 | 0,010 | 0,534 | 0,801 |
| **1-5** | 0,010 | 0,011 | 0,010 | 0,005 | 0,590 | 0,934 | 0,011 | 0,013 | 0,009 | 0,005 | 0,407 | 1,000 | 0,008 | 0,012 | 0,010 | 0,006 | 0,229 | 0,657 |
| **1-6** | 0,010 | 0,012 | 0,010 | 0,015 | 0,836 | 0,934 | 0,010 | 0,014 | 0,009 | 0,015 | 0,507 | 1,000 | 0,008 | 0,014 | 0,011 | 0,016 | 0,263 | 0,657 |
| **2-3** | 0,010 | 0,005 | 0,009 | 0,005 | 0,320 | 0,934 | 0,010 | 0,006 | 0,009 | 0,006 | 1,000 | 1,000 | 0,009 | 0,005 | 0,010 | 0,007 | 0,407 | 0,678 |
| **2-4** | 0,011 | 0,008 | 0,013 | 0,009 | 0,901 | 0,934 | 0,010 | 0,007 | 0,011 | 0,007 | 0,561 | 1,000 | 0,010 | 0,008 | 0,009 | 0,009 | 0,803 | 0,861 |
| **2-5** | 0,012 | 0,009 | 0,012 | 0,006 | 0,619 | 0,934 | 0,012 | 0,011 | 0,010 | 0,005 | 0,384 | 1,000 | 0,009 | 0,010 | 0,012 | 0,008 | 0,407 | 0,678 |
| **2-6** | 0,012 | 0,012 | 0,013 | 0,015 | 0,678 | 0,934 | 0,013 | 0,012 | 0,012 | 0,013 | 0,934 | 1,000 | 0,008 | 0,011 | 0,011 | 0,015 | 0,245 | 0,657 |
| **3-4** | 0,012 | 0,011 | 0,011 | 0,012 | 0,709 | 0,934 | 0,010 | 0,010 | 0,012 | 0,010 | 0,561 | 1,000 | 0,010 | 0,010 | 0,009 | 0,011 | 1,000 | 1,000 |
| **3-5** | 0,010 | 0,011 | 0,010 | 0,007 | 0,507 | 0,934 | 0,010 | 0,014 | 0,009 | 0,006 | 0,534 | 1,000 | 0,009 | 0,013 | 0,011 | 0,008 | 0,199 | 0,657 |
| **3-6** | 0,013 | 0,017 | 0,010 | 0,019 | 0,709 | 0,934 | 0,011 | 0,018 | 0,011 | 0,017 | 1,000 | 1,000 | 0,008 | 0,017 | 0,009 | 0,020 | 0,648 | 0,810 |
| **4-5** | 0,009 | 0,017 | 0,011 | 0,004 | 0,678 | 0,934 | 0,011 | 0,016 | 0,009 | 0,003 | 0,229 | 1,000 | 0,009 | 0,015 | 0,010 | 0,004 | 0,229 | 0,657 |
| **4-6** | 0,010 | 0,025 | 0,010 | 0,006 | 0,901 | 0,934 | 0,010 | 0,023 | 0,010 | 0,009 | 0,561 | 1,000 | 0,011 | 0,020 | 0,011 | 0,009 | 0,803 | 0,861 |
| **5-6** | 0,011 | 0,007 | 0,010 | 0,007 | 0,901 | 0,934 | 0,012 | 0,008 | 0,010 | 0,007 | 0,678 | 1,000 | 0,009 | 0,008 | 0,012 | 0,007 | 0,068 | 0,657 |

# C. Statistical Analysis: Conventional Reintegration Group (CRG)

Table **C-1**.: Wilcoxon test results. CRG PRE vs. CRG POST

| RoIs | CRG PRE vs. CRG POST | | | | | |
|---|---|---|---|---|---|---|
| | CRG PRE | | CRG POST | | p-value | q-value |
| | MEDIAN | STD | MEDIAN | STD | | |
| **RoI1-RoI2** | 0,0105 | 0,0113 | 0,0123 | 0,0108 | **0,0060** | 0,0449 |
| **RoI1-RoI3** | 0,0126 | 0,0130 | 0,0123 | 0,0128 | 0,3104 | 0,4657 |
| **RoI1-RoI4** | 0,0141 | 0,0179 | 0,0142 | 0,0212 | 0,9120 | 0,9120 |
| **RoI1-RoI5** | 0,0127 | 0,0184 | 0,0142 | 0,0178 | 0,7046 | 0,7982 |
| **RoI1-RoI6** | 0,0124 | 0,0165 | 0,0136 | 0,0195 | 0,7450 | 0,7982 |
| **RoI2-RoI3** | 0,0119 | 0,0100 | 0,0133 | 0,0123 | 0,0513 | 0,1755 |
| **RoI2-RoI4** | 0,0116 | 0,0143 | 0,0124 | 0,0175 | 0,1989 | 0,4657 |
| **RoI2-RoI5** | 0,0145 | 0,0179 | 0,0132 | 0,0186 | 0,3015 | 0,4657 |
| **RoI2-RoI6** | 0,0129 | 0,0135 | 0,0130 | 0,0173 | 0,2738 | 0,4657 |
| **RoI3-RoI4** | 0,0132 | 0,0177 | 0,0128 | 0,0200 | 0,2858 | 0,4657 |
| **RoI3-RoI5** | 0,0136 | 0,0205 | 0,0144 | 0,0184 | 0,7140 | 0,7982 |
| **RoI3-RoI6** | 0,0139 | 0,0191 | 0,0127 | 0,0202 | 0,7437 | 0,7982 |
| **RoI4-RoI5** | 0,0114 | 0,0102 | 0,0132 | 0,0193 | **0,0414** | 0,1755 |
| **RoI4-RoI6** | 0,0118 | 0,0145 | 0,0143 | 0,0268 | 0,0585 | 0,1755 |
| **RoI5-RoI6** | 0,0131 | 0,0120 | 0,0154 | 0,0203 | **0,0041** | 0,0449 |

Table **C-2**.: Wilcoxon test results (Condition × group).

| RoIs | Condition × group (CRG PRE vs. CRG POST)) | | | | | | | | | | | | | | | | | |
|---|---|---|---|---|---|---|---|---|---|---|---|---|---|---|---|---|---|---|
| | Negative | | | | | | Neutral | | | | | | Positive | | | | | |
| | PRE | | POST | | p | q | PRE | | POST | | p | q | PRE | | POST | | p | q |
| | $\widetilde{x}$ | STD | $\widetilde{x}$ | STD | | | $\widetilde{x}$ | STD | $\widetilde{x}$ | STD | | | $\widetilde{x}$ | STD | $\widetilde{x}$ | STD | | |
| **1-2** | 0,011 | 0,010 | 0,011 | 0,009 | 0,171 | 0,963 | 0,011 | 0,012 | 0,012 | 0,011 | 0,150 | 0,829 | 0,011 | 0,012 | 0,013 | 0,011 | 0,060 | 0,312 |
| **1-3** | 0,012 | 0,011 | 0,012 | 0,012 | 0,299 | 0,963 | 0,013 | 0,014 | 0,012 | 0,014 | 0,926 | 0,948 | 0,013 | 0,014 | 0,013 | 0,013 | 0,551 | 0,689 |
| **1-4** | 0,014 | 0,020 | 0,014 | 0,021 | 0,863 | 0,963 | 0,014 | 0,017 | 0,014 | 0,022 | 0,696 | 0,948 | 0,014 | 0,017 | 0,016 | 0,020 | 0,730 | 0,783 |
| **1-5** | 0,012 | 0,019 | 0,013 | 0,016 | 0,893 | 0,963 | 0,013 | 0,018 | 0,014 | 0,020 | 0,896 | 0,948 | 0,013 | 0,018 | 0,015 | 0,017 | 0,521 | 0,689 |
| **1-6** | 0,014 | 0,016 | 0,013 | 0,018 | 0,963 | 0,963 | 0,012 | 0,017 | 0,011 | 0,021 | 0,423 | 0,829 | 0,012 | 0,017 | 0,018 | 0,019 | 0,210 | 0,393 |
| **2-3** | 0,012 | 0,010 | 0,013 | 0,012 | 0,260 | 0,963 | 0,012 | 0,010 | 0,012 | 0,012 | 0,301 | 0,829 | 0,012 | 0,010 | 0,014 | 0,013 | 0,262 | 0,393 |
| **2-4** | 0,012 | 0,016 | 0,011 | 0,017 | 0,937 | 0,963 | 0,012 | 0,014 | 0,013 | 0,018 | 0,357 | 0,829 | 0,012 | 0,014 | 0,013 | 0,018 | 0,184 | 0,393 |
| **2-5** | 0,015 | 0,018 | 0,014 | 0,020 | 0,592 | 0,963 | 0,014 | 0,018 | 0,013 | 0,017 | 0,442 | 0,829 | 0,014 | 0,018 | 0,014 | 0,019 | 0,662 | 0,763 |
| **2-6** | 0,014 | 0,013 | 0,012 | 0,019 | 0,952 | 0,963 | 0,013 | 0,014 | 0,011 | 0,017 | 0,784 | 0,948 | 0,013 | 0,014 | 0,014 | 0,016 | 0,083 | 0,312 |
| **3-4** | 0,013 | 0,020 | 0,012 | 0,020 | 0,845 | 0,963 | 0,013 | 0,017 | 0,012 | 0,021 | 0,609 | 0,948 | 0,013 | 0,017 | 0,015 | 0,019 | 0,243 | 0,393 |
| **3-5** | 0,013 | 0,021 | 0,014 | 0,018 | 0,730 | 0,963 | 0,014 | 0,021 | 0,014 | 0,020 | 0,838 | 0,948 | 0,014 | 0,021 | 0,015 | 0,018 | 0,959 | 0,959 |
| **3-6** | 0,014 | 0,019 | 0,013 | 0,021 | 0,583 | 0,963 | 0,014 | 0,019 | 0,012 | 0,022 | 0,948 | 0,948 | 0,014 | 0,019 | 0,016 | 0,019 | 0,210 | 0,393 |
| **4-5** | 0,012 | 0,012 | 0,012 | 0,021 | 0,521 | 0,963 | 0,011 | 0,009 | 0,013 | 0,020 | 0,340 | 0,829 | 0,011 | 0,009 | 0,015 | 0,017 | 0,069 | 0,312 |
| **4-6** | 0,013 | 0,016 | 0,014 | 0,029 | 0,514 | 0,963 | 0,012 | 0,014 | 0,014 | 0,025 | 0,167 | 0,829 | 0,012 | 0,014 | 0,015 | 0,026 | 0,239 | 0,393 |
| **5-6** | 0,015 | 0,014 | 0,016 | 0,021 | 0,096 | 0,963 | 0,013 | 0,011 | 0,014 | 0,021 | 0,178 | 0,829 | 0,013 | 0,011 | 0,018 | 0,019 | 0,059 | 0,312 |

Table **C-3**.: Wilcoxon test results (Condition × band (DELTA) × group)

| RoIs | **Condition × Delta(0.1 - 3.99 Hz) × group (CRG PRE vs. CRG POST )** | | | | | | | | | | | | | | | | | |
|---|---|---|---|---|---|---|---|---|---|---|---|---|---|---|---|---|---|---|
| | **Negative** | | | | | | **Neutral** | | | | | | **Positive** | | | | | |
| | **PRE** | | **POST** | | **p** | **q** | **PRE** | | **POST** | | **p** | **q** | **PRE** | | **POST** | | **p** | **q** |
| | $\widetilde{x}$ | **STD** | $\widetilde{x}$ | **STD** | | | $\widetilde{x}$ | **STD** | $\widetilde{x}$ | **STD** | | | $\widetilde{x}$ | **STD** | $\widetilde{x}$ | **STD** | | |
| **1-2** | 0,017 | 0,014 | 0,018 | 0,008 | 0,573 | 0,929 | 0,015 | 0,015 | 0,019 | 0,013 | 0,837 | 1,000 | 0,015 | 0,015 | 0,022 | 0,011 | 0,473 | 1,000 |
| **1-3** | 0,018 | 0,013 | 0,014 | 0,009 | 0,959 | 1,000 | 0,020 | 0,018 | 0,015 | 0,013 | 0,330 | 1,000 | 0,020 | 0,018 | 0,012 | 0,013 | 0,356 | 1,000 |
| **1-4** | 0,022 | 0,025 | 0,027 | 0,015 | 1,000 | 1,000 | 0,019 | 0,019 | 0,016 | 0,015 | 0,356 | 1,000 | 0,019 | 0,019 | 0,022 | 0,018 | 0,918 | 1,000 |
| **1-5** | 0,016 | 0,017 | 0,025 | 0,018 | 0,644 | 0,929 | 0,023 | 0,019 | 0,019 | 0,030 | 0,682 | 1,000 | 0,023 | 0,019 | 0,027 | 0,025 | 0,644 | 1,000 |
| **1-6** | 0,021 | 0,015 | 0,021 | 0,027 | 0,837 | 1,000 | 0,020 | 0,020 | 0,009 | 0,035 | 0,151 | 1,000 | 0,020 | 0,020 | 0,025 | 0,030 | 0,959 | 1,000 |
| **2-3** | 0,018 | 0,010 | 0,023 | 0,012 | 0,383 | 0,929 | 0,015 | 0,010 | 0,024 | 0,012 | 0,124 | 1,000 | 0,015 | 0,010 | 0,026 | 0,012 | 0,200 | 1,000 |
| **2-4** | 0,024 | 0,023 | 0,015 | 0,012 | 0,383 | 0,929 | 0,020 | 0,014 | 0,018 | 0,009 | 0,644 | 1,000 | 0,020 | 0,014 | 0,019 | 0,016 | 0,682 | 1,000 |
| **2-5** | 0,020 | 0,018 | 0,029 | 0,019 | 0,608 | 0,929 | 0,023 | 0,015 | 0,025 | 0,023 | 1,000 | 1,000 | 0,023 | 0,015 | 0,021 | 0,024 | 1,000 | 1,000 |
| **2-6** | 0,022 | 0,013 | 0,017 | 0,027 | 0,644 | 0,929 | 0,020 | 0,013 | 0,015 | 0,023 | 0,959 | 1,000 | 0,020 | 0,013 | 0,020 | 0,024 | 0,878 | 1,000 |
| **3-4** | 0,027 | 0,028 | 0,017 | 0,014 | 0,259 | 0,929 | 0,022 | 0,022 | 0,015 | 0,012 | 0,412 | 1,000 | 0,022 | 0,022 | 0,022 | 0,020 | 1,000 | 1,000 |
| **3-5** | 0,022 | 0,015 | 0,030 | 0,016 | 0,608 | 0,929 | 0,029 | 0,018 | 0,025 | 0,028 | 0,918 | 1,000 | 0,029 | 0,018 | 0,026 | 0,027 | 0,878 | 1,000 |
| **3-6** | 0,024 | 0,015 | 0,023 | 0,029 | 0,505 | 0,929 | 0,021 | 0,017 | 0,012 | 0,032 | 0,573 | 1,000 | 0,021 | 0,017 | 0,022 | 0,028 | 0,837 | 1,000 |
| **4-5** | 0,017 | 0,018 | 0,020 | 0,010 | 0,682 | 0,929 | 0,018 | 0,009 | 0,021 | 0,017 | 0,758 | 1,000 | 0,018 | 0,009 | 0,020 | 0,017 | 0,305 | 1,000 |
| **4-6** | 0,030 | 0,017 | 0,023 | 0,017 | 0,918 | 1,000 | 0,022 | 0,016 | 0,017 | 0,026 | 0,918 | 1,000 | 0,022 | 0,016 | 0,016 | 0,036 | 0,918 | 1,000 |
| **5-6** | 0,018 | 0,014 | 0,029 | 0,019 | 0,101 | 0,929 | 0,021 | 0,011 | 0,032 | 0,027 | 0,259 | 1,000 | 0,021 | 0,011 | 0,025 | 0,026 | 0,238 | 1,000 |

Table **C-4**.: Wilcoxon test results (Condition × band (THETA) × group)

| RoIs | Condition × Delta (4.0 - 7.99 Hz) × group (CRG PRE vs. CRG POST) | | | | | | | | | | | | | | | | | |
|---|---|---|---|---|---|---|---|---|---|---|---|---|---|---|---|---|---|---|
| | Negative | | | | | | Neutral | | | | | | Positive | | | | | |
| | PRE | | POST | | p | q | PRE | | POST | | p | q | PRE | | POST | | p | q |
| | $\widetilde{x}$ | STD | $\widetilde{x}$ | STD | | | $\widetilde{x}$ | STD | $\widetilde{x}$ | STD | | | $\widetilde{x}$ | STD | $\widetilde{x}$ | STD | | |
| **1-2** | 0,012 | 0,009 | 0,013 | 0,010 | 0,473 | 0,716 | 0,015 | 0,010 | 0,021 | 0,014 | 0,644 | 0,806 | 0,015 | 0,010 | 0,014 | 0,013 | 0,878 | 0,959 |
| **1-3** | 0,015 | 0,011 | 0,018 | 0,012 | 0,305 | 0,716 | 0,021 | 0,008 | 0,018 | 0,015 | 0,644 | 0,806 | 0,021 | 0,008 | 0,017 | 0,013 | 0,837 | 0,959 |
| **1-4** | 0,022 | 0,017 | 0,036 | 0,030 | 0,505 | 0,716 | 0,022 | 0,014 | 0,027 | 0,028 | 0,238 | 0,596 | 0,022 | 0,014 | 0,025 | 0,026 | 0,473 | 0,959 |
| **1-5** | 0,023 | 0,027 | 0,019 | 0,021 | 0,412 | 0,716 | 0,022 | 0,026 | 0,021 | 0,025 | 1,000 | 1,000 | 0,022 | 0,026 | 0,020 | 0,019 | 0,644 | 0,959 |
| **1-6** | 0,017 | 0,015 | 0,020 | 0,016 | 0,758 | 0,812 | 0,021 | 0,018 | 0,013 | 0,018 | 0,720 | 0,830 | 0,021 | 0,018 | 0,023 | 0,014 | 0,330 | 0,959 |
| **2-3** | 0,013 | 0,008 | 0,016 | 0,009 | 0,259 | 0,716 | 0,015 | 0,006 | 0,016 | 0,011 | 0,878 | 0,940 | 0,015 | 0,006 | 0,012 | 0,015 | 0,644 | 0,959 |
| **2-4** | 0,017 | 0,014 | 0,034 | 0,021 | 0,124 | 0,716 | 0,016 | 0,012 | 0,030 | 0,023 | 0,065 | 0,487 | 0,016 | 0,012 | 0,025 | 0,020 | 0,473 | 0,959 |
| **2-5** | 0,020 | 0,023 | 0,024 | 0,030 | 0,573 | 0,716 | 0,020 | 0,019 | 0,026 | 0,020 | 0,383 | 0,772 | 0,020 | 0,019 | 0,017 | 0,026 | 0,918 | 0,959 |
| **2-6** | 0,017 | 0,012 | 0,028 | 0,023 | 0,151 | 0,716 | 0,016 | 0,011 | 0,025 | 0,018 | 0,137 | 0,499 | 0,016 | 0,011 | 0,029 | 0,015 | **0,027** | 0,341 |
| **3-4** | 0,016 | 0,014 | 0,036 | 0,028 | 0,101 | 0,716 | 0,016 | 0,013 | 0,029 | 0,029 | 0,051 | 0,487 | 0,016 | 0,013 | 0,023 | 0,026 | 0,356 | 0,959 |
| **3-5** | 0,023 | 0,031 | 0,024 | 0,026 | 0,918 | 0,918 | 0,022 | 0,029 | 0,029 | 0,021 | 0,412 | 0,772 | 0,022 | 0,029 | 0,022 | 0,020 | 0,959 | 0,959 |
| **3-6** | 0,021 | 0,012 | 0,029 | 0,024 | 0,442 | 0,716 | 0,015 | 0,019 | 0,021 | 0,021 | 0,505 | 0,806 | 0,015 | 0,019 | 0,027 | 0,016 | **0,046** | 0,341 |
| **4-5** | 0,019 | 0,013 | 0,018 | 0,027 | 0,573 | 0,716 | 0,017 | 0,011 | 0,017 | 0,028 | 0,608 | 0,806 | 0,017 | 0,011 | 0,014 | 0,020 | 0,918 | 0,959 |
| **4-6** | 0,019 | 0,023 | 0,020 | 0,050 | 0,758 | 0,812 | 0,013 | 0,018 | 0,026 | 0,035 | 0,166 | 0,499 | 0,013 | 0,018 | 0,019 | 0,034 | 0,573 | 0,959 |
| **5-6** | 0,026 | 0,019 | 0,032 | 0,030 | 0,282 | 0,716 | 0,023 | 0,015 | 0,027 | 0,026 | 0,151 | 0,499 | 0,023 | 0,015 | 0,026 | 0,022 | 0,305 | 0,959 |

Table **C-5**.: Wilcoxon test results (Condition × band (ALPHA) × group)

| RoIs | **Condition × Alpha (8.0 - 13.99 Hz) × group (CRG PRE vs. CRG POST)** | | | | | | | | | | | | | | | | | |
|---|---|---|---|---|---|---|---|---|---|---|---|---|---|---|---|---|---|---|
| | **Negative** | | | | | | **Neutral** | | | | | | **Positive** | | | | | |
| | **PRE** | | **POST** | | **p** | **q** | **PRE** | | **POST** | | **p** | **q** | **PRE** | | **POST** | | **p** | **q** |
| | $\widetilde{x}$ | **STD** | $\widetilde{x}$ | **STD** | | | $\widetilde{x}$ | **STD** | $\widetilde{x}$ | **STD** | | | $\widetilde{x}$ | **STD** | $\widetilde{x}$ | **STD** | | |
| **1-2** | 0,013 | 0,012 | 0,012 | 0,014 | 0,878 | 0,940 | 0,011 | 0,018 | 0,018 | 0,013 | 0,305 | 0,997 | 0,011 | 0,018 | 0,017 | 0,015 | 0,166 | 0,416 |
| **1-3** | 0,014 | 0,015 | 0,015 | 0,019 | 0,959 | 0,959 | 0,013 | 0,021 | 0,019 | 0,020 | 0,538 | 0,997 | 0,013 | 0,021 | 0,019 | 0,018 | 0,282 | 0,416 |
| **1-4** | 0,017 | 0,027 | 0,016 | 0,026 | 0,682 | 0,940 | 0,022 | 0,025 | 0,016 | 0,032 | 0,959 | 1,000 | 0,022 | 0,025 | 0,031 | 0,024 | 0,356 | 0,445 |
| **1-5** | 0,020 | 0,020 | 0,019 | 0,017 | 0,758 | 0,940 | 0,015 | 0,020 | 0,015 | 0,013 | 0,758 | 0,997 | 0,015 | 0,020 | 0,022 | 0,012 | 0,573 | 0,661 |
| **1-6** | 0,018 | 0,023 | 0,028 | 0,019 | 0,837 | 0,940 | 0,020 | 0,022 | 0,016 | 0,021 | 0,505 | 0,997 | 0,020 | 0,022 | 0,027 | 0,017 | 0,282 | 0,416 |
| **2-3** | 0,015 | 0,014 | 0,015 | 0,019 | 0,720 | 0,940 | 0,014 | 0,017 | 0,017 | 0,016 | 0,798 | 0,997 | 0,014 | 0,017 | 0,021 | 0,017 | 0,112 | 0,416 |
| **2-4** | 0,017 | 0,016 | 0,011 | 0,024 | 0,644 | 0,940 | 0,017 | 0,022 | 0,015 | 0,025 | 0,538 | 0,997 | 0,017 | 0,022 | 0,018 | 0,025 | 0,238 | 0,416 |
| **2-5** | 0,022 | 0,021 | 0,015 | 0,016 | 0,073 | 0,940 | 0,021 | 0,027 | 0,017 | 0,013 | 0,330 | 0,997 | 0,021 | 0,027 | 0,018 | 0,010 | 1,000 | 1,000 |
| **2-6** | 0,018 | 0,018 | 0,018 | 0,013 | 0,758 | 0,940 | 0,021 | 0,022 | 0,013 | 0,019 | 1,000 | 1,000 | 0,021 | 0,022 | 0,029 | 0,012 | 0,259 | 0,416 |
| **3-4** | 0,017 | 0,026 | 0,015 | 0,021 | 0,837 | 0,940 | 0,016 | 0,023 | 0,014 | 0,029 | 0,918 | 1,000 | 0,016 | 0,023 | 0,027 | 0,020 | 0,182 | 0,416 |
| **3-5** | 0,020 | 0,024 | 0,018 | 0,015 | 0,218 | 0,940 | 0,018 | 0,025 | 0,015 | 0,013 | 0,330 | 0,997 | 0,018 | 0,025 | 0,022 | 0,009 | 0,720 | 0,771 |
| **3-6** | 0,022 | 0,032 | 0,018 | 0,019 | 0,682 | 0,940 | 0,014 | 0,032 | 0,016 | 0,024 | 0,758 | 0,997 | 0,014 | 0,032 | 0,030 | 0,015 | 0,151 | 0,416 |
| **4-5** | 0,018 | 0,009 | 0,017 | 0,032 | 0,878 | 0,940 | 0,013 | 0,012 | 0,020 | 0,027 | 0,473 | 0,997 | 0,013 | 0,012 | 0,020 | 0,022 | 0,051 | 0,416 |
| **4-6** | 0,015 | 0,013 | 0,023 | 0,030 | 0,305 | 0,940 | 0,015 | 0,016 | 0,019 | 0,028 | 0,305 | 0,997 | 0,015 | 0,016 | 0,019 | 0,027 | 0,218 | 0,416 |
| **5-6** | 0,024 | 0,012 | 0,022 | 0,016 | 0,644 | 0,940 | 0,017 | 0,009 | 0,018 | 0,013 | 0,608 | 0,997 | 0,017 | 0,009 | 0,020 | 0,013 | 0,305 | 0,416 |

Table **C-6**.: Wilcoxon test results (Condition × band (BETA) × group)

| RoIs | Condition × Beta (14.0 - 29.99 Hz) × group (CRG PRE vs. CRG POST) | | | | | | | | | | | | | | | | | |
|---|---|---|---|---|---|---|---|---|---|---|---|---|---|---|---|---|---|---|
| | Negative | | | | | | Neutral | | | | | | Positive | | | | | |
| | PRE | | POST | | p | q | PRE | | POST | | p | q | PRE | | POST | | p | q |
| | $\widetilde{x}$ | STD | $\widetilde{x}$ | STD | | | $\widetilde{x}$ | STD | $\widetilde{x}$ | STD | | | $\widetilde{x}$ | STD | $\widetilde{x}$ | STD | | |
| **1-2** | 0,010 | 0,003 | 0,012 | 0,004 | 0,442 | 0,757 | 0,010 | 0,005 | 0,011 | 0,009 | 0,218 | 0,852 | 0,010 | 0,005 | 0,014 | 0,005 | **0,021** | 0,289 |
| **1-3** | 0,011 | 0,003 | 0,011 | 0,004 | 0,644 | 0,806 | 0,010 | 0,006 | 0,012 | 0,007 | 0,305 | 0,852 | 0,010 | 0,006 | 0,013 | 0,005 | 0,412 | 0,687 |
| **1-4** | 0,009 | 0,005 | 0,010 | 0,006 | 0,442 | 0,757 | 0,011 | 0,005 | 0,012 | 0,005 | 0,608 | 0,852 | 0,011 | 0,005 | 0,011 | 0,008 | 1,000 | 1,000 |
| **1-5** | 0,010 | 0,002 | 0,012 | 0,006 | **0,040** | 0,604 | 0,011 | 0,004 | 0,010 | 0,009 | 0,682 | 0,852 | 0,011 | 0,004 | 0,014 | 0,007 | 0,200 | 0,500 |
| **1-6** | 0,010 | 0,004 | 0,013 | 0,008 | 0,101 | 0,756 | 0,010 | 0,005 | 0,011 | 0,011 | 0,538 | 0,852 | 0,010 | 0,005 | 0,010 | 0,010 | 0,383 | 0,687 |
| **2-3** | 0,010 | 0,004 | 0,011 | 0,006 | 0,473 | 0,757 | 0,011 | 0,004 | 0,010 | 0,009 | 0,644 | 0,852 | 0,011 | 0,004 | 0,013 | 0,007 | 0,182 | 0,500 |
| **2-4** | 0,009 | 0,004 | 0,009 | 0,003 | 0,573 | 0,781 | 0,009 | 0,003 | 0,009 | 0,003 | 0,878 | 0,918 | 0,009 | 0,003 | 0,011 | 0,002 | 0,200 | 0,500 |
| **2-5** | 0,011 | 0,003 | 0,011 | 0,008 | 1,000 | 1,000 | 0,011 | 0,002 | 0,009 | 0,007 | 0,644 | 0,852 | 0,011 | 0,002 | 0,010 | 0,009 | 0,959 | 1,000 |
| **2-6** | 0,009 | 0,003 | 0,010 | 0,004 | 0,959 | 1,000 | 0,010 | 0,003 | 0,009 | 0,003 | 0,918 | 0,918 | 0,010 | 0,003 | 0,010 | 0,005 | 0,412 | 0,687 |
| **3-4** | 0,009 | 0,005 | 0,009 | 0,004 | 0,918 | 1,000 | 0,010 | 0,004 | 0,011 | 0,003 | 0,682 | 0,852 | 0,010 | 0,004 | 0,011 | 0,004 | 0,720 | 0,900 |
| **3-5** | 0,010 | 0,003 | 0,011 | 0,008 | 0,282 | 0,757 | 0,012 | 0,004 | 0,011 | 0,010 | 0,918 | 0,918 | 0,012 | 0,004 | 0,011 | 0,010 | 0,878 | 1,000 |
| **3-6** | 0,009 | 0,005 | 0,011 | 0,008 | 0,505 | 0,757 | 0,010 | 0,006 | 0,010 | 0,007 | 0,644 | 0,852 | 0,010 | 0,006 | 0,011 | 0,010 | 0,720 | 0,900 |
| **4-5** | 0,011 | 0,004 | 0,012 | 0,004 | 0,505 | 0,757 | 0,009 | 0,002 | 0,010 | 0,004 | 0,383 | 0,852 | 0,009 | 0,002 | 0,011 | 0,005 | 0,058 | 0,289 |
| **4-6** | 0,011 | 0,003 | 0,012 | 0,007 | 0,442 | 0,757 | 0,010 | 0,003 | 0,011 | 0,011 | 0,505 | 0,852 | 0,010 | 0,003 | 0,011 | 0,006 | 0,473 | 0,709 |
| **5-6** | 0,011 | 0,003 | 0,011 | 0,004 | 0,412 | 0,757 | 0,009 | 0,003 | 0,011 | 0,006 | 0,081 | 0,852 | 0,009 | 0,003 | 0,011 | 0,007 | 0,058 | 0,289 |

Table **C-7**.: Wilcoxon test results (Condition × band (GAMMA) × group

| RoIs | **Condition × Gamma (30.0 - 59.99 Hz) × (CRG PRE vs. CRG POST)** | | | | | | | | | | | | | | | | | |
|---|---|---|---|---|---|---|---|---|---|---|---|---|---|---|---|---|---|---|
| | **Negative** | | | | | | **Neutral** | | | | | | **Positive** | | | | | |
| | **PRE** | | **POST** | | **p** | **q** | **PRE** | | **POST** | | **p** | **q** | **PRE** | | **POST** | | **p** | **q** |
| | $\widetilde{x}$ | **STD** | $\widetilde{x}$ | **STD** | | | $\widetilde{x}$ | **STD** | $\widetilde{x}$ | **STD** | | | $\widetilde{x}$ | **STD** | $\widetilde{x}$ | **STD** | | |
| **1-2** | 0,009 | 0,002 | 0,010 | 0,003 | 0,238 | 0,596 | 0,010 | 0,003 | 0,010 | 0,003 | 0,412 | 0,772 | 0,010 | 0,003 | 0,008 | 0,006 | 0,837 | 0,918 |
| **1-3** | 0,009 | 0,002 | 0,010 | 0,002 | 0,182 | 0,596 | 0,009 | 0,002 | 0,009 | 0,003 | 0,878 | 0,878 | 0,009 | 0,002 | 0,010 | 0,006 | 0,837 | 0,918 |
| **1-4** | 0,010 | 0,009 | 0,010 | 0,001 | 0,505 | 0,673 | 0,010 | 0,012 | 0,009 | 0,002 | 0,073 | 0,363 | 0,010 | 0,012 | 0,008 | 0,003 | 0,081 | 0,918 |
| **1-5** | 0,009 | 0,003 | 0,008 | 0,002 | 0,137 | 0,596 | 0,009 | 0,003 | 0,010 | 0,002 | 0,682 | 0,852 | 0,009 | 0,003 | 0,008 | 0,004 | 0,330 | 0,918 |
| **1-6** | 0,010 | 0,007 | 0,008 | 0,002 | 0,200 | 0,596 | 0,010 | 0,009 | 0,009 | 0,002 | 0,051 | 0,363 | 0,010 | 0,009 | 0,009 | 0,002 | 0,200 | 0,918 |
| **2-3** | 0,008 | 0,003 | 0,009 | 0,002 | 0,505 | 0,673 | 0,008 | 0,005 | 0,010 | 0,002 | 0,356 | 0,763 | 0,008 | 0,005 | 0,008 | 0,003 | 0,918 | 0,918 |
| **2-4** | 0,008 | 0,004 | 0,010 | 0,003 | 0,200 | 0,596 | 0,010 | 0,004 | 0,008 | 0,003 | 0,798 | 0,855 | 0,010 | 0,004 | 0,008 | 0,004 | 0,798 | 0,918 |
| **2-5** | 0,010 | 0,004 | 0,009 | 0,001 | 0,644 | 0,744 | 0,011 | 0,004 | 0,009 | 0,002 | 0,218 | 0,648 | 0,011 | 0,004 | 0,009 | 0,002 | 0,200 | 0,918 |
| **2-6** | 0,009 | 0,007 | 0,010 | 0,004 | 0,442 | 0,673 | 0,009 | 0,007 | 0,009 | 0,003 | 0,758 | 0,855 | 0,009 | 0,007 | 0,009 | 0,003 | 0,878 | 0,918 |
| **3-4** | 0,010 | 0,004 | 0,010 | 0,003 | 0,538 | 0,673 | 0,010 | 0,006 | 0,008 | 0,004 | 0,124 | 0,465 | 0,010 | 0,006 | 0,008 | 0,004 | 0,644 | 0,918 |
| **3-5** | 0,009 | 0,002 | 0,008 | 0,002 | 0,166 | 0,596 | 0,009 | 0,003 | 0,009 | 0,002 | 0,538 | 0,852 | 0,009 | 0,003 | 0,009 | 0,002 | 0,383 | 0,918 |
| **3-6** | 0,010 | 0,006 | 0,009 | 0,002 | 0,798 | 0,798 | 0,010 | 0,005 | 0,008 | 0,003 | 0,259 | 0,648 | 0,010 | 0,005 | 0,009 | 0,003 | 0,412 | 0,918 |
| **4-5** | 0,009 | 0,003 | 0,009 | 0,002 | 0,538 | 0,673 | 0,010 | 0,002 | 0,009 | 0,001 | 0,573 | 0,852 | 0,010 | 0,002 | 0,009 | 0,002 | 0,918 | 0,918 |
| **4-6** | 0,009 | 0,003 | 0,009 | 0,001 | 0,282 | 0,603 | 0,011 | 0,002 | 0,009 | 0,002 | 0,073 | 0,363 | 0,011 | 0,002 | 0,009 | 0,002 | 0,442 | 0,918 |
| **5-6** | 0,010 | 0,003 | 0,009 | 0,002 | 0,798 | 0,798 | 0,010 | 0,003 | 0,010 | 0,003 | 0,682 | 0,852 | 0,010 | 0,003 | 0,010 | 0,004 | 0,644 | 0,918 |

# Bibliography


[1] N. R. Council, "Internal Displacement Monitoring Centre (IDMC) norwegian refugee council," http://www.internal-displacement.org/americas/colombia/, 2017, Accessed: 2016-10-10.

[2] K. Theidon, "Transitional subjects: The disarmament, demobilization and reintegration of former combatants in colombia," *International Journal of Transitional Justice*, vol. 1, no. 1, pp. 66–90, 2007.

[3] A. R. Nilsson, "Dangerous liaisons: Why ex-combatants return to violence," *Cases from the Republic of Congo and Sierra Leone (dissertation)*, 2008.

[4] A. Jiménez, "Salud mental en el posconflicto colombiano," *Revista criminalidad*, vol. 51, no. 1, pp. 179–192, 2009.

[5] E. Van Diessen, T. Numan, E. Van Dellen, A. Van Der Kooi, M. Boersma, D. Hofman, R. van Lutterveld, B. van Dijk, E. van Straaten, A. Hillebrand *et al.*, "Opportunities and methodological challenges in EEG and MEG resting state functional brain network research," *Clinical Neurophysiology*, vol. 126, no. 8, pp. 1468–1481, 2015.

[6] K. J. Friston, "Functional and effective connectivity: a review," *Brain connectivity*, vol. 1, no. 1, pp. 13–36, 2011.

[7] P. Fries, D. Nikolić, and W. Singer, "The gamma cycle," *Trends in neurosciences*, vol. 30, no. 7, pp. 309–316, 2007.

[8] P. Lang and M. M. Bradley, "The international affective picture system (IAPS) in the study of emotion and attention," *Handbook of emotion elicitation and assessment*, vol. 29, 2007.

[9] J. A. Mikels, B. L. Fredrickson, G. R. Larkin, C. M. Lindberg, S. J. Maglio, and P. A. Reuter-Lorenz, "Emotional category data on images from the international affective picture system," *Behavior research methods*, vol. 37, no. 4, pp. 626–630, 2005.

[10] C. P. Moreno, V. E. Quezada, and A. Antivilo, "Identifying fear-evoking pictures from the international affective picture system (IAPS) in a chilean sample," *Terapia Psicológica*, vol. 34, no. 3, 2016.

[11] J. Y. Lee, K. A. Lindquist, and C. S. Nam, "Emotional granularity effects on event-related brain potentials during affective picture processing," *Frontiers in human neuroscience*, vol. 11, 2017.

[12] P. Vuilleumier, "How brains beware: neural mechanisms of emotional attention," *Trends in cognitive sciences*, vol. 9, no. 12, pp. 585–594, 2005.

[13] A. Carballedo, J. Scheuerecker, E. Meisenzahl, V. Schoepf, A. Bokde, H.-J. Möller, M. Doyle, M. Wiesmann, and T. Frodl, "Functional connectivity of emotional processing in depression," *Journal of affective disorders*, vol. 134, no. 1, pp. 272–279, 2011.

[14] L. Pan, S. Hassel, A. Segreti, S. Nau, D. Brent, and M. L. Phillips, "Differential patterns of activity and functional connectivity in emotion processing neural circuitry to angry and happy faces in adolescents with and without suicide attempt," *Psychological medicine*, vol. 43, no. 10, pp. 2129–2142, 2013.

[15] S. Haufe, V. V. Nikulin, K.-R. Müller, and G. Nolte, "A critical assessment of connectivity measures for EEG data: a simulation study," *Neuroimage*, vol. 64, pp. 120–133, 2013.

[16] R. K. Pitman, S. P. Orr, B. Altman, R. E. Longpre, R. E. Poiré, and M. L. Macklin, "Emotional processing during eye movement desensitization and reprocessing therapy of vietnam veterans with chronic posttraumatic stress disorder," *Comprehensive psychiatry*, vol. 37, no. 6, pp. 419–429, 1996.

[17] B. T. Litz, S. M. Orsillo, D. Kaloupek, and F. Weathers, "Emotional processing in posttraumatic stress disorder." *Journal of Abnormal Psychology*, vol. 109, no. 1, p. 26, 2000.

[18] C. T. Taft, D. G. Kaloupek, J. A. Schumm, A. D. Marshall, J. Panuzio, D. W. King, and T. M. Keane, "Posttraumatic stress disorder symptoms, physiological reactivity, alcohol problems, and aggression among military veterans." *Journal of abnormal psychology*, vol. 116, no. 3, p. 498, 2007.

[19] A. Etkin and T. D. Wager, "Functional neuroimaging of anxiety: a meta-analysis of emotional processing in PTSD, social anxiety disorder, and specific phobia," *American Journal of Psychiatry*, vol. 164, no. 10, pp. 1476–1488, 2007.

[20] R. A. Morey, C. M. Petty, D. A. Cooper, K. S. LaBar, and G. McCarthy, "Neural systems for executive and emotional processing are modulated by symptoms of posttraumatic stress disorder in Iraq war veterans," *Psychiatry Research: Neuroimaging*, vol. 162, no. 1, pp. 59–72, 2008.

[21] C. Tobón, D. C. Aguirre-Acevedo, L. Velilla, J. Duque, C. P. Ramos, and D. Pineda, "Perfil psiquiátrico, cognitivo y de reconocimiento de características emocionales de un grupo de excombatientes de los grupos armados ilegales en colombia," *Revista Colombiana de Psiquiatría*, vol. 45, no. 1, pp. 28–36, 2016.

[22] C. Tobón, A. Ibañez, L. Velilla, J. Duque, J. Ochoa, N. Trujillo, J. Decety, and D. Pineda, "Emotional processing in colombian ex-combatants and its relationship with empathy and executive functions," *Social neuroscience*, vol. 10, no. 2, pp. 153–165, 2015.

[23] A. Quintero-Zea, L. M. Sepúlveda-Cano, M. R. Calvache, S. T. Orrego, N. T. Orrego, and J. D. López, "Characterization framework for ex-combatants based on EEG and behavioral features," in *VII Latin American Congress on Biomedical Engineering CLAIB 2016, Bucaramanga, Santander, Colombia, October 26th-28th, 2016*. Springer, 2017, pp. 205–208.

[24] S. Trujillo, S. Valencia, N. Trujillo, J. Ugarriza, J. Lopez, M. Rodriguez, J. Rendon, D. Pineda, A. Ibanez, and M. Parra, "Atypical modulations of N170 component during emotional processing and their links to social behaviors in ex-combatants," *Frontiers in Human Neuroscience*, vol. 11, p. 244, 2017. [Online]. Available: http://journal.frontiersin.org/article/10.3389/fnhum.2017.00244

[25] C. Brunner, M. Billinger, M. Seeber, T. R. Mullen, and S. Makeig, "Volume conduction influences scalp-based connectivity estimates," *Frontiers in Computational Neuroscience*, vol. 10, 2016.

[26] A. Khadem and G.-A. Hossein-Zadeh, "Comparing the robustness of brain connectivity measures to volume conduction artifact," in *Biomedical Engineering (ICBME), 2013 20th Iranian Conference on*. IEEE, 2013, pp. 209–214.

[27] M. Teplan *et al.*, "Fundamentals of EEG measurement," *Measurement science review*, vol. 2, no. 2, pp. 1–11, 2002.

[28] M. Rodríguez-Calvache, A. Quintero-Zea, S. T. Orrego, N. T. Orrego, and J. D. López, "Classifying artifacts and neural EEG components using SVM," in *Computational Intelligence (LA-CCI), 2016 IEEE Latin American Conference on*. IEEE, 2016, pp. 1–5.

[29] ACR, "La Reintegracion en cifras," http://www.reintegracion.gov.co/es/la-reintegracion/Paginas/cifras.aspx/, 2017, Accessed: 2017-02-10.

[30] R. Weierstall, C. P. B. Castellanos, F. Neuner, and T. Elbert, "Relations among appetitive aggression, post-traumatic stress and motives for demobilization: a study in former colombian combatants," *Conflict and health*, vol. 7, no. 1, p. 9, 2013.

[31] J. H. Newby, J. E. McCarroll, R. J. Ursano, Z. Fan *et al.*, "Positive and negative consequences of a military deployment," *Military medicine*, vol. 170, no. 10, p. 815, 2005.

[32] L. Carretié, J. Iglesias, T. Garcia, and M. Ballesteros, "N300, P300 and the emotional processing of visual stimuli," *Electroencephalography and clinical Neurophysiology*, vol. 103, no. 2, pp. 298–303, 1997.

[33] R. Plutchik, "A general psychoevolutionary theory of emotion," *Theories of emotion*, vol. 1, no. 3-31, p. 4, 1980.

[34] M. Batty and M. J. Taylor, "Early processing of the six basic facial emotional expressions," *Cognitive Brain Research*, vol. 17, no. 3, pp. 613–620, 2003.

[35] R. Plutchik, "The nature of emotions human emotions have deep evolutionary roots, a fact that may explain their complexity and provide tools for clinical practice," *American scientist*, vol. 89, no. 4, pp. 344–350, 2001.

[36] D. A. Pizzagalli *et al.*, "Electroencephalography and high-density electrophysiological source localization," *Handbook of psychophysiology*, vol. 3, pp. 56–84, 2007.

[37] G. R. Müller-Putz, R. Riedl, and S. C. Wriessnegger, "Electroencephalography (EEG) as a research tool in the information systems discipline: foundations, measurement, and applications," *Communications of the Association for Information Systems*, vol. 37, no. 1, p. 46, 2015.

[38] K. Korjus, A. Uusberg, H. Uusberg, N. Kuldkepp, K. Kreegipuu, J. Allik, R. Vicente, and J. Aru, "Personality cannot be predicted from the power of resting state EEG," *Frontiers in human neuroscience*, vol. 9, 2015.

[39] T. W. Picton, O. G. Lins, and M. Scherg, "The recording and analysis of event-related potentials," *Handbook of neuropsychology*, vol. 10, pp. 3–3, 1995.

[40] E. Hurtado, A. Haye, R. González, F. Manes, and A. Ibáñez, "Contextual blending of ingroup/outgroup face stimuli and word valence: LPP modulation and convergence of measures," *BMC neuroscience*, vol. 10, no. 1, p. 69, 2009.

[41] M. Rubinov and O. Sporns, "Complex network measures of brain connectivity: uses and interpretations," *Neuroimage*, vol. 52, no. 3, pp. 1059–1069, 2010.

[42] E. W. Lang, A. M. Tomé, I. R. Keck, J. Górriz-Sáez, and C. G. Puntonet, "Brain connectivity analysis: a short survey," *Computational intelligence and neuroscience*, vol. 2012, p. 8, 2012.

[43] W. Hasenkamp and L. W. Barsalou, "Effects of meditation experience on functional connectivity of distributed brain networks," *Frontiers in human neuroscience*, vol. 6, p. 38, 2012.

[44] S. B. Rutkove, "Introduction to volume conduction," in *The clinical neurophysiology primer*. Springer, 2007, pp. 43–53.

[45] M. X. Cohen, *Analyzing neural time series data: theory and practice*. MIT Press, 2014.

[46] W. Schneider, A. Eschman, and A. Zuccolotto, "E-prime, version 1.1," *Pittsburgh, PA: Psychology Software Tools*, 2002.

[47] C. A. Gantiva Díaz, P. Guerra Muñoz, and J. Vila Castellar, "Colombian validation of the international affective picture system: Evidence of cross-cultural origins of emotion," *Acta Colombiana de Psicología*, vol. 14, no. 2, pp. 103–111, 2011.

[48] P. L. Nunez and R. Srinivasan, *Electric fields of the brain: the neurophysics of EEG*. Oxford University Press, USA, 2006.

[49] C. Neuroscan, "Neuroscan 4.5 [computer software]," *North Carolina: Compumedics USA*, 2008.

[50] V. Milnik, "Anleitung zur elektrodenplatzierung des internationalen 10–20-systems," *Das Neurophysiologie-Labor*, vol. 31, no. 1, pp. 1–35, 2009.

[51] V. Jurcak, D. Tsuzuki, and I. Dan, "10/20, 10/10, and 10/5 systems revisited: their validity as relative head-surface-based positioning systems," *Neuroimage*, vol. 34, no. 4, pp. 1600–1611, 2007.

[52] A. Delorme and S. Makeig, "EEGLAB: an open source toolbox for analysis of single-trial eeg dynamics including independent component analysis," *Journal of neuroscience methods*, vol. 134, no. 1, pp. 9–21, 2004.

[53] C. J. James and C. W. Hesse, "Independent component analysis for biomedical signals," *Physiological measurement*, vol. 26, no. 1, p. R15, 2004.

[54] N. Mammone, G. Inuso, F. La Foresta, and F. Carlo Morabito, "Multiresolution ICA for artifact identification from electroencephalographic recordings," in *Knowledge-Based Intelligent Information and Engineering Systems*. Springer, 2007, pp. 680–687.

[55] N. P. Castellanos and V. A. Makarov, "Recovering eeg brain signals: artifact suppression with wavelet enhanced independent component analysis," *Journal of neuroscience methods*, vol. 158, no. 2, pp. 300–312, 2006.

[56] A. Greco, N. Mammone, F. C. Morabito, and M. Versaci, "Kurtosis, Renyis entropy and independent component scalp maps for the automatic artifact rejection from EEG data," *International Journal of Signal Processing*, vol. 2, no. 4, pp. 240–244, 2006.

[57] D. Dharmaprani, H. K. Nguyen, T. W. Lewis, D. De Los Ángeles, J. O. Willoughby, and K. J. Pope, "A comparison of independent component analysis algorithms and measures to discriminate between EEG and artifact components," in *Engineering in Medicine and Biology Society (EMBC), 2016 IEEE 38th Annual International Conference of the*. IEEE, 2016, pp. 825–828.

[58] A. Hyviirinen, J. Karhunen, and E. Oja, "Independent component analysis," *Wileyand Sons*, 2001.

[59] A. J. Bell and T. J. Sejnowski, "An information-maximization approach to blind separation and blind deconvolution," *Neural computation*, vol. 7, no. 6, pp. 1129–1159, 1995.

[60] S. Makeig, A. J. Bell, T.-P. Jung, T. J. Sejnowski *et al.*, "Independent component analysis of electroencephalographic data," *Advances in neural information processing systems*, pp. 145–151, 1996.

[61] T.-P. Jung, S. Makeig, C. Humphries, T.-W. Lee, M. J. Mckeown, V. Iragui, and T. J. Sejnowski, "Removing electroencephalographic artifacts by blind source separation," *Psychophysiology*, vol. 37, no. 02, pp. 163–178, 2000.

[62] V. N. Vapnik, *The Nature of Statistical Learning Theory*, 2nd ed. New York, NY: Springer–Verlag, 1995, ch. Methods of Pattern Recognition, pp. 138–155.

[63] C. Cortes and V. Vapnik, "Support-vector networks," *Machine learning*, vol. 20, no. 3, pp. 273–297, 1995.

[64] L. Shoker, S. Sanei, and J. Chambers, "Artifact removal from electroencephalograms using a hybrid BSS-SVM algorithm," *IEEE Signal Processing Letters*, vol. 12, no. 10, pp. 721–724, 2005.

[65] A. Belouchrani, K. Abed-Meraim, J.-F. Cardoso, and E. Moulines, "A blind source separation technique using second-order statistics," *IEEE Transactions on signal processing*, vol. 45, no. 2, pp. 434–444, 1997.

[66] S. Halder, M. Bensch, J. Mellinger, M. Bogdan, A. Kübler, N. Birbaumer, and W. Rosenstiel, "Online artifact removal for brain-computer interfaces using support vector machines and blind source separation," *Computational intelligence and neuroscience*, vol. 2007, 2007.

[67] L. Tong, R.-W. Liu, V. C. Soon, and Y.-F. Huang, "Indeterminacy and identifiability of blind identification," *IEEE Transactions on circuits and systems*, vol. 38, no. 5, pp. 499–509, 1991.

[68] J.-F. Cardoso, "High-order contrasts for independent component analysis," *Neural computation*, vol. 11, no. 1, pp. 157–192, 1999.

[69] E. Bingham and A. Hyvärinen, "A fast fixed-point algorithm for independent component analysis of complex valued signals," *International journal of neural systems*, vol. 10, no. 01, pp. 1–8, 2000.

[70] G. Bartels, L.-C. Shi, and B.-L. Lu, "Automatic artifact removal from EEG: - a mixed approach based on double blind source separation and support vector machine," in *Engineering in Medicine and Biology Society (EMBC), 2010 Annual International Conference of the IEEE*. IEEE, 2010, pp. 5383–5386.

[71] S.-Y. Shao, K.-Q. Shen, C. J. Ong, E. P. Wilder-Smith, and X.-P. Li, "Automatic EEG artifact removal: a weighted support vector machine approach with error correction," *Biomedical Engineering, IEEE Transactions on*, vol. 56, no. 2, pp. 336–344, 2009.

[72] A. J. Smola and B. Schölkopf, *Learning with kernels*. GMD-Forschungszentrum Informationstechnik, 1998.

[73] G.-Y. Shi and S. Liu, "Model selection of RBF kernel for C-SVM based on genetic algorithm and multithreading," in *2012 International Conference on Machine Learning and Cybernetics*, vol. 1, July 2012, pp. 382–386.

[74] C.-C. Chang and C.-J. Lin, "LIBSVM: a library for support vector machines," *ACM Transactions on Intelligent Systems and Technology (TIST)*, vol. 2, no. 3, p. 27, 2011.

[75] N. M. Kleinhans, T. Richards, L. Sterling, K. C. Stegbauer, R. Mahurin, L. C. Johnson, J. Greenson, G. Dawson, and E. Aylward, "Abnormal functional connectivity in autism spectrum disorders during face processing," *Brain*, vol. 131, no. 4, pp. 1000–1012, 2008.

[76] C. S. Monk, S. J. Peltier, J. L. Wiggins, S.-J. Weng, M. Carrasco, S. Risi, and C. Lord, "Abnormalities of intrinsic functional connectivity in autism spectrum disorders," *Neuroimage*, vol. 47, no. 2, pp. 764–772, 2009.

[77] A. Meyer-Lindenberg, J.-B. Poline, P. D. Kohn, J. L. Holt, M. F. Egan, D. R. Weinberger, and K. F. Berman, "Evidence for abnormal cortical functional connectivity during working memory in schizophrenia," *American Journal of Psychiatry*, vol. 158, no. 11, pp. 1809–1817, 2001.

[78] M.-E. Lynall, D. S. Bassett, R. Kerwin, P. J. McKenna, M. Kitzbichler, U. Muller, and E. Bullmore, "Functional connectivity and brain networks in schizophrenia," *Journal of Neuroscience*, vol. 30, no. 28, pp. 9477–9487, 2010.

[79] M. Ullsperger and S. Debener, *Simultaneous EEG and fMRI: recording, analysis, and application*. Oxford University Press, 2010.

[80] W. Klimesch, "EEG alpha and theta oscillations reflect cognitive and memory performance: a review and analysis," *Brain research reviews*, vol. 29, no. 2, pp. 169–195, 1999.

[81] A. K. Engel and P. Fries, "Beta-band oscillations-signalling the status quo?" *Current opinion in neurobiology*, vol. 20, no. 2, pp. 156–165, 2010.

[82] G. Buzsaki, *Rhythms of the Brain*. Oxford University Press, 2006.

[83] M. A. Brazier and J. U. Casby, "Crosscorrelation and autocorrelation studies of electroencephalographic potentials," *Electroencephalography and clinical neurophysiology*, vol. 4, no. 2, pp. 201–211, 1952.

[84] G. Pfurtscheller and C. Andrew, "Event-related changes of band power and coherence: methodology and interpretation," *Journal of clinical neurophysiology*, vol. 16, no. 6, p. 512, 1999.

[85] G. Nolte, O. Bai, L. Wheaton, Z. Mari, S. Vorbach, and M. Hallett, "Identifying true brain interaction from EEG data using the imaginary part of coherency," *Clinical neurophysiology*, vol. 115, no. 10, pp. 2292–2307, 2004.

[86] C. J. Stam, G. Nolte, and A. Daffertshofer, "Phase lag index: assessment of functional connectivity from multi channel EEG and MEG with diminished bias from common sources," *Human brain mapping*, vol. 28, no. 11, pp. 1178–1193, 2007.

[87] R. A. Fisher, "The use of multiple measurements in taxonomic problems," *Annals of eugenics*, vol. 7, no. 2, pp. 179–188, 1936.

[88] P. Xanthopoulos, P. M. Pardalos, and T. B. Trafalis, "Linear discriminant analysis," in *Robust Data Mining*. Springer, 2013, pp. 27–33.

[89] G. Chung, D. M. Tucker, P. West, G. F. Potts, M. Liotti, P. Luu, and A. L. Hartry, "Emotional expectancy: Brain electrical activity associated with an emotional bias in interpreting life events," *Psychophysiology*, vol. 33, no. 3, pp. 218–233, 1996.

[90] M. Esslen, R. Pascual-Marqui, D. Hell, K. Kochi, and D. Lehmann, "Brain areas and time course of emotional processing," *Neuroimage*, vol. 21, no. 4, pp. 1189–1203, 2004.

[91] P. Vuilleumier and G. Pourtois, "Distributed and interactive brain mechanisms during emotion face perception: evidence from functional neuroimaging," *Neuropsychologia*, vol. 45, no. 1, pp. 174–194, 2007.

[92] G. Niso, R. Bruña, E. Pereda, R. Gutiérrez, R. Bajo, F. Maestú, and F. Del-Pozo, "Hermes: towards an integrated toolbox to characterize functional and effective brain connectivity isacm," *International Society for the Advancement of Clinical Magnetoencephalography*, p. 38453, 2013.

[93] R. Adolphs, "Cognitive neuroscience of human social behaviour," *Nature Reviews Neuroscience*, vol. 4, no. 3, pp. 165–178, 2003.

[94] A. Olsson and K. N. Ochsner, "The role of social cognition in emotion," *Trends in cognitive sciences*, vol. 12, no. 2, pp. 65–71, 2008.

[95] E. A. Yildirim, M. Kasar, and M. G̈dük, "Investigation of the reliability of the" reading the mind in the eyes test" in a turkish population," *Turk Psikiyatri Dergisi*, vol. 22, no. 3, p. 177, 2011.

[96] T. Fujimura, Y.-T. Matsuda, K. Katahira, M. Okada, and K. Okanoya, "Categorical and dimensional perceptions in decoding emotional facial expressions," *Cognition & emotion*, vol. 26, no. 4, pp. 587–601, 2012.

[97] A. N. Clausen, A. J. Francisco, J. Thelen, J. Bruce, L. E. Martin, J. McDowd, W. K. Simmons, and R. L. Aupperle, "PTSD and cognitive symptoms relate to inhibition-related prefrontal activation and functional connectivity," *Depression and anxiety*, vol. 34, no. 5, pp. 427–436, 2017.

[98] F. Wilcoxon, "Individual comparisons by ranking methods," *Biometrics bulletin*, vol. 1, no. 6, pp. 80–83, 1945.

[99] L. J. Larson-Prior, J. M. Zempel, T. S. Nolan, F. W. Prior, A. Z. Snyder, and M. E. Raichle, "Cortical network functional connectivity in the descent to sleep," *Proceedings of the National Academy of Sciences*, vol. 106, no. 11, pp. 4489–4494, 2009.

[100] D. M. Goldenholz, J. J. Tharayil, R. Kuzniecky, P. Karoly, W. H. Theodore, and M. J. Cook, "Simulating clinical trials with and without intracranial EEG data," *Epilepsia Open*, 2016.

[101] K. Singh, Y. D. Shah, D. Luciano, D. Friedman, O. Devinsky, and S. V. Kothare, "Safety and efficacy of perampanel in children and adults with various epilepsy syndromes: A single-center postmarketing study," *Epilepsy & Behavior*, vol. 61, pp. 41–45, 2016.

[102] E. Whitley and J. Ball, "Statistics review 6: Nonparametric methods," *Critical Care*, vol. 6, no. 6, p. 509, 2002.

[103] Y. Benjamini and Y. Hochberg, "Controlling the false discovery rate: a practical and powerful approach to multiple testing," *Journal of the royal statistical society. Series B (Methodological)*, pp. 289–300, 1995.

[104] A. K. Singh and S. Phillips, "Hierarchical control of false discovery rate for phase locking measures of EEG synchrony," *NeuroImage*, vol. 50, no. 1, pp. 40–47, 2010.

[105] Y.-Y. Lee and S. Hsieh, "Classifying different emotional states by means of EEG-based functional connectivity patterns," *PloS one*, vol. 9, no. 4, p. e95415, 2014.

[106] M. Balconi and C. Lucchiari, "EEG correlates (event-related desynchronization) of emotional face elaboration: a temporal analysis," *Neuroscience letters*, vol. 392, no. 1, pp. 118–123, 2006.

[107] T. Costa, E. Rognoni, and D. Galati, "EEG phase synchronization during emotional response to positive and negative film stimuli," *Neuroscience letters*, vol. 406, no. 3, pp. 159–164, 2006.

[108] S. Trujillo, N. Trujillo, J. Lopez, D. Gomez, S. Valencia, J. Rendon, D. Pineda, and M. Parra, "Social cognitive training improves emotional processing and reduces aggressive attitudes in ex-combatants," *Frontiers in Psychology*, vol. 8, p. 510, 2017. [Online]. Available: http://journal.frontiersin.org/article/10.3389/fpsyg.2017.00510